The role of the salvage pathway of phytol, geranylgeraniol, and farnesol phosphorylation in *Arabidopsis thaliana*

Dissertation

zur
Erlangung des Doktorgrades (Dr. rer. nat.)
der
Mathematisch-Naturwissenschaftlichen Fakultät
der
Rheinischen Friedrich-Wilhelms-Universität Bonn

vorgelegt von

Jill Romer
aus
Biberach an der Riß

Bonn, Oktober 2020

Angefertigt mit Genehmigung der Mathematisch-Naturwissenschaftlichen Fakultät der Rheinischen Friedrich-Wilhelms-Universität Bonn.

Erster Gutachter: Prof. Dr. Peter Dörmann
Zweiter Gutachter: Prof. Dr. Gabriel Schaaf
Tag der Promotion: 10.02.2021
Erscheinungsjahr: 2021

Table of Contents

Table of Figures

List of Tables

Abbreviations

% (v/v)	Percent volume per volume (ml per 100 ml)
% (w/v)	Percent weight per volume (g per 100 ml)
ACN	Acetonitrile
ad	Latin: *ad* = fill up to
APS	Ammonium persulfate
A. thaliana	*Arabidopsis thaliana*
ATP	Adenosine triphosphate
bp	Base pairs
BR	Brassinosteroid
BSA	Bovine serum albumin
CHAPS	3-[(3-Cholamidopropyl)dimethylammonio]-1-propanesulfonate
CHLG	Chlorophyll synthase
cps	Counts per second
CTAB	Cetyltrimethylammonium bromide
CTP	Cytidine triphosphate
ddH_20	Double deionized water
DEE	Diethylether
DGDG	Digalactosyldiacylglycerol
DMAPP	Dimethylallyl-pyrophosphate
DMSO	Dimethyl sulfoxide
DNA	Deoxyribonucleic acid
dNTPs	Deoxyribonucleotide triphosphates (dATP, dCTP, dTTP, dGTP)
DW	Dry weight
E. coli	*Escherichia coli*
EDTA	Ethylenediaminetetraacetic acid
ESI	Electrospray ionization
et al.	Latin: *et alii* = and others
EtOH	Ethanol
FAME	Fatty acid methyl ester
Farnesyl-P/-PP	Farnesyl-phosphate/-pyrophosphate
FLD	Fluorescence light detector
FOLK	Farnesol kinase
FW	Fresh weight
GC-FID	Gas chromatography-flame ionization detection
GC-MS	Gas chromatography-mass spectrometry
GFP	Green fluorescent protein
GG-P/-PP	Geranylgeranyl-phosphate/-pyrophosphate
GGR	Geranylgeranyl reductase
GTP	Guanosine triphosphate
HEPES	4-(2-hydroxyethyl)-1-piperazineethanesulfonic acid
HGA	Homogentisate
HGGT	Homogentisate geranylgeranyltransferase
HPLC	High-performance liquid chromatography
HPT	Homogentisate phytyltransferase (= VTE2)
IPP	Isopentenyl-pyrophosphate
I.S.	Internal standard
kDa	Kilo Dalton
LB medium	Luria-Bertani medium

LC-MS	Liquid chromatography coupled to mass spectrometry
MCS	Multiple cloning site
MeOH	Methanol
MGDM	Monogalactosyldiacylglycerol
mol%	Molar percentage
MRM	Multiple reaction monitoring
MS	Mass spectrometry
MS medium	Murashige and Skoog medium
MSTFA	N-methyl-N-(trimethylsilyl) trifluoroacetamide
m/z	Mass/charge ratio
N. benthamiana	*Nicotiana benthamiana*
NTPs	Ribonucleotide triphosphates (ATP, CTP, UTP, GTP)
OD	Optical density
ORF	Open reading frame
P	Phosphate
PAO	Pheophorbide a oxygenase
PAR	Photosynthetic active radiation
PC-8	Plastochromanol-8
PCR	Polymerase chain reaction
PES	Phytyl Ester Synthase
Phytyl-P/-PP	Phytyl-phosphate/-pyrophosphate (= diphosphate)
PP	Pyrophosphate (= diphosphate)
PSI	Photosystem I
Q-TOF MS	Quadrupole Time-of-Flight Mass Spectrometer
Q-Trap MS	Quadrupole Iontrap Mass Spectrometer
rcf	Relative centrifugal force
RNA	Ribonucleic acid
ROS	Reactive oxygen species
rpm	Revolutions per minute
RT	Room temperature
RT-PCR	Reverse transcription PCR
SD	Standard deviation
SDS PAGE	Sodium dodecyl sulfate polyacrylamide gel electrophoresis
SGR	Stay-green
SPE	Solid phase extraction
TEMED	Tetramethylethylenediamine
Tris	Tris(hydroxymethyl)aminomethane
UTP	Uridine triphosphate
VTE	Vitamin E deficient
VTE1	Vitamin E deficient 1 (tocopherol cyclase)
VTE2	Vitamin E deficient 2 (= HPT, homogentisate phytyltransferase)
VTE5	Vitamin E deficient 5 (phytol kinase)
VTE6	Vitamin E deficient 6 (phytyl-phosphate kinase)
WT	Wild type

Lipid terminology

Isoprenoid chains are abbreviated according to the number of carbon atoms in their structure in the following format: **Cx.** While the number "x" stands for the number of carbon atoms, the "C" is the abbreviation for carbon.

Fatty acids are abbreviated in numbers in the following format: **X:Y**. The "X" indicates the number of C-atoms, "Y" indicates the number of double bonds. Fatty acid alcohols are additionally substituted by "ol" at the end.

Arabidopsis thaliana

The entire work was done using the model organism *Arabidopsis thaliana* (*A. thaliana*). In the following, this organism name will be simplified and called Arabidopsis.

1 Introduction

Cellular metabolism of animals and plants is based on the economic use of resources. These resources comprise in particular metabolites containing essential elements, and energy conserved in energy-rich bonds. The *de novo* synthesis of metabolic compounds consumes a lot of energy. Instead of *de novo* synthesizing the building blocks, degradation and turnover products from the catabolism can be remobilized in salvage pathways, e.g. by phosphorylation, as precursors for the biosynthesis of essential metabolites. One of the most critical of these processes in plants is the turnover of the photosynthetic machinery which includes the degradation and turnover of the photosynthetic pigment chlorophyll. Chlorophyll is the key pigment in photosynthesis, where light energy is used to convert inorganic carbon into organic compounds, under the release of oxygen (Katz and Norris, 1973; von Wettstein *et al.*, 1995). The chlorophyll structure can be separated into two main parts: a porphyrin head group and a C20 phytyl side chain derived from the diphosphorylated isoprenoid alcohol phytyl diphosphate (-PP). This phytyl side chain is cleaved off during chlorophyll degradation and the free isoprenoid alcohol phytol is released. Recently, it was shown that phytol can be remobilized by phosphorylation for tocopherol (vitamin E) and phylloquinone (vitamin K1) biosynthesis (vom Dorp *et al.*, 2015; Wang *et al.*, 2017). Isoprenoids are the most diverse class of organic compounds found in nature. They are synthesized *de novo* from the C5 isoprene monomers isopentenyl pyrophosphate (IPP) and dimethylallyl pyrophosphate (DMAPP). These two precursors are attached by condensation reactions forming the C10 isoprenoid alcohol phosphate geranyl-PP, the precursor of the monoterpenes. Condensation of one or two additional C5 monomers leads to the formation of the sesquiterpene precursor farnesyl-PP (C15) and the diterpene precursor geranylgeranyl-PP (C20). Important plant molecules derived from farnesyl-PP are, for example, sterols. Geranylgeranyl-PP is the precursor for the biosynthesis of photosynthetic pigments, such as chlorophyll and carotenoids, and for some phytohormones. Phytyl-PP is not a direct product of the isoprenoid *de novo* synthesis but can be produced from geranylgeranyl-PP after reduction. Phytyl-PP differs from geranylgeranyl-PP by the reduction of three double bonds and forms the side chain of tocopherols (vitamin E) and phylloquinone (vitamin K1). The variety of biosynthetic pathways dependent on the presence of

phosphorylated isoprenoid alcohols underlines their metabolic importance. Further, phytol from chlorophyll degradation can be remobilized by phosphorylation for the biosynthesis of tocopherol and phylloquinone. This shows that isoprenoid alcohol phosphates can be part of salvage pathways.

1.1 Plant isoprenoids

1.1.1 Isoprenoid *de novo* synthesis in plants: MVA and MEP pathways

Isoprenoids encompass a large number of important compounds and form the most diverse molecule class found in nature. In plants, next to phytohormones, sterols, and photosynthetic pigments, they are also building blocks of vitamins, including vitamin E (tocochromanols) and vitamin K1 (phylloquinone). Isoprenoids are synthesized *de novo* in plants via two pathways, the mevalonate (MVA) and the non-mevalonate or 2-C-methyl-D-erythritol 4-phosphate (MEP) pathway (Figure 1). The two pathways differ from each other in their subcellular location and the precursor molecules. The MVA pathway is located to the cytosol. In plants, some reactions of the MVA pathway are shown to also take place in the peroxisomes (Simkin *et al.*, 2011; Clastre *et al.*, 2011; Gutbrod *et al.*, 2019). While all eukaryotes harbor the MVA pathway for the *de novo* synthesis of isoprenoids, some bacteria, plants, and algae also possess of the additional MVA independent pathway, the MEP pathway (Lichtenthaler *et al.*, 1997; Rohmer, 1999; Calisto *et al.*, 2007). The MEP pathway is evolutionary derived from cyanobacteria and is located to the plastids in plants. Although the two pathways are separated in different subcellular localizations, radiolabeled intermediates of the cytosolic MVA pathway were also found inside the plastids (Rohmer, 1999). Presumably, isoprene precursors can be exchanged between the two pathways, but the exact processes are still unclear. Isoprenoid synthesis in the cytosolic MVA pathway starts with the condensation of two molecules of acetyl-CoA under the release of one CoA (coenzyme A) molecule catalyzed by acetyl-CoA-acetyltransferase (ACAT). This step presumably takes place in the cytosol, but one of the two Arabidopsis ACAT homologs (ACAT2) is present in peroxisomes (Carrie *et al.*, 2007; Reumann *et al.*, 2007). The resulting acetoacetyl-CoA molecule is elongated by 3-hydroxy-3-methylglutaryl-CoA synthase (HMGS) to form 3-hydroxy-3-methylglutaryl-CoA (HMG-CoA). This elongation happens by acetylation with another acetyl-CoA molecule. HMG-

CoA is reduced by the HMG-CoA reductase (HMGR) to form mevalonate, the name-giving intermediate of this pathway (Ferguson *et al.*, 1959; Durr and Rudney, 1960). Mevalonate is processed by two subsequent phosphorylation steps catalyzed by mevalonate kinase (MK) and 5-phospho-mevalonate kinase (PMK). Diphosphorylated mevalonate is decarboxylated to the C5 isoprenoid key molecule isopentenyl-PP (IPP), which can be converted to its isomer dimethylallyl-PP (DMAPP) by isopentenyl-PP isomerase.

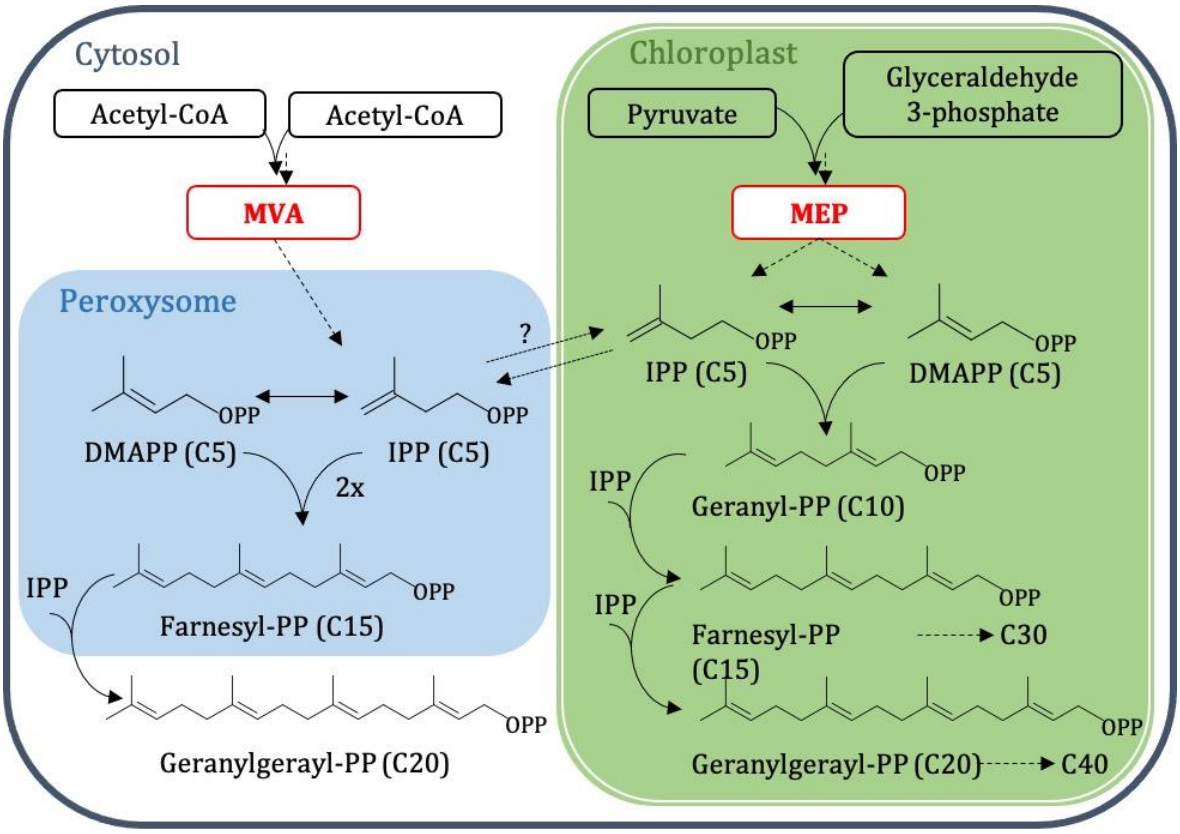

Figure 1 Schematic overview of the isoprenoid *de novo* synthesis in plants: MVA and MEP pathways.

Plants are able to produce isoprenoids via two pathways, the cytosolic mevalonate (MVA) and the chloroplast localized 2-C-methyl-D-erythritol 4-phosphate (MEP) pathway. Both pathways have in common the production of the isoprenoid C5 building blocks isopentenyl-PP (IPP) and dimethylallyl-PP (DMAPP). From these C5 isoprenyl units, larger isoprenoids like the C10 geranyl-PP, the C15 farnesyl-PP or the C20 geranylgeranyl-PP are formed. Figure modified after Gutbrod *et al.*, 2019.

In plants, the isoprene building blocks IPP and DMAPP can also be synthesized inside plastids via the non-mevalonate or MEP pathway (Lichtenthaler *et al.*, 1997). Here the starting molecule is pyruvate instead of acetyl-CoA, which is condensed with glyceraldehyde-3-phosphate under the release of carbon dioxide. The product 1-deoxyxylulose-5-P (DOXP) is converted by a reductoisomerase (DXR) into 2-C-methyl-

D-erythritol 4-phosphate (MEP), the name-giving molecule of this pathway. IPP and DMAPP are synthesized from MEP in five steps (Lichtenthaler, 1999; Schwender *et al.*, 1999). First, MEP is esterified with a cytidine triphosphate (CTP) molecule under the release of one phosphate group to form 2-methyl-4-CDP-erythritol (CDP-MEP). This step is followed by an ATP dependent phosphorylation at the C2 position of CDP-MEP. Dephosphorylation of the CDP moiety leads to cyclization between the remaining phosphate group of CMP and the phosphate group at the C2 atom forming 2-methylerythritol-2,4-cyclodiphosphate (MEcPP). Dehydration of this ring structure leads to ring opening and formation of 4-hydroxy-3-methyl-2-enyl-PP, which is the precursor for the two C5 isoprene units IPP and DMAPP. IPP and DMAPP formation is catalyzed by 4-hydroxy-3-methylbut-2-enyl-PP reductase (HDR) under the release of water and oxidation of $NADPH+H^+$ (Hsieh and Goodman, 2005).

IPP and DMAPP from the cytosolic MVA as well as from the plastidial MEP pathway are the precursors of larger isoprene units. Larger isoprene units are formed by condensation of IPP with DMAPP (Figure 1). The so-called head-to-tail condensation is most common, while head-to-head or tail-to-tail condensations are relatively rare. Condensation of the two C5 isoprene subunits is catalyzed by geranyl diphosphate synthase forming the C10 monoterpene precursor geranyl-PP. Further attachment of one more C5 isoprene unit to geranyl-PP leads to the synthesis of the C15 sesquiterpene farnesyl-PP catalyzed by farnesyl diphosphate synthase. Two molecules of farnesyl-PP are condensed to form the precursor for the C30 triterpenes. Farnesyl-PP is elongated by condensation with another C5 isoprene unit to form the C20 diterpene geranylgeranyl-PP. Geranylgeranyl-PP is also the precursor for the C40 tetraterpenes after condensation of two C20 units. Condensation reactions are catalyzed by the respective synthases (Kellogg and Poulter, 1997). Phytol, which is also a C20 isoprene, shares the same structure with geranylgeranyl-PP with the exception that it carries only one double bond in the carbon chain while geranylgeranyl-PP carries four (Gutbrod *et al.*, 2019). Geranylgeranyl-PP can be reduced to phytyl-PP by the geranylgeranyl reductase (GGR) (Keller *et al.*, 1998).

1.1.2 Farnesol, geranylgeraniol, and phytol

Free isoprenoid alcohols are only low abundant compounds in Arabidopsis under normal conditions. Farnesol, geranylgeraniol, and phytol have a similar

structure derived from isoprenoid subunits. Farnesol and geranylgeraniol differ from each other in the number of C-atoms present in the isoprenoid chain. Farnesol is a C15 isoprenoid alcohol, and geranylgeraniol with one additional isoprene unit is a C20 isoprenoid alcohol (Figure 2). Phytol shares the same number of 20 C-atoms present in the isoprenyl chain with geranylgeraniol but differs from geranylgeraniol in the number of double bonds. While geranylgeraniol is unsaturated with four double bonds, phytol has only one double bond (Figure 2). *De novo* synthesized farnesyl-PP and geranylgeranyl-PP in plants can be hydrolyzed to the respective isoprenoid alcohols. Plant extracts are often used in the perfume industry, because the presence of free isoprenoid alcohols in plant oils is oftentimes accompanied by a strong odor (Zhang *et al.*, 2017). Further, free isoprenoid alcohols can be released during plant metabolism upon degradation or turnover. For example, free farnesol or geranylgeraniol can be released from farnesylated or geranylgeranylated proteins during protein degradation. The main function of farnesylation or geranylgeranylation is to anchor proteins in the lipid bilayer of the plasma membranes. The discovery of a nuclear farnesol receptor (FXR) in 1995 provided evidence, that free farnesol might act as a regulator of diverse metabolic processes (Forman *et al.*, 1995). Later studies using radiolabeled substrates showed that farnesol and geranylgeraniol can be phosphorylated in two consecutive steps to their respective activated diphosphorylated forms by enzymes present in *Nicotiana tabacum* cells (Thai *et al.*, 1999). A gene encoding an enzyme with farnesol kinase activity (*FOLK*) was described later in Arabidopsis (Fitzpatrick *et al.*, 2011) but the respective farnesyl phosphate kinase gene is still missing. Activated diphosphorylated farnesol (farnesyl-PP) is an important precursor in plant sterol and sesquiterpene biosynthesis, while activated geranylgeraniol (geranylgeranyl-PP) is an important precursor in the biosynthesis of photosynthetic pigments including carotenoids and chlorophyll. Free phytol can be released from chlorophyll during chlorophyll turnover or degradation. The function of free phytol in plants is unclear but high amounts of phytol can affect the integrity of lipid membranes as it has detergent-like characteristics. The same is true for farnesol and geranylgeraniol, this is why these compounds are supposed to be rapidly metabolized, for example by esterification or phosphorylation.

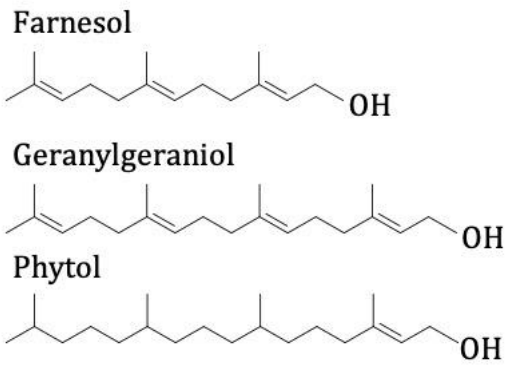

Figure 2 Chemical structure of farnesol, geranylgeraniol, and phytol.

Farnesol, geranylgeraniol, and phytol are isoprenoid alcohols that carry a hydroxy group at the C1 position. Farnesol has a C15 isoprenoid chain with three double bonds while geranylgeraniol has a C20 isoprenoid chain with four double bonds. Phytol shares the same C20 isoprenoid structure as geranylgeraniol but carries only one double bond at the C2 position.

1.2 Isoprenoid alcohol phosphates: intermediates in the biosynthesis of sterols, phytohormones, photosynthetic pigments, vitamin E and vitamin K1

1.2.1 Farnesyl-PP and geranylgeranyl-PP are precursors for sterols, some phytohormones and photosynthetic pigments

Sterols are synthesized from squalene which is synthesized from farnesyl-PP of the cytosolic MVA pathway (Schaeffer *et al.*, 2001). Phytosterols are a complex compound class. The predominant sterols in plants are β-sitosterol, stigmasterol and campesterol (Hartmann, 1998; Schaller *et al.*, 1998). While the phytosterols are synthesized from farnesyl-PP derived from the cytosolic MVA pathway, other plant compounds are synthesized from isoprenoid alcohol phosphates derived from the plastidial MEP pathway. The C20 diterpene geranylgeranyl-PP, synthesized in the MEP pathway, for example, represents an important precursor in the biosynthesis of photosynthetic pigments including chlorophyll, β-carotene, lutein, zeaxanthin, violaxanthin, and antheraxanthin (Cunningham and Gantt, 1998; Shalygo *et al.*, 2009; Gutbrod *et al.*, 2019). Chlorophyll synthesis includes the attachment of a geranylgeranyl side chain to the porphyrin head first forming geranylgeranyl-chlorophyll. This geranylgeranyl side chain is subsequently reduced to a phytyl chain by geranylgeranyl reductase (GGR) to form chlorophyll a. Further, some phytohormones are synthesized from geranylgeranyl-PP, for example, the phytohormones gibberellic acid (GA) and abscisic acid (ABA). ABA is synthesized from the carotenoid zeaxanthin in several steps (Xiong and Zhu, 2003; Gupta and Chakrabarty, 2013).

1.2.2 Phytyl-PP is a precursor for tocopherol (vitamin E) and phylloquinone (vitamin K1)

1.2.2.1 Tocopherol (vitamin E)

Tocopherols, also known as vitamin E, together with tocomonoenols, tocotrienols, and plastochromanol-8 (PC-8) belong to the class of tocochromanols. Tocochromanols are important antioxidants able to scavenge reactive oxygen species. They are synthesized predominantly in plants and algae but also in some cyanobacteria and *Plasmodium falciparum*. For humans and other vertebrates, they are an essential dietary nutrition factor. Tocochromanols include four forms of tocopherols, four forms of tocotrienols, four forms of tocomonoenols and plastochromanol-8. All compounds have in common their prenylquinone structure consisting of a chromanol ring in the head group, which is derived from homogentisic acid (HGA) and an isoprenoid side chain. Tocopherols consist of a methylated chromanol head group to which a phytyl side chain is attached. Tocotrienols carry a geranylgeranyl side chain (Figure 3).

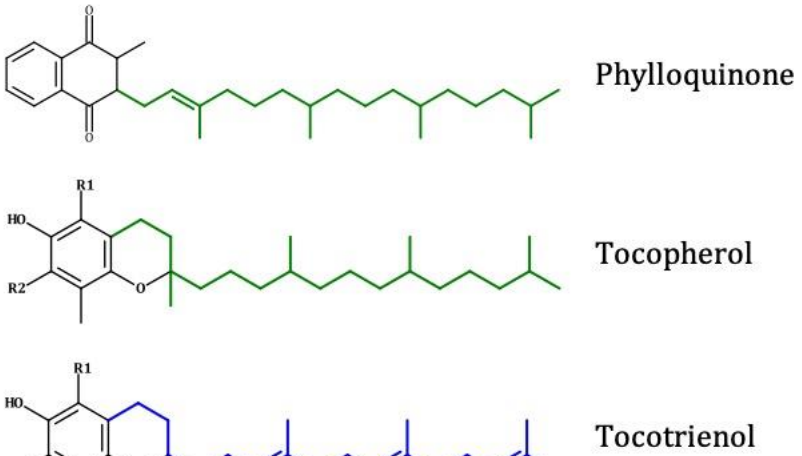

	α	β	γ	δ
R1	CH_3	CH_3	H	H
R2	CH_3	H	CH_3	H

Figure 3 Chemical structure of phylloquinone, tocopherol, and tocotrienol.

Tocopherols (vitamin E) and phylloquinone (vitamin K1) carry a phytyl-PP derived side chain (green), while tocotrienols have a geranylgeranyl-PP derived side chain (blue). Phylloquinone consists of a naphthoquinone head attached to a phytyl-PP derived side chain. Tocopherols and tocotrienols have a chromanol head group and differ from each other by the origin of their isoprenoid side chain. Depending on different methylation of the prenylquinone head group, α,β,γ and δ form of tocopherols and tocotrienols can be distinguished.

The biosynthesis of tocochromanols is located in chloroplasts and starts with the synthesis of homogentisic acid (homogentisate, HGA). HGA is derived from chorismate, an important intermediate of the shikimate pathway. In the rate-limiting step of tocopherol biosynthesis, HGA is condensed with phytyl-PP to form 2-methyl-6-phytyl-benzoquinone (MPBQ) catalyzed by the homogentisic acid phytyltransferase (HPT/VTE2) (Collakova and DellaPenna, 2001) (Figure 4). Phytyl-PP can either come from isoprenoid *de novo* synthesis by reduction of geranylgeranyl-PP catalyzed by geranylgeranyl reductase (GGR) (Keller *et al.*, 1998), or from phosphorylation of free phytol. In Arabidopsis, phytyl-PP for the biosynthesis of tocopherols is exclusively derived from phytol phosphorylation catalyzed by phytol kinase (VTE5) and the phytyl-phosphate kinase (VTE6) (Valentin *et al.*, 2006; vom Dorp *et al.*, 2015). MPBQ can be further methylated to DMPBQ by VTE3. A ring closure of either MPBQ or DMPBQ, catalyzed by the tocopherol cyclase VTE1 (Porfirova *et al.*, 2002; Sattler *et al.*, 2003), leads to the formation of the δ- and γ-forms of tocopherol, respectively. A further methyltransferase reaction catalyzed by VTE4 leads to the formation of the α- and β- forms of tocopherol from the δ- and γ-form, respectively (Shintani and DellaPenna, 1998; Bergmüller *et al.*, 2003). Therefore, depending on the degree of methylation on the chromanol head group, the four forms, α, β, δ, and γ are defined (Figure 3). Depending on the isoprenoid side chain attached to HGA in the initial biosynthesis step, tocopherols are distinguished from tocotrienols, tocomonoenols, and plastochromanol-8. While tocopherols carry a C20 phytyl side-chain derived from the attachment of phytyl-PP, tocotrienols carry a geranylgeranyl-derived side chain with three double bonds (Figure 3). In the case of tocomenoenols the side chain is derived from the C20 tetrahydrogeranylgeraniol, which has two double bonds. In contrast to the C20 derived tocopherols and tocotrienols, plastochromanol-8 carries a much longer side chain derived from solanesyl-PP with 45 C-atoms. The tocochromanol content and composition of different forms differ among plant species. Arabidopsis only contains tocopherols and plastochromanol-8, while tocotrienols are, for example, highly abundant in seeds of monocots. Further, the abundance of specific tocochromanol forms ($\alpha, \beta, \gamma, \delta$) also differs in plant organs. For example, in Arabidopsis leaves, the main tocopherol form is α-tocopherol, while seeds mainly contain γ-tocopherol.

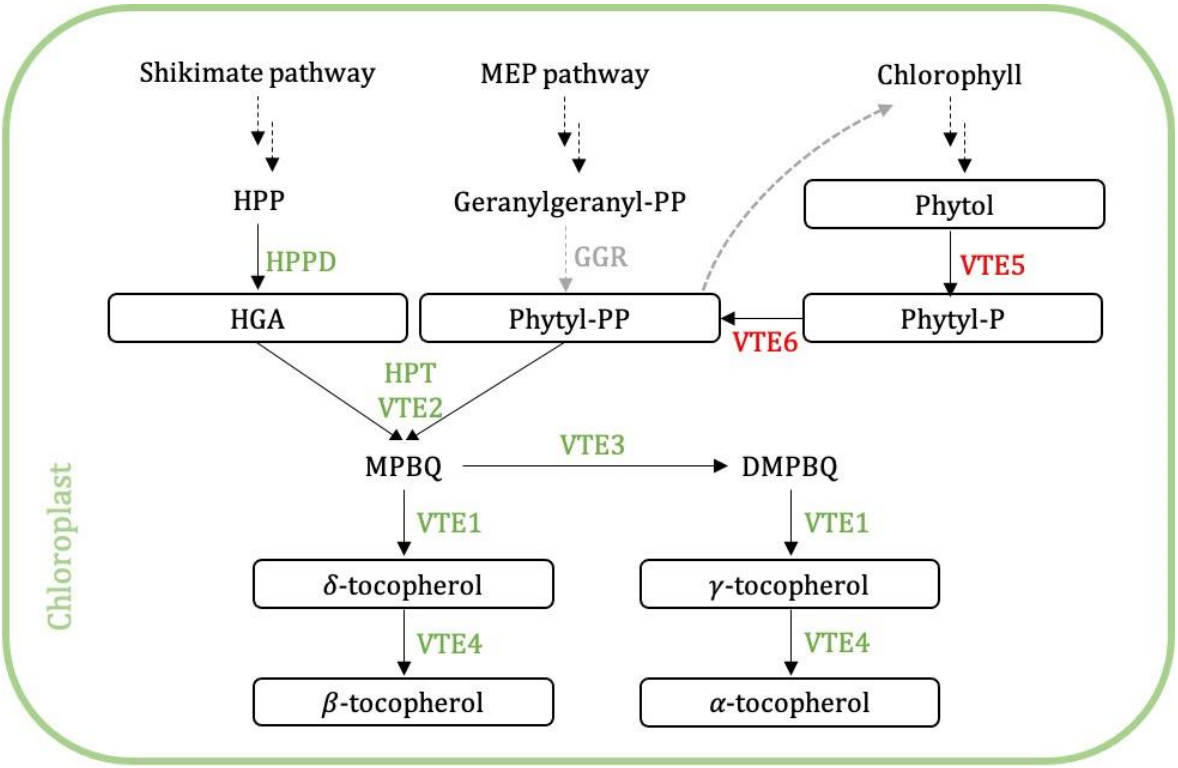

Figure 4 Schematic overview of tocopherol biosynthesis in Arabidopsis.

The initial and rate-limiting step of tocopherol biosynthesis is the condensation of homogentisate (HGA) with phytyl-PP. Phytyl-PP can either be produced from reduction of geranylgeranyl-PP catalyzed by geranylgeranyl reductase (GGR) or in the phytol phosphorylation pathway (red enzymes) from phosphorylation of phytol catalyzed by phytol kinase (VTE5) and phytyl-P kinase (VTE6). Condensation of HGA and phytyl-PP is performed by the homogentisate phytyl transferase (HPT, VTE2). The product 2-methyl-6-phytyl-benzoquinol (MPBQ) can either be directly converted to δ-tocopherol by tocopherol cyclase (VTE1) or first methylated by VTE3 to form 2,3-dimethyl-5-phytyl-benzoquinol (DMPBQ) and then converted by VTE1 to form γ-tocopherol. δ-Tocopherol and γ-tocopherol are finally converted to β- and α-tocopherol, respectively, by the methyltransferase VTE4.

1.2.2.2 Phylloquinone (vitamin K1)

Phylloquinone, also is known as vitamin K1, consists of a methylated naphthoquinone ring structure to which a phytyl-PP derived side chain is attached (Figure 3). It is an important electron carrier in photosystem I in plants, algae, and cyanobacteria (Lohmann *et al.*, 2006; Basset *et al.*, 2017). Additionally, phylloquinone can act as an electron acceptor and is essential in the human diet. In humans, phylloquinone can be converted to menaquinone-4 (vitamin K2) which acts as a co-factor during posttranslational protein modifications including γ-carboxylation of glutamate residues of proteins involved in blood coagulation (Reumann, 2013). Biosynthesis of phylloquinone starts from chorismate and is localized in chloroplasts with some reactions taking place in peroxisomes (Gutbrod *et al.* 2019). Chorismate is a cyclic intermediate in the shikimate pathway and precursor to all aromatic amino acids. Chorismate is converted in several steps into 1,4-dihydroxy-2-naphthoate

(DHNA), the unmethylated form of the naphthoquinone head group of phylloquinone. The phytyl side chain derived from phytyl-PP is attached to the ring in the next step by the DHNA phytyltransferase (MenA) to form the unmethylated phylloquinone precursor 2-phytyl-1,4-naphtoquinone. Next, the naphthoquinone ring is methylated by 2-phytyl-1,4-naphthoquinone methyltransferase (MenG). Arabidopsis mutants lacking MenG activity are phylloquinone deficient (Lohmann *et al.*, 2006). Also phylloquinone deficient are Arabidopsis mutants lacking phytyl-P kinase (VTE6) activity (Wang *et al.*, 2017).

The biosynthesis of phylloquinone, as well as tocopherol in *Arabidopsis* is well studied and is presented in several review articles including Mène-Saffrané (2018) and Gutbrod *et al.* (2019). Arabidopsis phytyl-P kinase mutants (*vte6*) are deficient in tocopherol and phylloquinone (vom Dorp *et al.*, 2015; Wang *et al.*, 2017). Therefore, the origin for the phytyl-PP side chain of tocopherol and phylloquinone is derived from phosphorylation of phytol via phytyl-P to phytyl-PP. The two studies corroborated the hypothesis that phytol phosphorylation is the preferred pathway over *de novo* synthesis of phytyl-PP from geranylgeranyl-PP for the biosynthesis of tocopherol and phylloquinone. This shows, that the salvage pathway of isoprenoid alcohol phosphorylation can play an important role for the biosynthesis of metabolites. Free phytol is released from chlorophyll upon degradation and turnover. The released phytol side chain can be remobilized in a phosphorylation salvage pathway for the biosynthesis of tocopherol and phylloquinone (vom Dorp *et al.*, 2015; Wang *et al.*, 2017).

1.3 Salvage pathway of phytol from chlorophyll degradation

Chlorophyll is the most abundant photosynthetic pigment found in nature. Its structure consists of a porphyrin head group that carries a magnesium cation bound in a chelate form in its center (Fleming, 1967). The isoprenoid derived C20 phytol side-chain is esterified to the porphyrin head. As chlorophyll occurs in nature in very high amounts, the phytyl side chain is also highly abundant. The phytyl side-chain is able to anchor the chlorophyll molecule to proteins of photosystem I and II or the light-harvesting complex located in the thylakoid membrane. Chlorophyll molecules are organized in light-harvesting complexes and they are key molecules in photosystem I and II. Plants contain two different forms of chlorophyll, chlorophyll a and b. While

chlorophyll a carries a methyl group at position 3 of the porphyrin ring, in chlorophyll b, this group is exchanged with a formyl group (von Wettstein *et al.*, 1995). The porphyrin carries a central Mg^{2+} cation. This structure enables light absorption, which is coupled to energy production during photosynthesis. Chlorophyll can be degraded during senescence and is constantly undergoing turnover (Figure 5). The degradation of chlorophyll is visible in the nature during seasonal changes in the form of spectacular changes of color from green to yellow and red leaves. Next to this, chlorophyll is also degraded during stress conditions like nutrient starvation or dryness. Additionally, chlorophyll constantly undergoes turnover in the cell throughout the plant life cycle. Chlorophyll degradation during senescence or stress, and chlorophyll turnover occurs in two different pathways, both starting from chlorophyll a (Figure 5). Chlorophyll degradation as part of the senescence pathway starts with the removal of the central magnesium cation by a magnesium dechetalase (STAY-GREEN, SGR), which leads to the formation of pheophytin a. In the genome of Arabidopsis, three different *SGR* (*SGR1*, *SGR2*, and *SGRL*) genes can be found. Magnesium was shown to be removed from chlorophyll a in *in vitro* assays after incubation with recombinant SGR1 or SGR2 protein (Shimoda *et al.*, 2016). In contrast, the preferred substrate for SGRL is chlorophyllide a, which is formed during chlorophyll turnover. Chlorophyllide a is formed from chlorophyll after dephytylation catalyzed by chlorophyll dephytylase (CLD1).

Chlorophyll degradation, after removal of the central magnesium cation and formation of pheophytin a, continues with the removal of the phytyl side-chain catalyzed by pheophytinase (PPH). The dephytylated form of pheophytin a is pheophorbide a. Further breakdown of pheophorbide a includes the cleavage of the chlorophyll ring structure. This key step in chlorophyll breakdown is catalyzed by pheophorbide a oxygenase (PAO), the name-giving compound of the PAO pathway (Pružinská *et al.*, 2005; Hörtensteiner, 2013). Ring-opening leads to the formation of red chlorophyll catabolites (RCC), which are precursors of all further breakdown products.

Phytol is a side product of chlorophyll degradation and turnover. Due to its chemical properties, free phytol has detergent-like properties, which can be harmful to membranes and proteins. Therefore, it is toxic for plants in high amounts. While in animals, a degradation pathway for phytol is described, the existence of the corresponding pathway in plants is still unclear. Phytol degradation starts with the production of phytenal by an alcohol dehydrogenase (ALD), and is followed in animals

by α- and β-oxidation. Besides degradation, phytol can be further metabolized by esterification or phosphorylation. Previous studies showed that radiolabeled phytol is incorporated in tocopherols (vitamin E), fatty acid phytyl esters and chlorophyll, in addition to being degraded (Ischebeck *et al.*, 2006).

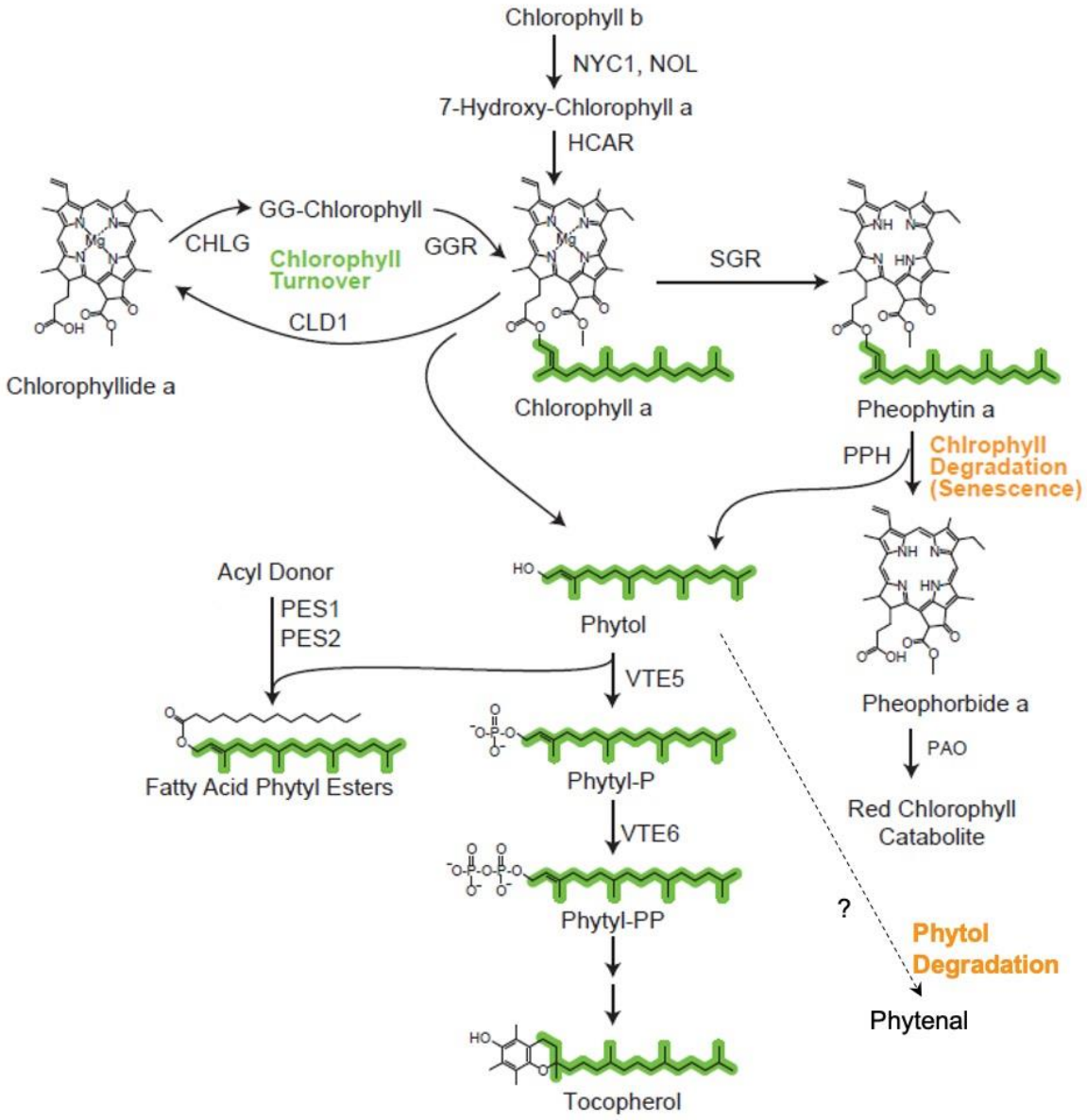

Figure 5 Chlorophyll turnover, degradation, and phytol metabolism in Arabidopsis.

During chlorophyll turnover, chlorophyll is hydrolyzed to chlorophyllide a by CLD1. Chlorophyll can also enter the PAO pathway for chlorophyll degradation. Chlorophyll degradation starts with the removal of the central Mg^{2+} ion by SGR and leads to the production of pheophytin a. Pheophytin a is hydrolyzed by PPH to produce pheophorbide a and phytol. Free phytol can either be esterified by PES1 and PES2 to fatty acid phytyl esters, or phytol can be phosphorylated to phytyl-P by VTE5 and further to phytyl-PP by VTE6. Phytyl-PP from phytol phosphorylation can enter the biosynthesis pathway of tocopherol. In mammals, phytol degradation to phytenal is described, but the existence of this pathway remains unclear in Arabidopsis. Figure modified from Gutbrod *et al.*, 2019.

1.3.1 Phytol metabolism in Arabidopsis

Free phytol can be esterified to fatty acid phytyl esters or phosphorylated (Ischebeck *et al.*, 2006). After Ischebeck *et al.* showed in 2006 that free phytol can be metabolized by esterification to form fatty acid phytyl esters (FAPEs), two enzymes were characterized in Arabidopsis in 2012 which are able to catalyze the respective esterification reaction; PHYTYL ESTER SYNTHASE 1 and 2 (PES1 and PES2) (Lippold *et al.*, 2012). PES1 and PES2 are members of the so-called ELT (esterase/lipase/thioesterase) family, which encompasses next to PES1 and PES2, four more members with putative acyltransferase activity (Lippold *et al.*, 2012; Wehler, 2017). Homologs of PES1 and PES2 are also present in other plant species, including tomato (PALE YELLOW PETALS (PYP)).

Next to the esterification, phytol can be phosphorylated in a phytol phosphorylation pathway (Ischebeck *et al.*, 2006; Valentin *et al.*, 2006; vom Dorp *et al.*, 2015; vom Dorp, 2015; Wang *et al.*, 2017). For the incorporation of free phytol into tocopherols (vitamin E), phylloquinone (vitamin K1), and chlorophyll, phytol needs to be activated by phosphorylation. In Arabidopsis, two kinases were identified as key enzymes in this process. Phytol kinase (VTE5) catalyzes the first phosphorylation step followed by a second phosphorylation catalyzed by phytyl-phosphate kinase (VTE6) (Valentin *et al.*, 2006; vom Dorp *et al.*, 2015) (Figure 5 and Figure 6).

1.4 Arabidopsis phytol kinase (VTE5), phytyl-phosphate kinase (VTE6), and farnesol kinase (FOLK)

Phosphorylation of free phytol takes place in Arabidopsis in two subsequent steps. The first step, where free phytol is converted to phytyl-P, is catalyzed by phytol kinase (VTE5) (Valentin *et al.*, 2006). Characterization of Arabidopsis mutant plants carrying a premature stop codon in At5g04490 (*vte5-1*) showed an overall tocopherol reduction in seeds down to 20% of wild type levels, while in leaves, the tocopherol content was reduced by around 50% (Valentin *et al.*, 2006). Due to its impact on tocopherol levels, the At5g04490 gene was named *VTE5 (VITAMIN E PATHWAY GENE 5)*. Enzyme assays showed that VTE5 has phytol kinase activity because it catalyzes the phosphorylation of free phytol. The *vte5-1* mutant plants carry a null mutation of *VTE5*, but the plants still contain residual amounts of tocopherol. Therefore, the biosynthesis pathway of tocopherol was believed to use phytyl-PP derived from reduction of

geranylgeranyl-PP from isoprenoid *de novo* synthesis in addition to phytyl-P from phytol phosphorylation. This alternative route would include the activity of geranylgeranyl reductase (GGR/CHLR) which can reduce geranylgeranyl-PP to phytyl-PP as described for several plant species, including Arabidopsis (Keller *et al.*, 1998; Tanaka *et al.*, 1999; Wang *et al.*, 2014). Plants with a defect in GGR are strongly impaired in chlorophyll and tocopherol biosynthesis. Nevertheless, the identification of a second gene involved in phytol phosphorylation in Arabidopsis, *VTE6*, demonstrated that the contribution of the alternative pathway to tocopherol synthesis is negligible because the *vte6* mutant is completely devoid of tocopherol. VTE6 encodes phytyl-P kinase (vom Dorp *et al.*, 2015) (Figure 6). The respective Arabidopsis *vte6* null mutant completely lacks tocopherol and phylloquinone (vom Dorp *et al.*, 2015; Wang *et al.*, 2017). These findings showed the essential role of phytol phosphorylation for the biosynthesis of tocopherol and phylloquinone and underlined that phytol phosphorylation is the preferred pathway for the production of phytyl-PP for the biosynthesis of tocopherol and phylloquinone.

In addition to tocopherol and phylloquinone deficiency, Arabidopsis *vte6* mutant lines show a very strong growth retardation. Arabidopsis *vte6* mutant plants are dwarf and do not develop mature leaves nor siliques or seeds. It is interesting to mention that growth of other tocopherol deficient Arabidopsis mutant lines is unaffected (*vte1* and *vte2*) (Collakova and DellaPenna, 2001; Sattler *et al.*, 2004; Kanwischer *et al.*, 2005). The growth retardation of *vte6* mutant plants remains an open question that needs to be answered.

Tocopherol analysis of *vte5* and *vte6* null mutant lines showed that phytol phosphorylation is essential for the production of phytyl-PP for the biosynthesis of tocopherol. While the Arabidopsis *vte6* mutant lines are completely tocopherol deficient, the *vte5* mutant lines still contain reduced amounts of tocopherol, raising the question whether another gene with phytol kinase similar to that of *VTE5* might exist in Arabidopsis. Protein BLAST searches by Valentin *et al*. revealed that only one gene with high sequence similarity to *VTE5* exists, which is At5g58560. The protein encoded by the At5g58560 gene is able to phosphorylate geraniol, farnesol, and, to a lesser extent, also geranylgeraniol (Fitzpatrick *et al.*, 2011). As the preferred substrate was farnesol, the enzyme was named farnesol kinase (FOLK) (Figure 6). Interestingly the putative phytol kinase activity of the FOLK protein was never investigated.

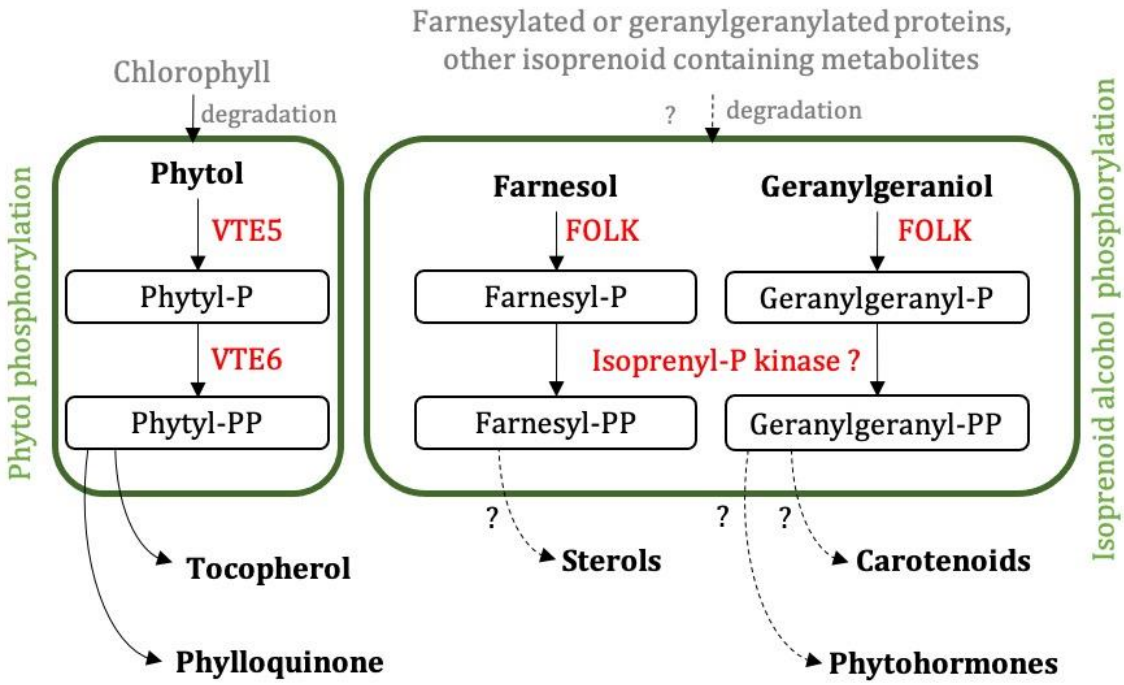

Figure 6 Phytol, geranylgeraniol, and farnesol phosphorylation in Arabidopsis catalyzed by VTE5 and FOLK.

The Arabidopsis phytol kinase (VTE5) is able to phosphorylate phytol, which is released from chlorophyll upon degradation. A second phosphorylation step catalyzed by the phytyl-P kinase (VTE6) leads to the production of phytyl-PP, which can enter the biosynthesis of tocopherol and phylloquinone. The farnesol kinase (FOLK) is able to phosphorylate free farnesol, geranylgeraniol, and to a lesser extent geraniol. It is unclear whether farnesyl-P and geranylgeranyl-P are converted to the respective diphosphates which might be precursors for the synthesis of other compounds such as sterols, carotenoids, or phytohormones.

1.5 Objectives

Phytol phosphorylation is essential during the mobilization of phytol for the biosynthesis of tocopherols and phylloquinone. Nevertheless, little is known about the role of the phosphorylation salvage pathway of other isoprenoid alcohols, including farnesol and geranylgeraniol. The aim of this study is to investigate the role of the salvage pathway of phytol, geranylgeraniol, and farnesol phosphorylation during the biosynthesis of the two vitamins tocopherol (vitamin E) and phylloquinone (vitamin K1), photosynthetic pigments including chlorophyll and carotenoids, phytohormones including abscisic acid (ABA) and gibberellic acid (GA), and sterols, in Arabidopsis. All compounds are synthesized from farnesyl-PP, geranylgeranyl-PP, or phytyl-PP. In Arabidopsis, farnesyl-P and geranylgeranyl-P can be produced by the farnesol kinase FOLK, and phytyl-P can be formed by the phytol kinase VTE5, using the respective

isoprenoid alcohols farnesol, geranylgeraniol, or phytol as substrates. The phytyl-P kinase VTE6 converts phytyl-P into phytyl-PP.

In this work, the Arabidopsis double mutant *vte5-2 folk-2* lacking the two isoprenoid alcohol kinases VTE5 and FOLK has been generated. The double mutant and the respective single mutant plants are used to investigate the role of isoprenoid alcohol phosphorylation for the activation of phytol, farnesol, or geranylgeraniol. The contents of chlorophyll, tocopherol, phylloquinone, sterols, carotenoids, and ABA are measured to evaluate the importance of isoprenoid alcohol kinase activity of FOLK and VTE5 for the biosynthesis of these compounds. Additionally, the subcellular localization of Arabidopsis VTE5 and FOLK, as well as their substrate specificities, are analyzed in detail. For localization studies, VTE5 and FOLK fusion constructs with GFP are transiently expressed in *N. benthamiana* leaves after infiltration with recombinant *A. tumefaciens* cells. *VTE5* and *FOLK* are cloned in *E. coli* for heterologous expression and enzyme assays. The Arabidopsis *vte6* mutant affected in phytyl-P kinase activity shows strong growth retardation. The reason for the dwarf growth of *vte6-1* is investigated in this work by growing the mutant on medium containing the growth hormone gibberellic acid (GA) to test whether GA can in part compensate for the growth restriction. Furthermore, the *vte6-1* mutant is crossed with the *pao1* mutant deficient in chlorophyll degradation to test whether the block in phytol released from chlorophyll degradation can alleviate the strong growth defect of *vte6*.

2 Materials and Methods

2.1 Equipment

Autoclave		Systec (Linden, D)
Balance	PG503-S	Mettler Toledo (Gießen, D)
Balance	XS205	Mettler Toledo (Gießen, D)
Binocular microscope	SZX16	Olympus (Hamburg, D)
Centrifuge	5417R	Eppendorf (Hamburg, D)
Centrifuge	5810R	Eppendorf (Hamburg, D)
Confocal Microscope	LSM 780	Zeiss (Oberkochen, D)
Cool trap	RV4104 refrigerated vapor trap, ThermoSavant	ThermoScientific (Schwerte, D)
Chemiluminescence documentation system	ChemiDoc	Bio-Rad (München, D)
Chlorophyll fluorimeter	Junior Pulse-amplitude modulator (Junior PAM)	WALZ (Effeltrich, D)
Electrophoresis chamber	Horizontal	Cti (Idstein, D)
Electrophoresis chamber	Vertical, mighty small II for 8x7 cm gels	Amersham Biosciences (Piscataway, USA)
Electrophoresis power supply	PowerBac Basic	Bio-Rad (München, D)
Electroporation device	Micro pulser	Bio-Rad (München, D)
Gas Chromatograph (GC) with Mass Spectrometer (MS)	7890A GC system with Agilent 5975C inert XL MSD with triple-axis detector	Agilent (Böblingen, D)
Heating block	SBH130D/3	Bibby Scientific (Staffordshire, USA)
High Performance Liquid Chromatograph (HPLC) with Diode Array Detector (DAD)	1100 Series, DAD 1200 series	Agilent (Böblingen, D)
High Performance Liquid Chromatograph (HPLC) with Fluorescent Light Detector (FLD)	1200 Series	Agilent (Böblingen, D)
Homogenizer	Precellys®24	PeQlab (Erlangen, D)
Incubation shaker	Multitron 28570	INFORS (Bottmingen, CH)
Incubator for plant cultivation on plates		Percival (Iowa, USA)

Liquid Chromatography-Mass Spectrometer (LC-MS) with Q-Trap	LC 1260 Infinity, QTrap 6500+	LC System: Agilent (Böblingen, D), Q-Trap: AB Sciex (Darmstadt, D)
Liquid Chromatography-Mass Spectrometer (LC-MS) with Q-TOF	LC 1200 Series, Agilent QTOF 6530 Accurate-Mass Quadrupole Time-of-Flight (Q-TOF) LC/MS	Agilent (Böblingen, D)
Magnetic stirrer	MR30001	Heidolph Instruments (Schwabach, D)
pH Meter	pH-Level 1	InoLab WTW (Weilheim, D)
Phytochamber	SIMATIC OP17	York International (York, USA)
Spectrophotometer	Nanodrop 1000	PeQlab (Erlangen, D)
Spectrophotometer	Specord 205	Analytik Jena (Jena, D)
SpeedVac	SPD121P Savant Speed Vac	ThermoScientific (Schwerte, D)
Sterile bench	Holten LaminAir Model 1.8	ThermoScientific (Schwerte, D)
Thermocycler	TProfessional 96	Biometra (Göttingen, D)
Ultracentrifuge	Sorvall RC5B Plus	ThermoScientific (Schwerte, D)
Vortex	Genie2	Scientific Industries (New York, USA)
Western blot device	Trans-Blot SD semi-dry transfer cell	Bio-Rad (München, D)

2.2 Materials

2.2.1 Consumables

Glass vials with thread	8 mL	VWR (Darmstadt, D)
Glass vials with thread	40 mL	Schmidlin (Neuheim, CH)
PTFE screw caps	for 8 mL glass vials	Schott (Mainz, D)
Plastic screw caps	for 40 mL glass vials	Schmidlin (Neuheim, CH)
Teflon septa for screw caps	13.3 and 22.4 mm	Schmidlin (Neuheim, CH)
Glass vials without thread	8 mL	VWR (Darmstadt, D)
Pasteur (glass) pipettes	150 and 225 mm	Brand (Wertheim, D)
Sample vials (GC and LC)	Vials with inserts and screw caps with teflon-septa	Macherey and Nagel (Düren, D) or Agilent (Böblingen, D)
Soil for plant cultivation	Classic Profi Substrat	Einheitserde (Sinntal, D)
SPE columns	Strata Si-1 silica, 55 µm, 70 Å, 100 mg/1 mL	Macherey and Nagel (Düren, D)
Parafilm M	4 IN. X 125 FT. roll	Sigma-Aldrich (Taufkirchen, D)

Petri dishes	94×16 and 145×20 mm	Greiner Bio-One (Frickenhausen, D)
Plastic tips for micropipettes		Labomedic (Bonn, D)
Pots for plant cultivation		Pöppelmann (Lohne, D)
Reaction tubes	1.5 mL and 2 mL	Sarstedt (Nümbrecht, D)
Reaction tubes for PCR	8 × 0.2 mL, stripes	BRAND (Wertheim, D)
Vermiculite		Klemens Rolfs (Siegburg, D)

2.2.2 Chemicals

Acetic acid	AppliChem (Darmstadt, D)
Acetone	Fisher Scientific (Schwerte, D)
Acetonitrile	VWR (Darmstadt, D)
Acetosyringone	Sigma-Aldrich (Taufkirchen, D)
Agarose	PeQlab (Erlangen, D)
Ammonium acetate (NH_4OAc)	Carl Roth (Karlsruhe, D)
Ammonium hydroxide solution (NH_4OH, 32%)	AppliChem (Darmstadt, D)
Bacto-Agar	Formedium (Norfolk, UK)
BCA (Bicinchoninic acid solution)	Sigma-Aldrich (Taufkirchen, D)
Bovine serum albumin (BSA)	Sigma-Aldrich (Taufkirchen, D)
CHAPS (3-[(3-Cholamidopropyl) dimethylammonio]-1-propanesulfonate)	AppliChem (Darmstadt, D)
Chloroform	VWR (Darmstadt, D)
CTAB (Cetyltrimethylammonium bromide)	Roth (Karlsruhe, D)
$CuSO_4$ (Copper(II)sulfate anhydrous)	Merck (Darmstadt, D)
Dichloromethane	AppliChem (Darmstadt, D)
Diethylether	Fisher Scientific (Schwerte, D)
Ethanol	VWR (Darmstadt, D)
Ethidium bromide	Roth (Karlsruhe, D)
Formic acid	AppliChem (Darmstadt, D)
Glucose	Duchefa (Haarlem, NL)
HEPES (2-(4-(2-Hydroxyethyl)-1-piperazineethansulfonic acid)	Formedium (Hunstanton, UK)
Isopropanol	AppliChem (Darmstadt, D)
KH_2PO_4	Merck (Darmstadt, D)
K_2HPO_4	Merck (Darmstadt, D)
LB broth	Formedium (Norfolk, UK)
Lysozyme	AppliChem (Darmstadt, D)
Methanol	VWR (Darmstadt, D)
Methoxylamine hydrochloride	Sigma-Aldrich (Taufkirchen, D)
MS salts including vitamins	Duchefa (Haarlem, NL)
MSTFA (N-Methyl-N-(trimethylsilyl) trifluoroacetamide	Roth (Karlsruhe, D)
n-Hexane	Merck (Darmstadt, D)
Phytoagar	Duchefa (Haarlem, NL)
Proplant (fungicide)	Arysta LifeScience (Düsseldorf, D)
Pyridine	Sigma-Aldrich (Taufkirchen, D)

Sodium orthovanadate	Sigma-Aldrich (Taufkirchen, D)
Sorbitol	AppliChem (Darmstadt, D)
Substral Celaflor Careo Schädlingsfrei	Bayer
Sucrose	Duchefa (Haarlem, NL)
Tertiary butylmethylether (TBME)	Roth (Karlsruhe, D)
Trichloroacetonitrile	Sigma-Aldrich (Taufkirchen, D)
Triethylamine	Sigma-Aldrich (Taufkirchen, D)
Tris (tris(hydroxymethyl)aminomethane) base	Duchefa (Haarlem, NL)
Triton-X-100	Sigma-Aldrich (Taufkirchen, D)
Yeast extract	Duchefa (Haarlem, NL)

2.2.3 Antibiotics

All antibiotics were obtained from Duchefa (Haarlem, The Netherlands). Stock solutions for ampicillin (Amp), carbenicillin (Carb), gentamicin (Gent), kanamycin (Kan), spectinomycin (Spec), and streptomycin (Strep) were prepared in water. The stock solution of rifampicin (Rif) was prepared in dimethylsulfoxide (DMSO). Stock solutions were stored at -20°C.

2.2.4 Kits and Enzymes

CloneJET PCR Cloning Kit	Thermo Fisher Scientific (Karlsruhe, D)
DCS DNA Polymerase	DNA Cloning Service (Hamburg, D)
Lysozyme	Sigma-Aldrich (Darmstadt, D)
NucleoSpin® Gel and PCR Clean-up	Macherey-Nagel (Düren, D)
NucleoSpin® Plasmid	Macherey-Nagel (Düren, D)
Restriction enzymes	New England Biolabs (Frankfurt, D)
T_4 DNA Ligase	New England Biolabs (Frankfurt, D)
Q5® high fidelity DNA polymerase	New England Biolabs (Frankfurt, D)

2.2.5 Bacteria strains

Table 1 Bacteria strains

Bacteria strain	Purpose	IMBIO stock
A. tumefaciens GV3101	Transient transformation of *N. benthamiana* or stable transformation of *A. thaliana*	bn76
E. coli Electroshox	High yield plasmid amplification	bn1218
E. coli Rosetta (DE3)	Heterologous expression, a strain containing codons rarely used in *E. coli*	bn1100

2.2.6 Recombinant plasmids

Table 2 Recombinant plasmids

Vector	Insert	Purpose	IMBIO stock
pETDuet-1	empty	Dual expression vector for *E. coli*	bn1132
pETDuet FOLK/-	FOLK	Expression of FOLK	bn1133
pETDuet VTE5/-	VTE5	Expression of VTE5	bn 1423
pJet1.2/blunt		Blunt end vector for PCR product ligation	CloneJET PCR Cloning Kit
pJet1.2/blunt	VTE6-eGFP	Template for eGFP amplification	bn573
pLH9000	eGFP-WSD6	pLH9000 vector backbone after removal of eGFP-WSD6	bn1176
pLH9000	FOLK-eGFP	Expression after transient *N. benthamiana* leaf infiltration	bn1285
pLH9000	VTE5-eGFP	Expression after transient *N. benthamiana* leaf infiltration	bn1286
pM	P19	Helper plasmid, *N. benthamiana* leaf co-infiltration	bn856

Vector maps and cloning of pETDuet FOLK/- and pETDuet VTE5/- are described in 7.1.1. Vector maps and cloning of pLH9000 FOLK-eGFP and pLH9000 VTE5-eGFP are described in 7.1.2.

2.2.7 Synthetic oligonucleotides

Oligonucleotides were obtained from IDT Genomics (Leuven, BE). The oligonucleotide sequences used in this study are listed in Table 8 in the appendix.

2.2.8 Arabidopsis ecotypes and insertion lines

Table 3 Arabidopsis ecotypes and insertion lines

Genotype	Ecotype	Gene	Stock center code	Origin
Wild type Col-0	Col-0			IMBIO institute (Bonn, D)
Wild type Ds11	No-0		Ds1-388-5 (CS8511), donor line of pst12490	RIKEN (Ibaraki, JP)
Wild type Ds3	No-0		Ds3-390-1, donor line of pst15134	RIKEN (Ibaraki, JP)
folk-2	Col-0	At5g58560	SALK_123564	SIGnAL (La Jolla, USA)
pao1	Col-0	At3g44880	SALK_111333	Dr. Stefan Hörtensteiner, University of Zurich (Zürich, CH)
vte6-1	No-0	At1g78620	pst15134	RIKEN (Ibaraki, JP)
vte5-2	No-0	At5g04490	pst12490 (line 11-5074-1)	RIKEN (Ibaraki, JP)
vte5-2 folk-2	No-0 and Col-0	At5g04490 At5g58560	pst12490 crossed with SALK_123564	Jill Romer, generated by crossing during this work
vte5-2 vte6-1	No-0	At5g04490 At1g78620	pst12490 crossed with pst15134	Dr. Georg Hölzl, IMBIO institute (Bonn, D)
vte6-1 pao1	No-0 and Col-0	At1g78620 At3g44880	pst15134 crossed with SALK_111333	Jill Romer, generated by crossing during this work

2.3 Plant cultivation, methods, and plant crossing

2.3.1 Seed sterilization and sterile plant cultivation on Petri dishes (*A. thaliana*)

Arabidopsis seedlings were germinated under sterile conditions on synthetic MS medium containing 1% sucrose (Murashige and Skoog, 1962). For sterile cultivation, seeds were surface-sterilized either by a liquid sterilization protocol or by dry gas sterilization. For the sterilization using gas, ~20 mg seeds were filled in 1.5 mL reaction tubes and placed in a desiccator with half-opened reaction tube lids. Chloric gas was produced inside the desiccator by mixing commercially available chlorine

bleach cleaner with concentrated HCl (37%) in a 100:4 ratio. The desiccator lid was closed after adding the concentrated HCl into the bleach cleaner solution to prevent escaping of the developing chorine gas. The desiccator was kept under a fume hood during the whole sterilization process. Seeds were incubated in the gas for 2 h. Afterward, the reaction tube lids were carefully closed, and the seeds sown on MS medium containing 1% sucrose under a sterile bench. For liquid seed surface sterilization, ~20 mg seeds were filled in 1.5 mL reaction tubes, and 1 mL of sterilization solution containing sodium hypochlorite (10-12%), ddH_2O, and 10% triton-X-100 (10:10:0.2; v/v/v) was added. Seeds were incubated in this solution for 10 min while shaking. Then, the seeds were washed once with 1 mL 99% ethanol and three times with sterile ddH_2O. After washing, the seeds were sown by pipetting water droplets, containing the seeds, on MS medium containing 1% sucrose under a sterile bench.

After sowing the surface-sterilized seeds on MS containing plates, the plates were first kept for 24-72 h at 4 °C for stratification. Finally, the plates were transferred to a growth cabinet (Percival Scientific). In the growth cabinet, the plants were cultivated under long day conditions (16 h light, 8000-10000 Lux), 22 °C and 55% relative humidity. Seedlings were pricked out to fresh MS medium or soil after two weeks of growth.

MS medium	
0.4405% (w/v)	MS salts including vitamins
1% (w/v)	Sucrose
0.213% (w/v)	MES
pH 6.0	adjusted with KOH
0.8% (w/v)	Phytoagar

2.3.2 Plant cultivation on soil (*A. thaliana* and *N. benthamiana*)

For cultivation on soil, Arabidopsis seeds were sown and precultured under sterile conditions on synthetic MS medium containing 1% sucrose for two weeks (section 2.3.1), while *N. benthamiana* seeds were directly sown on soil.

Soil for plant cultivation was mixed in a 1:3 ratio with vermiculite and soaked with water containing 1 mL/L boric acid and 1.5 mL/L Proplant® to reduce pests and

algal growth. Additionally, for the reduction of pests in the soil, pots were watered from the top with a 1 mL/L nematode suspension. Plants on soil were cultivated in a phytochamber under long-day conditions (16 h light, 150 µE), 22 °C and 55% relative humidity. Pots were watered with tap water every two to three days. Plants infested with aphids were watered with 1 mL/L Substral Celaflor (Careo Schädlingsfrei).

For Arabidopsis seed amplification, plants were grown on soil, and the first inflorescence were cut to increase the number of developing inflorescences. Plants were grown for approximately five to six weeks until siliques were fully developed. Siliques were covered with paper bags when the siliques began to turn yellow. Then plants were watered for two more weeks. Afterward, watering was stopped, and plants kept on soil until the plants, siliques, and seeds were dry. Dry shoots were cut off together with the paper bags. Seeds were liberated inside the paper bag from the siliques by gently rubbing the paper bags with the hands. Liberated seeds were sieved three times with a 350 µm mesh sieve (Retsch) to remove remaining plant parts. Sieved seeds were filled in glass tubes and incubated with open lid for 24 h under vacuum in a desiccator containing silica beads, to achieve complete dryness of the seeds. Dry seeds were stored at 4 °C in the dark until usage.

2.3.3 Arabidopsis cultivation for nitrogen deprivation experiments

For analysis of the plant lipid composition after nitrogen deprivation, plants were cultivated under sterile conditions on Petri dishes containing synthetic medium. Seeds were sterilized, sown, and cultivated on MS medium containing 1% sucrose for the first two weeks, as described in section 2.3.1. After two weeks of growth, the seedlings were transferred to fresh Petri dishes containing synthetic medium lacking nitrogen (-N medium) or nitrogen containing (+N medium) as control. Plants were cultivated for further 10-14 days until the plants growing under -N conditions started to turned yellow. Complete rosettes were harvested, roots, and shoots were removed, and the fresh weight was determined. Leaf material was frozen in liquid nitrogen in 2 mL reaction tubes containing ceramic beads and used directly for lipid extractions or was stored at -80 °C.

+N medium		-N medium	
2.5 mM	KNO_3	2.5 mM	KCl
1 mM	$MgSO_4$ (anhydrous)	1 mM	$MgSO_4$ (anhydrous)
1 mM	$Ca(NO_3)_2$	1 mM	$CaCl_2$
1 mM	KH_2PO_4	1 mM	KH_2PO_4
1 mM	NH_4NO_3	25 mM	Fe-EDTA
25 mM	Fe-EDTA	0.05% (v/v)	Arabidopsis micronutrients
0.05% (v/v)	Arabidopsis micronutrients	1% (w/v)	Sucrose
1% (w/v)	Sucrose	0.8% (w/v)	Agarose
0.8% (w/v)	Agarose		

2.3.4 Arabidopsis cultivation for feeding experiments in liquid MES-KOH buffer

Arabidopsis plants were cultivated under sterile conditions on Petri dishes containing MS medium supplemented with 1% sucrose for three weeks as described in section 2.3.1. After three weeks, the seedlings were transferred to 250 mL Erlenmeyer flasks containing 40 mL of 20 mM MES-KOH (pH 6.5) buffer. Four seedlings per flask were carefully transferred with forceps so that the roots were submerged while the rosette leaves were floating on the buffer surface. Control plants were transferred to 20 mM MES-KOH buffer without any supplemented substrate. Plants for substrate feeding were either transferred to buffer containing 5 mM phytol, 5 mM farnesol, or 5 mM geranylgeraniol. Plants were incubated with gentle shaking in the respective buffer in a phytochamber under non-sterile conditions for 24 h under long-day conditions. Afterward, plants were harvested and washed with tap water to remove residual buffer and substrates from the plant surface. Roots and shoots were separated, and the fresh weight of the leaf material was determined. Afterward, the material was frozen in liquid nitrogen in 2 mL reaction tubes containing ceramic beads. Frozen leaf material was directly used for lipid extractions or stored at – 80 °C.

2.3.5 Arabidopsis cultivation for homogentisic acid (HGA) supplementation experiments

For lipid extractions from plants that were grown on HGA supplemented synthetic medium, Arabidopsis plants were first sown and cultivated under sterile conditions on Petri dishes containing MS medium supplemented with 1% sucrose for

two weeks as described in section 2.3.1. After two weeks, the seedlings were transferred to sterile Petri dishes containing MS medium supplemented with 1% sucrose together with 5 mM HGA. HGA was added as a sterile filtrated solution to the fresh autoclaved liquid MS medium after cooling down to around 40 °C, right before pouring the plates. HGA containing media changed the color from milky white to brown after several days of cultivation, due to polymer formation. Control plants were transferred to Petri dishes containing MS medium supplemented with 1% sucrose but without HGA. Plants were cultivated on HGA containing or HGA-free (control) MS medium under sterile conditions for nine more days. Afterward, leaf material was harvested, the fresh weight determined and the leaves frozen in liquid nitrogen in 2 mL reaction tubes containing ceramic beads. Samples were either directly extracted for tocopherol and tocotrienol analysis or stored until extraction at – 80 °C.

MS medium containing 5 mM HGA

0.4405% (w/v)	MS salts including vitamins
1% (w/v)	Sucrose
0.213% (w/v)	MES
pH 6.0	adjusted with KOH
0.8% (w/v)	Phytoagar
5 mM	HGA (added as sterile filtrated solution after autoclaving)

2.3.6 Arabidopsis cultivation for gibberellic acid (GA) supplementation

For analysis of the effect of exogenous supplementation with GA to Arabidopsis *vte6-1*, plants were first grown under sterile conditions on Petri dishes containing MS medium supplemented with 1% sucrose for two weeks as described in section 2.3.1. Afterward, plants were transferred to MS plates without sucrose and either supplemented with 0 µM GA, 10 µM GA, or 100 µM GA. GA (GA3, Olchemin) was added as a sterile filtrated aqueous solution to the fresh autoclaved liquid MS medium after cooling down to around 40 °C and right before pouring the plates. Plants were further cultivated under sterile conditions for eight days and the growth was documented daily.

MS medium containing GA

0.4405% (w/v)	MS salts including vitamins
0.213% (w/v)	MES
pH 6.0	adjusted with KOH
0.8% (w/v)	Phytoagar
0 µM, 10 µM or 100 µM	GA3 (added as sterile filtrated aqueous solution after autoclaving)

2.3.7 Crossing of Arabidopsis mutants for the generation of double homozygous *vte5-2 folk-2* and *vte6-1 pao1* mutant plants

For the generation of Arabidopsis *vte5-2 folk-2* mutant plants, heterozygous transposon insertion null mutant *vte5-2* plants (At5g04490, pst12490 (RIKEN)) (vom Dorp *et al.*, 2015) had previously been crossed with heterozygous T-DNA insertion null mutant *folk-2* plants (At5g58560, SALK_123564 (SIGnAL SALK)) (Fitzpatrick *et al.*, 2011) by Dr. Georg Hölzl (IMBIO Institute, University of Bonn). The seeds derived from this crossing were harvested and the F1 plants screened by genotyping PCR (2.5.4.1) for plants carrying an insertion in both loci; *vte5* and *folk*. Plants heterozygous for the two loci were identified in the F1 generation, and F2 seeds were harvested. Plants of the F2 generation were again screened for the presence of an insertion in both loci. No double homozygous F2 plants could be detected after the screening of around 200 plants. Therefore, seeds from F2 plants homozygous for one locus and heterozygous for the other locus were collected and again germinated. In the F3 generation, double homozygous *vte5-2 folk-2* plants were identified, which were used for further experiments.

For the generation of the Arabidopsis *vte6-1 pao1* mutant, heterozygous *vte6-1* plants (At1g78520, pst15134 (RIKEN)) (vom Dorp *et al.*, 2015) were crossed with homozygous *pao1* mutant (At3g44880, SALK_111333 (SIGnAL SALK) (Pružinská *et al.*, 2005) plants. The F1 seeds from this crossing were harvested and F1 plants screened by genotyping PCR (2.5.4.1) for plants carrying insertions in the two loci. Thus, F1 plants heterozygous for both loci were identified. Seeds of these F1 plants were germinated, and F2 plants homozygous for *pao1* and heterozygous for *vte6-1* were detected after the screening of around 300 plants. F3 seeds, homozygous for *pao1* and segregating for *vte6-1,* were collected and germinated. In the F3 generation, double homozygous *vte6-1 pao1* plants were identified.

2.3.8 Seed longevity assay after accelerated seed aging

Longevity of Arabidopsis seeds from mutants with a defect in tocopherol biosynthesis was analyzed by determination of the germination rate after accelerated aging of the seeds. Accelerated aging was performed according to Sattler *et al.*, 2004 for 72 h, at 40 °C and 100% relative humidity. Aging was performed with seeds inside a desiccator where water was filled in the bottom to produce 100% humidity. Seeds from three plants per line as replicates were filled in 2 mL reaction tubes each, and placed with opened lids inside the desiccator above the water level. The desiccator was placed with a closed lid inside an oven. Seeds were aged in an accelerated way for 72 h at 40 °C with 100% humidity. After aging, 100 seeds from each replica were placed on water-soaked filter paper. As a control, seeds without accelerated aging treatment were used. Germination of seeds was defined as time point when the root extended from the seeds and was documented with a binocular. The germination rate was recorded every day for ten days.

2.3.9 Transient transformation of *N. benthamiana* leaves and subcellular localization

For transient expression experiments for subcellular localization studies, *N. benthamiana* leaves were infiltrated with *A. tumefaciens* strains which carried recombinant pLH9000 35S-VTE5-eGFP or pLH9000 35S-FOLK-eGFP constructs (7.1.2). Agrobacteria were grown for 20 h at 28 °C in 10 mL LB medium containing antibiotics. After 20 h of growth, 10 µL acetosyringone (100 mM in dimethyl sulfoxide) were added for induction of virulence genes. Bacteria were centrifuged at low speed (4000 g) for 10 min and cells resuspended in 5 mL infiltration medium containing 5 mM $MgCl_2$, 5 mM MES (pH 5.7), and 100 µM acetosyringone. Cell density was adjusted to an OD_{600}=0.4 for infiltration. To avoid RNA silencing in the infiltrated plant cells, Agrobacteria harboring the pMP19 helper plasmid (bn856) (Voinnet *et al.*, 2000) in the same cell density were always co-infiltrated. Four- to six-week-old *N. benthamiana* plants were used for leaf infiltration. Plants were well watered before infiltration to promote stomata opening. The abaxial leaf side was infiltrated with the bacterial suspension using a 3 mL plastic syringe. Expression and localization were analyzed after three to four days by fluorescence analysis. Fluorescence was observed by excitation at 488 and 543 nm under a laser scanning microscope (LSM 780; Zeiss, Jena,

Germany) with a ×40 lens (C-Apochromat 40x/1.2W Korr). Emitted light was collected at 493–523 nm (GFP), 663–723 nm (chlorophyll).

2.4 Bacteria cultivation and transformation methods

2.4.1 Cultivation of *Escherichia coli* and *Agrobacterium tumefaciens*

Bacterial pre-cultures were grown overnight in liquid medium. *E. coli* was grown in liquid LB medium containing antibiotics, while liquid YEP medium containing antibiotics was used for *A. tumefaciens.* For each preculture, 4 mL medium were prepared in glass tubes with loose lids and inoculated with single-cell colonies from solid medium plates, or from glycerol stocks. *E. coli* pre-cultures were incubated at 37°C, *A. tumefaciens* cultures at 28 °C while rotating at 40 rpm. Larger culture volumes were inoculated from pre-cultures to an initial OD_{600} of 0.1 for further cultivation and growth.

For bacteria cultivation on solidified medium plates, cells were streaked out from liquid culture with a Drigalski spatula, or from cell glycerol stocks in a three-phase streaking pattern using a sterile loop.

LB liquid medium

2% (w/v)	LB broth
pH 7.2	adjusted with NaOH

LB solid medium

LB medium liquid + 0.8% (w/v) bactoagar

YEP liquid medium

1% (w/v)	Peptone
1% (w/v)	Yeast extract
0.5% (w/v)	NaCl
pH 6.8	adjusted with NaOH

YEP solid medium

YEP medium liquid + 1.5% (w/v) bactoagar

2.4.2 Generation of electrocompetent bacteria cells for transformation

Bacteria cells were inoculated from frozen glycerol stocks in 20 mL SOB medium as pre-cultures. Cells were grown overnight while shaking at 37 °C for *E. coli* or at 28 °C for Agrobacteria. The next day, 400 mL SOB medium were inoculated with the pre-cultures. When the cultures reached the desired OD_{600}, of 0.5, cells were cooled on ice and harvested by centrifugation in precooled centrifuge tubes at 4 °C for 10 min at 4000 g. The bacteria pellets were resuspended in 50 mL cooled 1 mM HEPES buffer and finally washed three times with first 250 mL, then 100 mL, and finally with only 50 mL ice-cold ddH_2O. After the final washing step, cells were centrifuged, the supernatant discarded, and the cells were carefully resuspended in sterile and cold 20% (v/v) glycerol. Cells in glycerol were divided in 50 µL aliquots which were transferred into 1.5 mL pre-cooled reaction tubes and subsequently frozen in liquid nitrogen. Cells were stored at -80 °C until further use for bacteria electroporation.

SOB medium

2% (w/v)	peptone
0.5% (w/v)	yeast extract
0.06% (w/v)	NaCl
0.018% (w/v)	KCl

After autoclaving add the following solutions:

20% (v/v)	1 M $MgSO_4$ (sterile filtrated)
20% (v/v)	1 M $MgCl_2$ (sterile filtrated)

2.4.3 Bacteria transformation by electroporation

For transformation by electroshock, one frozen 50 µL aliquot of electrocompetent bacteria was mixed with 1 µL recombinant plasmid isolated from bacteria or with 10 µL of freshly ligated and desalted insert and vector combinations. For transformation of Agrobacteria, the cells were incubated on ice for 5 min together with the plasmid. *E. coli* cells were mixed with the plasmid and directly transformed. Transformation was performed in electroporation cuvettes by application of 1250 V in a MicroPulser (BioRad). Directly after applying the electroshock, cells were resuspended in cold and sterile 500 µL SOB medium (*E. coli*) or YEP medium (*A. tumefaciens*) without antibiotics. For recovery, transformed *E. coli* and *A. tumefaciens*

were incubated at 37 °C for 40 min or 28 °C for 120 min, respectively. After recovery, 100 µL cells were plated out on solid LB medium (*E. coli*) or solid YEP medium (*A. tumefaciens*) containing antibiotics for selection. *E. coli* transformants were visible after one day of growth at 37 °C, and *A. tumefaciens* colonies were visible after two days of growth at 28 °C. Single colonies were tested by colony PCR as described in 2.5.4.3, restriction digests, or sequencing.

2.5 Methods in molecular biology and biochemistry

2.5.1 DNA isolation from leaf tissue

Plant genomic DNA was isolated from leaves using cetyltrimethylammonium bromide (CTAB). 800 µL of CTAB buffer was filled into 2 mL reaction tubes, ceramic beads and approximately 10 mg leaf material were added. Leaves were ground in the buffer two times for 20 s at 6300 rpm using a Precellys homogenizer. Samples were centrifuged for 30 s at 2000 rpm to reduce the amount of foam after grinding. Afterward, samples were incubated at 65 °C while shaking at 400 rpm on a heat block for a minimum of 20 min. Then 300 µL chloroform were added, samples were vortexed, and centrifuged for 3 min at 3000 rcf for phase separation. The upper organic phase containing the DNA was transferred to fresh 1.5 mL reaction tubes containing 600 µL ice-cold isopropanol. Samples were mixed by gentle inverting ten times and then incubated at -20 °C for at least 20 min to overnight for DNA precipitation. DNA was pelleted by centrifugation at 14000 rpm for 5 min. The derived pellet was washed once with 500 µL 75% ethanol and again centrifuged for 5 min at 14000 rpm. After complete removal of ethanol, the DNA pellets were suspended in 40 µL sterile water.

CTAB buffer

140 mM	Sorbitol
220 mM	Tris (pH 8.0)
22 mM	EDTA
800 mM	NaCl
1% (w/v)	Sarcosyl
0.8% (w/v)	CTAB

2.5.2 Plasmid DNA isolation from bacteria cells

Plasmid DNA was isolated from 4 mL bacteria culture using the plasmid isolation kit (Nucleospin Plasmid, Macherey & Nagel) following the supplier's protocol with one modification. In contrast to this protocol, in the final step, plasmid DNA was eluted from the column with sterile water heated to 50 °C, instead of the elution buffer from the kit to avoid high salt concentrations in the plasmid preparation, which can affect the efficiency of restriction digests.

2.5.3 Plasmid DNA digestion using restriction enzymes

Isolated plasmids were digested with restriction enzymes (NEB) according to the supplier's recommendations. Conditions for digestion and suitable buffers were selected using the NEBcloner® online tool (nebcloner.neb.com/#!/redigest). Control digests were performed in a total volume of 10 µL, large digests for further cloning (7.1) were performed in a total volume of 50 µL.

2.5.4 Polymerase chain reaction (PCR)

2.5.4.1 Genotyping PCR for the identification of Arabidopsis insertional mutant lines

Arabidopsis transposon and T-DNA insertion mutant lines were identified by PCR with genomic DNA using gene-specific primers together with primers specifically binding to the inserted DNA fragment. For genotyping by PCR, genomic DNA was extracted from leaf material as described in 2.5.1. For one PCR reaction mixture, 1 µL containing at least 200 ng genomic DNA was used. The mix of the PCR reactions is indicated below this section. Primer combinations for the different mutant lines are indicated in Table 4. PCR parameters were set to 2 min initial denaturation at 95 °C followed by 35-37 cycles of denaturation at 95 °C (30 s), annealing (melting temperature of the primer -5 °C, 30 s per 1000 bp product), and elongation at 72 °C for 1 min. A final elongation step was performed at the end of the last cycle at 72 °C for 10 min before the PCR reaction was cooled down to 12 °C and completely stopped by the addition of agarose gel loading dye containing EDTA to stop enzymatic reactions.

Table 4 Oligonucleotides for genotyping PCR of Arabidopsis insertional mutant lines

Mutant Allele	3' primer	5' primer	Insertional primer	Product size [bp]
FOLK	bn2853	bn2854		1069
folk-2		bn2854	bn78	488-788
VTE5	bn771	bn772		1352
vte5-2	bn771		bn232	1080
VTE6	bn233	bn234		1255
vte6-1		bn234	bn232	970
PAO	bn3005	bn3004		927
pao1		bn3004	bn78	480-500

PCR reaction mix for genotyping

0.2 µL	DCS polymerase
0.3 µL	dNTPs (10 mM total)
1.5 µL	10 × buffer B (0.8 M Tris-HCl, 0.2 M $(NH_4)_2SO_4$)
1.5 µL	$MgCl_2$ (25 mM)
1.5 µL	5' primer or insertional primer (10 µM each)
1.5 µL	3' primer or insertional primer (10 µM each)
1 µL	Template DNA (approximately 200 ng)
ad 15 µL	ddH_2O

2.5.4.2 DNA amplification by PCR for cloning

Arabidopsis gene sequences to be cloned into bacteria strains for expression or localization studies were amplified with gene-specific oligonucleotide primers modified with desired restriction enzyme flanking sites. Sequences were amplified from cDNA obtained by reverse-transcription of Arabidopsis WT leaf RNA. Q5 polymerase was used for PCR according to the supplier's protocol and added during the initial denaturation step at 95 °C (hot start). PCR parameters were set to 30 s initial denaturation at 95 °C followed by 35 cycles of denaturation at 95 °C (10 s), annealing (melting temperature of the primer -5 °C, 30 s per 1000 bp product), and elongation at 72 °C for 80 sec. A final elongation step was performed at the end of the last cycle at 72 °C for 2 min before the PCR reaction was cooled down to 12 °C and completely

stopped by the addition of agarose gel loading dye containing EDTA to stop enzymatic reactions.

PCR reaction mix for DNA amplification

0.5 µL	Q5 polymerase
1 µL	dNTPs (10 mM total)
10 µL	Q5 reaction buffer (5×)
2.5 µL	forward primer (10 µM)
2.5 µL	reverse primer (10 µM)
1 µL	cDNA template
ad 50 µL	ddH_2O

2.5.4.3 Identification of bacteria clones by colony PCR

Colony PCR was performed to identify bacteria clones carrying the transformed plasmid with an integrated insert of interest. PCR was conducted using oligonucleotide pairs, specific for the insert, or flanking the multi cloning site into which the open reading frame was ligated. The thermostable DCS polymerase was used for PCR according to the supplier's protocol. The PCR reaction mix is listed below. A pipette tip was dipped into a single colony obtained from the transformation (2.4.3). The tip was then dipped on a fresh solid LB plate, containing antibiotics for selection, as a reference plate for the colony PCR. The very same tip was finally used to add bacteria material to the PCR mix by pipetting up and down the mixture several times. PCR parameters were set to 5 min initial denaturation at 95 °C followed by 35-37 cycles of denaturation at 95 °C (30 s), annealing (melting temperature of the primer -5 °C, 30 s per 1000 bp product), and elongation at 72 °C for 2 min. A final elongation step was performed at the end of the last cycle at 72 °C for 4 min before the PCR reaction was cooled down to 12 °C and completely stopped by the addition of agarose gel loading dye containing EDTA. The reference plate was incubated at the optimal growth temperature of the respective bacteria for several hours while PCR was running. Colonies from the reference plate were used for inoculation of overnight cultures from positive clones identified in the colony PCR.

PCR reaction mix for colony PCR

0.2 µL	DCS polymerase
0.3 µL	dNTPs (10 mM total)
1.5 µL	10 × buffer B (0.8 M Tris-HCl, 0.2 M $(NH_4)_2SO_4$)
1.5 µL	$MgCl_2$ (25 mM)
1.5 µL	forward primer (10 µM)
1.5 µL	reverse primer (10 µM)
ad 15 µL	ddH_2O
Bacteria material	

2.5.5 Agarose gel electrophoresis

DNA products from PCR amplification and plasmid fragments obtained from restriction digests, were separated and visualized by horizontal electrophoresis using agarose gels. Gels were prepared with 1× TAE buffer supplemented with 1% (w/v) agarose. Agarose was dissolved in TAE buffer by boiling the mixture in a microwave oven. TAE buffer with agarose was stored in a water bath at 65 °C to avoid solidification until gels were cast. Shortly before gel casting, the MidoriGreen Advance dye (Nippon Genetics) was added for in-gel staining, and visualization of DNA under green LED light according to the supplier's protocol. Agarose gels were placed horizontally in the electrophoresis chamber filled with 1× TAE buffer. DNA samples mixed with agarose loading dye were loaded into the gel slots and DNA fragments separated according to their size by application of 100 V resulting in a current of 400 mA. A 1 kb DNA ladder (GeneRuler 1 kb, Thermo Scientific) was loaded as size control. Sufficient separation of the DNA fragments was achieved after 30-45 min of electrophoresis.

50× TAE buffer

242 g	Tris base
57.1 mL	Glacial acetic acid
100 mL	0.5 M EDTA (pH 8.0)
ad 1 L	ddH_2O

2.5.6 Heterologous expression in *E. coli,* substrate feeding, and enzyme assays

For heterologous expression of *VTE5* and *FOLK* in *E. coli* Rosetta DE3, pETDuet-1 constructs were cloned as described in 7.1.1**,** and expression experiments performed. Bacteria cells were inoculated in 10 mL LB medium supplemented with antibiotics. These pre-cultures were grown overnight at 37 °C while shaking at 180 rpm for sufficient aeration. The next day, the main culture (50-250 mL Terrific broth medium, (Roth), supplemented with antibiotics) was inoculated with the pre-culture to an initial OD_{600} of 0.1. Cultures were cultivated at 37 °C while shaking until the cell density of an OD_{600} between 0.6 and 0.8 was reached. Protein expression was initiated by addition of sterile filtered 0.5 mM IPTG. Cells were further cultivated for expression overnight at 16 °C while shaking at 180 rpm. Afterward, cells in the culture were either fed with substrates in culture, or cells were harvested by centrifugation for protein isolation and further use in enzyme assays (section 2.5.6.2). For protein analysis using SDS PAGE (section 2.5.7.1) and Western blot (section 2.5.7.2), 1 ml cell culture was harvested by centrifugation.

2.5.6.1 E. coli feeding with phytol, farnesol, or geranylgeraniol

After heterologous expression of *VTE5* or *FOLK* in *E. coli* as described above (2.5.6), kinase substrates (phytol, geranylgeraniol, or farnesol) were directly added to the culture for *E. coli* feeding experiments. For this approach, *E. coli* cultures were divided into three 5 mL replicates after expression. Then either 5 mM phytol, geranylgeraniol, farnesol, or no alcohol as control, were added to the cultures. Cultures were cultivated in the presence of substrates for 3 h at 37 °C. Afterward, cells were harvested at 4 °C in 15 mL Falcon tubes by centrifugation for 10 min, 4000 rpm and cell pellets washed twice with 5 mL PBS buffer to remove excess substrates. In the last washing step, the OD_{600} was determined for later normalization, and cells finally harvested stepwise in 2 mL reaction tubes by centrifugation for 1 min, 10000 rcf at 4 °C. Cell pellets were supplemented with glass beads and shock frozen in liquid nitrogen for isoprenoid alcohol phosphate isolation and analysis.

2.5.6.2 Isoprenoid alcohol kinase assays after heterologous expression in E. coli Rosetta (DE3)

To analyze the substrate specificity of the isoprenoid alcohol kinases, VTE5 and FOLK, the proteins were isolated from *E. coli* cells after heterologous expression (2.5.6). Bacteria cells were harvested by centrifugation for 6 min at 3500 rpm at 4 °C. Cell pellets were washed once with 5 mL PBS buffer and again centrifuged for 5 min at 3500 rpm at 4 °C. Afterward, cell pellets were mixed with 5 mL homogenization buffer and transferred to several 2 mL reaction tubes, mixed with glass beads and thoroughly ground six times for 20 s at 6500 rpm in a Precellys homogenizer. In-between grinding steps, samples were kept on ice. After grinding, samples were combined in a 15 mL Falcon tube, and filled up to 10 mL with homogenization buffer. Cell debris was centrifuged down (3 min, 4000 rpm, 4 °C) so that the supernatant remained turbid. The supernatant was transferred to ultracentrifugation tubes and membrane proteins separated in the microsomal fraction from the soluble proteins by ultracentrifugation (1 h at 60000 rpm at 4 °C). The microsomal pellets were resuspended in 1 mL homogenization buffer, and the protein concentration was determined by an BCA assay as described in section 2.5.7.3. 50 nmol of the isoprenoid alcohols phytol, geranylgeraniol, or farnesol were used as substrates for the isoprenoid alcohol kinase assay. The enzyme assay was performed in assay buffer in a final assay volume of 100 µl containing 200 µg microsomal protein, and 20 nmol of an NTP mix as phosphate source, as listed below. The assay was started by addition of the protein and incubated at 30 °C for exactly 30 min. The reaction was stopped by freezing the samples in liquid nitrogen. Samples were stored at -80 °C or the isoprenoid alcohol phosphates were directly extracted for analysis (2.6.4 and 2.7.8).

<u>Homogenization buffer</u>

1 mM	EDTA
200 mM	Sucrose
100 mM	Tris-HCl (pH 7.4)

<u>Assay buffer</u>

0.25% (w/v)	CHAPS
20 mM	$MgCl_2$
50 mM	Na-orthovanadate

Enzyme assay setup

200 µg	Protein
20 nmol	NTP mix (10 mM ATP, 10 mM CTP, 10mM GTP, 10 mM UTP)
50 nmol	Isoprenoid alcohol (10 mM stock in ethanol)
ad 100 µL	Assay buffer

2.5.7 Protein analysis

2.5.7.1 Sodium dodecyl sulfate polyacrylamide gel electrophoresis (SDS PAGE)

Proteins were analyzed by SDS PAGE. After heterologous expression in *E. coli* as described in section 2.5.6, the cell density was determined at an OD of 600 nm. Cells from 1 mL cell culture were harvested in a 1.5 mL reaction tube by centrifugation at 11000 rcf for 30 s. The supernatant was discarded and the cell pellet resuspended in 80 µL ddH_2O per OD_{600} and 50 µL 4× Laemmli buffer per OD_{600}. The protein was denatured by incubation at 95 °C for 5 min. Protein samples were loaded into the slots of an SDS gel with a 10% acrylamide separating gel and a 4% acrylamide stacking gel. The gel was set up in a vertical electrophoresis chamber filled with running buffer. Proteins were separated according to their size by application of 200 V and 35 mA for approximately 1 h. To avoid damaging of the thin stacking gel only 25 mA were applied at the beginning and the current was increased to 35 mA as soon as the proteins reached the edge of the separating gel. 5 µL pre-stained protein standard broad range (NEB) was loaded as a size marker.

5× Laemmli buffer

0.03% (w/v)	Bromophenol blue
5 mM	EDTA
50% (v/v)	Glycerol
10% (w/v)	SDS
500 mM	Tris-HCl (pH 6.9)

4× Laemmli buffer was prepared by addition of 100 µL ddH_2O and 100 µL β-mercaptoethanol per 800 µL 5× buffer right before use (5× buffer was stored at -20 °C).

Running buffer

125 mM	Tris base
960 mM	Glycine
0.5% (w/v)	SDS

SDS polyacrylamide gel

Stacking gel (4%)	*Separating gel (10%)*	
2.66 mL	17 mL	Rotipherese® Mix (40% acrylamide/bisacrylamide 29:1 (v/v))
5 mL	—	0.5 M Tris-HCl (pH 6.8)
—	12.5 mL	1.5 M Tris-HCl (pH 8.8)
200 µL	500 µL	10% (w/v) SDS
10 µL	20 µL	TEMED
200 µL	300 µL	10% (w/v) APS
12 mL	20 mL	ddH_2O

For protein visualization, the SDS gel was stained with Coomassie brilliant blue R250 using a microwave oven staining protocol. For this purpose, the gel was removed from the electrophoresis chamber, the stacking gel removed, and the separating gel placed in a glass container with glass lid. The gel was covered in Coomassie staining solution, heated up in the microwave oven until boiling, and then shaken for 15 min. The staining solution was removed and exchanged with de-staining solution. The gel, covered with de-staining solution, was again boiled up in the microwave oven and shaken for 15 min. The de-staining was repeated three to five times.

Coomassie staining solution

50% (v/v)	Ethanol
7% (v/v)	Glacial acetic acid
0.252 (w/v)	Coomassie Brilliant Blue R250

De-staining solution

5% (v/v)	Glycerol
7.5% (v/v)	Glacial acetic acid

2.5.7.2 Analysis of His-tagged proteins by Western blot

For Western blot analysis, protein samples were first separated using SDS PAGE as described in section 2.5.7.1. After electrophoresis, the stacking gel was removed, and the remaining separation gel containing the proteins was incubated for 5 min in Towbin transfer buffer. A blotting sandwich for protein transfer (semi-dry) onto a nitrocellulose membrane was prepared. First, a stack of three filter papers (Whatman®) were placed on the anode of the Western blot device. On top of the filter papers, a nitrocellulose membrane (Amersham protran 0.45 µm NC) was placed and onto the membrane, the SDS gel was placed. Last, the gel was again covered with a stack of three filter papers. The sizes of the filter papers and the nitrocellulose membrane were adjusted to the size of the protein gel. All components of the blotting sandwich were soaked with Towbin transfer buffer before placing. The Western blot was carried out in a blotting apparatus for 1 h at 70 mA and 15 V. After the transfer, histidine (His) tagged proteins were visualized using the HIS Detector nickel-horseradish peroxidase (Ni-HRP) conjugate (Medac diagnostika). Nickel has a very high binding affinity to histidine. The unspecific protein binding sites on the membrane were blocked by incubation in TBSTXB buffer supplemented with 2% (w/v) BSA. The blocking was conducted for 1 h at room temperature or overnight at 4 °C while shaking. Afterward, the buffer was exchanged with fresh TBSTXSB buffer containing 2% (w/v) BSA and 0.005% (v/v) of the Ni-HRP conjugate. The membrane was again incubated while shaking at room temperature for 1 h. Afterward, the membrane was washed three times in TBSTXSB buffer while shaking for 15 min each. Bound Ni-HRP was visualized using the SuperSignal™ West Pico PLUS Chemiluminescent Substrate (ThermoScientific) according to the supplier's protocol. The luminescent signal was recorded using a ChemiDoc system (BioRad).

Towbin transfer buffer

0.303% (w/v)	Tris base
1.44% (w/v)	Glycine
20% (v/v)	Methanol
1% (v/v)	SDS (from 10% (w/v) stock)

TBSTXSB buffer

10 mM	Tris-HCl (pH 7.4)
0.01% (w/v)	Thimerosal
0.1% (v/v)	Triton X-100
0.05% (w/v)	SDS
0.1% (w/v)	BSA
0.9% (w/v)	NaCl

2.5.7.3 Protein quantification with bicinchoninic acid (BCA)

The protein concentration was determined with bicinchoninic acid (BCA) according to Smith *et al.*, 1985. Crude protein was diluted 1:10 and mixed with BCA reagent (BCA solution/4% $CuSO_4$ (49:1, v/v)) in a 1:100 ratio. For protein dependent reduction of Cu^{2+} ions to Cu^{+}, samples were incubated for 15 min at 60 °C. Purple complexes, which are formed by the reaction of Cu^{+} ions with BCA, were quantified photometrically at 562 nm using a Nanodrop photometer. Protein concentrations were determined by correlation to a BSA standard curve with known protein concentrations.

2.5.8 Pulse amplified modulation (PAM) fluorometry

To determine the photosynthetic quantum yield in Arabidopsis leaves, the fluorescence of chlorophyll was measured using PAM fluorometry. Before measuring, plants were dark adapted for 60 min. Afterward, the plants were exposed for 5 min to different light intensities at either 150 µmol m^{-2} s^{-1} (low light), 500 µmol m^{-2} s^{-1} (medium light), or 1000 and 1500 µmol m^{-2} s^{-1} (high light) photosynthetically active irradiation. After light exposure, chlorophyll fluorescence was measured using a Junior-PAM fluorometer according to the supplier's protocol. Quantum yield of photosystem II (YII) was calculated with the fluorescence emission using the WinControl-3 software according to the formula $(F_m\text{-}F)/F_m$, where F_m and F are the fluorescence emission of light-adapted plants under measuring light and after applying a saturation light pulse, respectively (Schreiber *et al.*, 1986). For each light condition, three different plants were measured and ten measurements per plant were performed.

2.5.9 Chloroplast ultrastructure analysis

Chloroplast ultrastructure was analyzed with transmission electron microscopy performed by Dr. Michael Melzer (IPK, Gatersleben) in leaves of four-week old Arabidopsis plants. Plants were grown on MS medium supplemented with 1% sucrose and dark adapted before sampling and leaf cross sectioning to reduce starch. Leaf cross sections were prepared as described in Schumann *et al.*, 2017.

2.6 Lipid extraction methods

2.6.1 Chlorophyll extraction with acetone

Chlorophyll was measured following Porra *et al.*, 1989. Approximately 10 mg Arabidopsis leaf material was frozen in 2 mL reaction tubes containing ceramic beads in liquid nitrogen. Leaves were homogenized in a Precellys homogenizer two times for 30 s at 6300 rpm and extracted two times with acetone. In the first step, 500 µL 80% (v/v) acetone were added, samples thoroughly vortexed for 10 s and then solid leaf debris pelleted by centrifugation. The supernatant was transferred to a new reaction tube and the extraction of the remaining pellet repeated using 500 µL 100% acetone. After vortexing and centrifugation, the supernatants were combined and the amount of chlorophyll determined by spectrophotometry as described in section 2.7.1.

2.6.2 Extraction of tocochromanols and chlorophyll with diethylether

For the extraction of tocochromanols, approximately 100 mg leaf material was frozen in liquid nitrogen. Plant material was ground in 2 mL reaction tubes containing ceramic beads at 6500 rpm, two times for 30 s in a Precellys homogenizer. In-between the two grinding steps and after grinding, the samples were kept in liquid nitrogen to prevent thawing of the plant material. To the ground plant material, 1 mL diethylether and 500 ng of internal standard for tocochromanol quantification (tocol) were added. Samples were vortexed and 300 µL of 300 mM ammonium acetate added. Samples were again thoroughly vortexed for approximately 10 s and centrifuged for phase separation for 3 min at 13000 rpm. The upper organic phase containing chlorophyll and tocochromanols was transferred to fresh glass vials. To the remaining aqueous phase, again 1 mL diethylether was added and samples once more ground for 15 s at 6500 rpm in a Precellys homogenizer. The aqueous phase was extracted three to four

times with 1 mL diethylether until the organic phase appeared colorless and not green any more. Organic phases were combined, an aliquot taken for chlorophyll measurement if needed (section 2.7.1), and the rest dried under nitrogen gas flow for tocochromanol analysis. To the dried samples, 200 µL n-hexane were added, samples were vortexed to dissolve lipids, and finally the n-hexane containing lipids were transferred to LC glass vials with glass inlays for HPLC FLD measurement as described in section 2.7.2. For analysis of tocochromanols by mass spectrometry, lipid extracts were dried after HPLC measurement under nitrogen gas flow, dissolved in 200 µL dichloromethane/methanol (1:5, v/v) and measured by LC Q-TOF MS/MS or LC Q-Trap MS/MS (2.7.3).

2.6.3 Isolation of fatty acid isoprenoid alcohol esters, free isoprenoid alcohols, tocochromanols, and free sterols by solid phase extraction using silica columns

The combined extraction protocol was performed with minor modifications according to vom Dorp *et al.*, 2015. Fatty acid isoprenoid alcohol esters, tocopherol, free sterols, and free isoprenoid alcohols; including phytol, geranylgeraniol, and farnesol, were extracted together from either approximately 100 mg leaf material or from 20 mg seeds. The weight of the plant material was determined, and samples frozen in liquid nitrogen in 2 mL reaction tubes containing ceramic beads. Frozen material was ground in a Precellys homogenizer two times for 20 s at 6300 rpm. Between the grinding steps the samples were stored in liquid nitrogen to prevent thawing. Afterward, 500 µL 100% diethylether, internal standard for the respective analytes (as listed in Table 5), and 250 µL of 300 mM ammonium acetate were added. Samples were thoroughly vortexed for 10 s and then centrifuged 5 min at 5000 rcf to obtain phase separation. The upper organic phase was transferred to fresh glass tubes and the lower aqueous phase was extracted two more times with 500 µL 100% diethylether. Organic phases were combined in the fresh glass tubes and at the end dried under nitrogen gas flow. Dried lipids were dissolved in 400 µL n-hexane and separated by solid phase extraction on silica columns by step gradient chromatography using n-hexane and diethylether.

Solid phase extraction

For solid phase separation of lipids, silica columns (Strata S1-1, 100 mg/1 mL, Phenomenex) were equilibrated by flushing with 3 mL n-hexane. Afterward, the lipid extract dissolved in in n-hexane was applied onto the column. Elution of lipids was carried out by first eluting hydrocarbons including squalene by flushing with 3 mL n-hexane, followed by flushing with 3 mL n-hexane/diethylether (99:1, v/v), eluting fatty acid isoprenoid alcohol esters (fraction I). Free isoprenoid alcohols were eluted together with tocochromanols by flushing with 3 mL n-hexane/diethylether (98:2, v/v) (fraction II). Free sterols were eluted last by flushing with 3 mL n-hexane/diethylether (85:15, v/v) (fraction III). All fractions were collected separately in fresh glass tubes and dried under nitrogen gas flow.

Fraction I: n-hexane/diethylether (99:1, v/v) – fatty acid isoprenoid alcohol esters

The lipids of fraction I were dissolved in 200 µL chloroform/methanol/300 mM ammonium acetate (300:665:35, v/v/v), vortexed and transferred to LC glass vials with inlay for analysis using direct infusion quadrupole Q-Tof MS/MS as described in section 2.7.7.

Fraction II: n-hexane/diethylether (98:2, v/v) – isoprenoid alcohols and tocochromanols

Lipids of fraction II were dissolved in 100 µL n-hexane, vortexed, and 50 µL transferred to HPLC glass vials with conical inlays for tocochromanol analysis using HPLC FLD as described in section 2.7.2. The remaining 50 µL from this fraction were dried again under nitrogen gas flow and derivatized for isoprenoid alcohol analysis by GC-MS. Alcohols were derivatized by addition of 80 µL N-methyl-N-(trimethylsilyl)trifluoracetamid (MSTFA) and incubation at 80 °C for 30 min. Afterward, the MSTFA was completely removed by evaporation with nitrogen gas. Derivatized dried isoprenoid alcohols, including phytol, geranylgeraniol, and farnesol, were dissolved in 50 µL n-hexane. Dissolved lipids were transferred to GC glass vials with conical inlays and free isoprenoid alcohols were measured using GC-MS as described in section 2.7.6.

Fraction III: n-hexane/diethylether (85:15, v/v) – free sterols

Lipids in fraction III were directly derivatized after drying under nitrogen gas flow by addition of 80 µL MSTFA, votexing and incubation for 30 min at 80 °C.

Afterward, remaining MSTFA was completely evaporated under nitrogen gas flow and derivatized free sterols dissolved in 100 µL n-hexane and transferred to GC glass vials with inlays. Samples were analyzed using GC-MS as described in section 2.7.6.

Table 5 Internal standards used for the quantification of fatty acid (FA) isoprenoid alcohol esters, free isoprenoid alcohols, tocochromanols and free sterols.

Analyte	Internal Standard	Final content in extraction	Supplier
Fatty acid isoprenoid alcohol esters	17:0-phytol	1 nmol	Synthesized in house (Dr. Katharina Gutbrod)
Free isoprenoid alcohols	Octadecenol (oleyl alcohol)	10 nmol	Sigma-Aldrich (Taufkirchen, D)
Free sterols	Cholestanol	0.5 nmol	Sigma-Aldrich (Taufkirchen, D)
Tocochromanols	Tocol	500 ng	Biotrend (Destin, USA)

2.6.4 Extraction of isoprenoid alcohol phosphates

Isoprenoid alcohol phosphates were extracted following vom Dorp *et al.*, 2015 with minor modifications. The internal standards 10:0-P and 10:0-PP were synthesized in house by Dr. Katharina Gutbrod according to Joo *et al.*, 1973 and quantified by LC MS/MS (Q-Trap) using commercial mono- and diphosphates (phytyl-P and geranylgeranyl-P for 10:0-P and phytyl-PP and geranylgeranyl-PP for 10:0-PP, derived from isoprenoids.com) as standards.

For isoprenoid alcohol phosphate extraction, 20 mg of Arabidopsis leaves or 20 mg dried seeds were frozen in liquid nitrogen in 2 mL reaction tubes containing ceramic beads. The samples were ground in a Precellys homogenizer at 5000 rpm for 20 s in two consecutive steps. In-between the steps the samples were kept in liquid nitrogen. To the ground plant material, 50 µL of internal standard (~200-500 pmol 10:0-P and 10:0-PP), were added together with 200 µL freshly prepared, cold extraction buffer (isopropanol/50 mM KH_2PO_4 (pH 7.2)/glacial acetic acid (1:1:0.025, v/v/v)). Samples dissolved in buffer were once more homogenized in the Precellys

homogenizer for 60 s at 6000 rpm. Non-polar lipids were separated from the polar lipids (isoprenoid alcohol phosphates) by washing four times with 200 µL, 50 °C warm, saturated n-hexane. Saturated n-hexane was prepared by shaking n-hexane with isopropanol and water (isopropanol/ddH_2O/n-hexane, 1:1:0.15, v/v/v). Phases were separated after vortexing by centrifugation at 2000 rpm for 1 min. The upper organic n-hexane phases containing the non-polar lipids were either discarded or combined for further analysis of the non-polar lipids as described in section 2.6.5.

Polar lipids including isoprenoid alcohol phosphates in the lower aqueous phase were harvested, and 5 µL saturated $(NH_4)_2SO_4$ and 600 µL methanol/chloroform (2:1, v/v) were added. Samples were thoroughly mixed and incubated at room temperature for 20 min. Afterward, samples were centrifuged for 2 min at 13500 rpm. The particle-free supernatant was transferred to fresh 1.5 mL reaction tubes and dried for around 2 h in a SpeedVac centrifuge with cool trap in auto run at 36 °C. When samples were completely dry, 50 µL methanol were added, samples vortexed and sonicated for 5 min. After sonication, particles were pelleted by centrifugation at 13500 rpm for 2 min. The particle-free supernatant was transferred to LC glass vials with conical inlays for measurement using LC MS/MS with a Q-Trap instrument as described in section 2.7.8.

2.6.5 Combined extraction of isoprenoid alcohol phosphates and non-polar lipids including free isoprenoid alcohols, tocochromanols, fatty acid isoprenoid alcohol esters and free sterols

Isoprenoid alcohol phosphates and non-polar lipids were extracted together as described in the thesis of Katharina vom Dorp (2015) with minor modifications. 20 mg plant material was frozen in 2 mL reaction tubes, together with ceramic beads, in liquid nitrogen. The material was ground to a fine powder in a Precellys homogenizer, two times for 20 s, 6800 rpm. In-between and after grinding steps, samples were stored in liquid nitrogen. Afterward, internal standards for isoprenoid alcohol phosphates (see section 2.6.4) and for the respective non-polar analytes (Table 5), were added. Then, isoprenoid alcohol phosphates were extracted as described in section 2.6.4. It is important, that the n-hexane phases containing the non-polar lipids were collected in fresh glass tubes, and dried under nitrogen gas flow. Dried non-polar lipids were later dissolved in 400 µL n-hexane, vortexed and used for solid phase extraction as described in section 2.6.3.

2.6.6 Extraction of photosynthetic pigments

Photosynthetic pigments were extracted according to Kanwischer, 2007. 80-100 mg leaf material was frozen in liquid nitrogen. Leaves were ground to a fine powder using ceramic beads in a Precellys homogenizer, two times at 6500 rpm. Samples were again placed in liquid nitrogen after grinding to prevent thawing. Afterward, 0.5 mL 80% (v/v) acetone was added, samples thoroughly vortexed and centrifuged for 1 min at 14000 rpm. The supernatant was transferred to a fresh reaction tube and the plant cell pellet once more extracted by addition of 0.5 mL 100% acetone. After centrifugation, the supernatants were combined in the fresh reaction tube. The supernatants were once more centrifuged for 1 min at 14000 rpm to spin down particles. 400 µL of the supernatant were transferred to HPLC glass vials with inlays for photosynthetic pigment analysis using HPLC DAD as described in section 2.7.5. The remaining supernatant was used for chlorophyll quantification with a spectrophotometer (section 2.7.1).

2.6.7 Extraction of phytohormones

Phytohormones were extracted from leaved according to Pan *et al.*, 2008. In contrast to the protocol published by Pan *et al.* (2008), samples were completely dried under nitrogen gas flow because the measurement of volatile phytohormones (e.g. ethylene) was not intended. After extraction samples were either directly measured, or stored dry and overlaid with nitrogen gas at -80 °C. For the measurement, samples were dissolved in methanol/ddH_2O (1:1, v/v) containing 0.1% formic acid. Phytohormones were measured following Pan *et al.* (2008), as described in the thesis of Victoria Kreszies (2019) using LC MS/MS analysis with Q-Trap.

2.6.8 Extraction of phylloquinone (vitamin K1)

Phylloquinone was isolated as described in the thesis of Marion Kanwischer (2007). The internal standard menaquinone-4 (vitamin K2) was dissolved in methanol to a working stock concentration of 0.01 g/µL. The correct concentration was confirmed spectrophotometrically by determination of the OD_{248} with an E1% value of 420 in methanol as described by Oostende, 2008 (Booth and Sadowski, 1997; Oostende *et al.*, 2008) (for 0.01 µg/µL OD_{248}=0.420).

For phylloquinone extraction, 80-100 mg leaf material was harvested and flash frozen in liquid nitrogen. The material was ground two times for 20 s at 6800 rpm to a fine powder using a Precellys homogenizer. Afterward, 800 µL isopropanol/n-hexane (3:1, v/v) and 500 ng internal standard (50 µL of 0.01 µg/µL working stock menaquinone-4) were added, samples mixed by vortexing, and centrifuged for 2 min at 13000 rpm. The supernatant was transferred to a fresh reaction tube and the pellet once more extracted with 600 µL n-hexane. The supernatants were combined and 600 µL methanol/ddH_2O (9:1, v/v) added. Samples were vortexed and centrifuged for 2 min at 13000 rpm to obtain a phase separation. The upper phases containing phylloquinone were transferred to fresh glass vials and dried under nitrogen gas flow. The dry analytes were dissolved in 100 µL methanol/dichloromethane (9:1, v/v) and transferred to LC vials with glass inlays. Phylloquinone was measured using HPLC FLD as described in section 2.7.4.

2.6.9 Extraction of phytenal

Phytenal was extracted from Arabidopsis leaves after a protocol established by Dr. Philipp Gutbrod (unpublished). 100 mg leaf tissue was harvested in liquid nitrogen and homogenized to a fine powder in a Precellys homogenizer. Afterward, 1 mL chloroform/methanol (2:1, v/v) was added together with 500 µL 0.3 M ammonium acetate. 3 nmol hexadecanal (Cayman Chemical) were added as internal standard. Samples were mixed by vortexing and centrifuged at 5000 rpm for 5 min to obtain phase separation. The organic phase was transferred to a fresh glass tube and the remaining aqueous phase once more extracted with 1 mL chloroform. Organic phases were combined and dried under nitrogen gas flow. When the samples were completely dry, 100 µL methoxylamine hydrochloride in pyridine (20 mg/mL) were added for derivatization (1 h at room temperature). Samples were then again dried under nitrogen gas flow, dissolved in 1 mL n-hexane and loaded onto a silica column (Strata S1-1 100 mg/1 mL; Phenomenex) which had been equilibrated with 3 mL n-hexane. After sample loading, the column was washed with 3 mL n-hexane. Long-chain aldehyde methoxylamine derivatives were then eluted from the column with 3 mL n-hexane/diethylether (99:1, v/v). This fraction was collected, dried under nitrogen gas flow and dissolved in 100 µL acetonitrile and measured using LC MS/MS with Q-Trap (2.7.9).

2.7 Lipid analysis

2.7.1 Chlorophyll analysis

Chlorophyll was extracted as described in section 2.6.1 or in section 2.6.2. Chlorophyll was quantified spectrophotometrically after Porra *et al.*, 1989. The absorption of chlorophyll extracts was measured in quartz cuvettes at 646.6, 663.6 and 750 nm. The contents of chlorophyll a and chlorophyll b were calculated with the following formulas:

$$Chlorophyll\ a = 12.25 \cdot (A_{663.6} - A_{750}) - 2.55 \cdot (A_{646.6} - A_{750})\ [\mu g]$$

$$Chlorophyll\ b = 20.31 \cdot (A_{646..6} - A_{750}) - 4.91 \cdot (A_{663..6} - A_{750})\ [\mu g]$$

2.7.2 Tocochromanol analysis using HPLC FLD

Tocochromanols were extracted according to the protocol in section 2.6.2 or 2.6.3 and analyzed using HPLC FLD. A diol column (Lichrospher 100-5 Diol 125 x 3 mm, Knauer) was used for chromatographic separation. Elution of tocochromanols from the column was achieved by isocratic flow at 1.2 mL/min using n-hexane/tertiary butylmethylether (96:4, v/v) as mobile phase. Tocochromanols were detected with a fluorescence detector (FLD) with an excitation at 290 nm and emission at 330 nm. Tocochromanols were quantified by comparison of the analyte peak areas with the peak area of the internal standard tocol. Analytes were identified by comparison of the retention time with external standards. The retention times of commercial tocopherol and tocotrienol mixtures (α-, β-, γ-, and δ-tocopherol, Calbiochem), tocotrienols (Cayman Chemical) and linseed oil containing PC-8 and γ-tocopherol (from the local supermarket) were determined in separate runs under the same conditions. Data were analyzed with the Chem Station software for LC 3D systems from Agilent.

2.7.3 Tocochromanol analysis using LC MS/MS with Q-Trap or Q-TOF

For highly sensitive measurements, tocochromanols were analyzed using LC MS/MS. The same samples could be analyzed first by HPLC-FLD (section 2.7.2) and then by LC MS/MS. Tocochromanol samples dissolved in n-hexane were dried under nitrogen gas and taken up in 200 µL dichloromethane/methanol (1:5, v/v) and 5 µL injected for analysis. A C18 Gemini column (5 µm, 150 × 2.00 mm; Phenomenex) was used for separation. The mobile phase contained 95% methanol and was pumped with

an isocratic flow rate of 0.6 mL/min. Ions were measured in positive ion mode. Targeted lists for MS/MS analysis are given in the appendix 7.3.

2.7.4 Phylloquinone analysis using HPLC FLD

Phylloquinone was analyzed using HPLC FLD as described in the thesis of Marion Kanwischer (2007). Samples were extracted as described in section 2.6.8 and quantified using the internal standard menaquinone-4. A C18 column (Eurospher-100-C18 250 × 4.6 mm, Knauer) was used for chromatographic separation. Elution of phylloquinone from the column was achieved by isocratic flow at 0.5 mL/min using dichloromethane/methanol (100:900, v/v, supplemented with 5 mL of a methanolic solution containing 1.37 g $ZnCl_2$, 0.41 g sodium acetate and 0.3 g acetic acid) as mobile phase. Phylloquinone and menaquinone-4 were detected after post-column reduction with Zn with a fluorescence detector (FLD) with an excitation at 243 nm and emission at 430 nm. Phylloquinone was quantified by comparison of the analyte peak area with the peak area of the internal standard menaquinone-4.

2.7.5 Photosynthetic pigment analysis using HPLC DAD

Photosynthetic pigments were isolated from leaf tissue as described in section 2.6.6 and analyzed with HPLC DAD according to the method provided in the thesis of Marion Kanwischer (Kanwischer, 2007). Photosynthetic pigments were quantified by comparison of the peak area with the peak area of chlorophyll. Chlorophyll was quantified in parallel by spectrophotometry according to Porra *et al*. (1989) as described in section 2.7.1. Peak areas of the photosynthetic pigments were corrected by dividing the peak area with the molar extinction coefficient at 440 nm as follows: Neoxanthin (e440=111520), violaxanthin (e440=144000), antheraxanthin (e440=125040), lutein (e440=124609), zeaxanthin (e440=106041, chlorophyll b (e440=59617), chlorophyll a (e440=33849) and β-carotene (e440=122514). Extinction coefficients of all pigments are given in $L \cdot mol^{-1} \cdot cm^{-1}$ and were taken from Jeffry S.W. *et al.*, 1997.

2.7.6 Analysis of free isoprenoid alcohols and free sterols with GC-MS

Free isoprenoid alcohols and free sterols were extracted as described in 2.6.3 and quantified as silylated derivatives by GC-MS analysis. Free phytol, geranylgeraniol and

farnesol were analyzed using octadecenol (18:1ol) as internal standard. Cholestanol was used as internal standard for sterol quantification. 2 µL of the lipid extract were injected via a splitless injector with an autosampler for GC-MS analysis. The injector was heated to 230 °C for sample evaporation. Evaporated samples were guided with a flow rate of 3.1450 mL/min through the HP-5MS column (Agilent, 30 m × 0.25 mm, 0.25 µm) with helium as carrier gas. The temperature gradient of the oven was set according to Table 6. Targeted lists for MS analysis of isoprenoid alcohols and sterols are given in the appendix 7.3. The data was evaluated using the Enhanced Chem Station software (Agilent).

Table 6 Temperature gradient for GC MS analysis of isoprenyl alcohols and sterols

	Rate [°C/min]	Value [°C]	Hold time [min]	Run time [min]
Initial	–	100	3	3
Ramp 1	5	200	1	24
Ramp 2	20	310	3	32.5
Ramp 3	20	100	3	46

2.7.7 Analysis of fatty acid isoprenoid alcohol esters by direct infusion Q-TOF MS/MS

Fatty acid isoprenoid alcohol esters were extracted as described in section 2.6.3 and analyzed by direct infusion MS/MS with Q-TOF detection (Agilent). MS/MS analysis was performed according to vom Dorp, 2015. Targeted lists for MS/MS analysis are given in the appendix 7.3.

2.7.8 Analysis of isoprenoid alcohol phosphates using LC Q-Trap MS/MS

Isoprenoid alcohol phosphates were extracted as described in section 2.6.4 or in a combined extraction together with non-polar lipids as described in section 2.6.5 and analyzed by LC Q-Trap MS/MS (Agilent and Sciex). A reversed phase column (Poroshell 120 EC-C8, 50×2.1 mm, 2.7 µm (Agilent)) was used for separation. Isoprenoid alcohol phosphates were eluted from the column using a solvent gradient with solvent A (H_2O/acetonitrile, 90:10 (v/v) + 5 mM NH_4OH), solvent B (acetonitrile + 5 mM NH_4OH) and solvent C (H_2O/acetonitrile, 30:70 (v/v) + 0.1% formic acid) according to Table 7 at a flow rate of 0.2 mL/min. Isoprenoid alcohol phosphates were

measured using a Q-Trap 6500 system with turbo V electrospray ion source (Sciex) via multiple reaction monitoring (MRM) in negative ion mode. Device settings were as following: 20 V curtain gas, medium collision gas and -4500 V ion spray voltage. Further, the ion source temperature was set to 150°C, the nebulizer and turbogas temperature to 25°C. Targeted lists for MS analysis are given in the appendix 7.3.

Table 7 Gradient protocol for the elution of isoprenoid alcohol phosphates.

Time [min]	Solvent A [%]	Solvent B [%]	Solvent C [%]
0 – 1	100	0	0
1.1-20	0	100	0
20 – 22	0	100	0
22.1 – 27	0	0	100
27.1 – 35	100	0	0

2.7.9 Analysis of phytenal by LC MS/MS with Q-Trap

Phytenal was analyzed by LC MS/MS with a Q-Trap (Sciex) after Gutbrod *et al.*, (unpublished). A reversed phase column (Eurospher II C8, 150×3 mm, with precolumn, 3 µm, Knauer) was used for the separation of derivatized aldehyde methoxylamines and eluted from the column using a solvent gradient with solvent A (H_2O/acetonitrile/formic acid (63:37:0.002, v/v)) and solvent B (acetonitrile) at a flow rate of 0.5 mL/min. The product ion used for the internal standard (hexadecanal methoxylamine) was 60.0455. For phytenal methoxylamine the product ion 96.0848 was used in MS/MS analysis.

2.8 Statistics

Statistical calculations were done using Microsoft Excel. The average and standard deviation of at least three replicates were calculated. The Student's t test was performed to detect significant differences between samples. Samples significantly different with $p<0.05$ are indicated with a single asterisk (*), values significantly different with $p<0.01$ are indicated with two asterisks (**) and with $p<0.005$ with three asterisks (***).

3 Results

3.1 Isoprenoid alcohol phosphorylation in Arabidopsis *vte5-2* and *folk-2* mutants

The phosphorylation of free phytol was shown to be a key process for the remobilization of phytol, which can be released from chlorophyll upon degradation. The Arabidopsis phytol kinase VTE5 and the phytyl-P kinase VTE6 are essential for the activation of phytol via phosphorylation for the biosynthesis of the vitamins tocopherol (vitamin E) and phylloquinone (vitamin K1). BLAST searches revealed that *FOLK* represents the only paralog of *VTE5* in Arabidopsis (Valentin *et al.*, 2006; Fitzpatrick *et al.*, 2011). To investigate the role of the salvage pathway of the phosphorylation of isoprenoid alcohols, Arabidopsis mutants with a defect in phytol kinase activity (At5g04490, VTE5) and in addition with a defect in farnesol kinase activity (At5g58560, FOLK) were analyzed. Null mutant lines of the respective genes described in previous studies were chosen. The *vte5-2* (pst12490) transposon insertion null mutant lacks phytol kinase activity (vom Dorp *et al.*, 2015) and was isolated in our institute. The *folk-2* (SALK_123564) null mutant (Fitzpatrick *et al*., 2011) lacking kinase activity for farnesol and to a lesser extent also for geraniol and geranylgeraniol kinase activity, is derived from the SALK collection and was obtained from the NASC stock center. The *vte5-2* and *folk-2* plants were crossed (section 2.3.7) to generate a double homozygous *vte5-2 folk-2* mutant.

3.1.1 The Arabidopsis *vte5-2 folk-2* double mutant plants are viable and develop normally

Double homozygous plants carrying a transposon insertion in the *VTE5* gene and a T-DNA insertion in the *FOLK* gene were identified in the F3 generation after crossing of the homozygous *vte5-2* (pst12490) and *folk-2* (SALK_123564) single mutant plants. The mutations in the double homozygous *vte5-2 folk-2* mutant plants were confirmed by genotyping PCR (Figure 7 A) as described in section 2.5.4.1. Growth of the double mutant plants was similar to the WT and the single mutant plants. The double mutant plants are able to grow on soil (Figure 7 B) and produce siliques and seeds. The *vte5-2* single mutant plant was generated in the Nossen (No-0) background donor line (Ds11). We obtained the No-0 line from the RIKEN stock center, and these

plants showed slightly bigger and more round leaves in comparison to the Col-0 WT. Col-0 represents the background line of the *folk-2* single mutant.

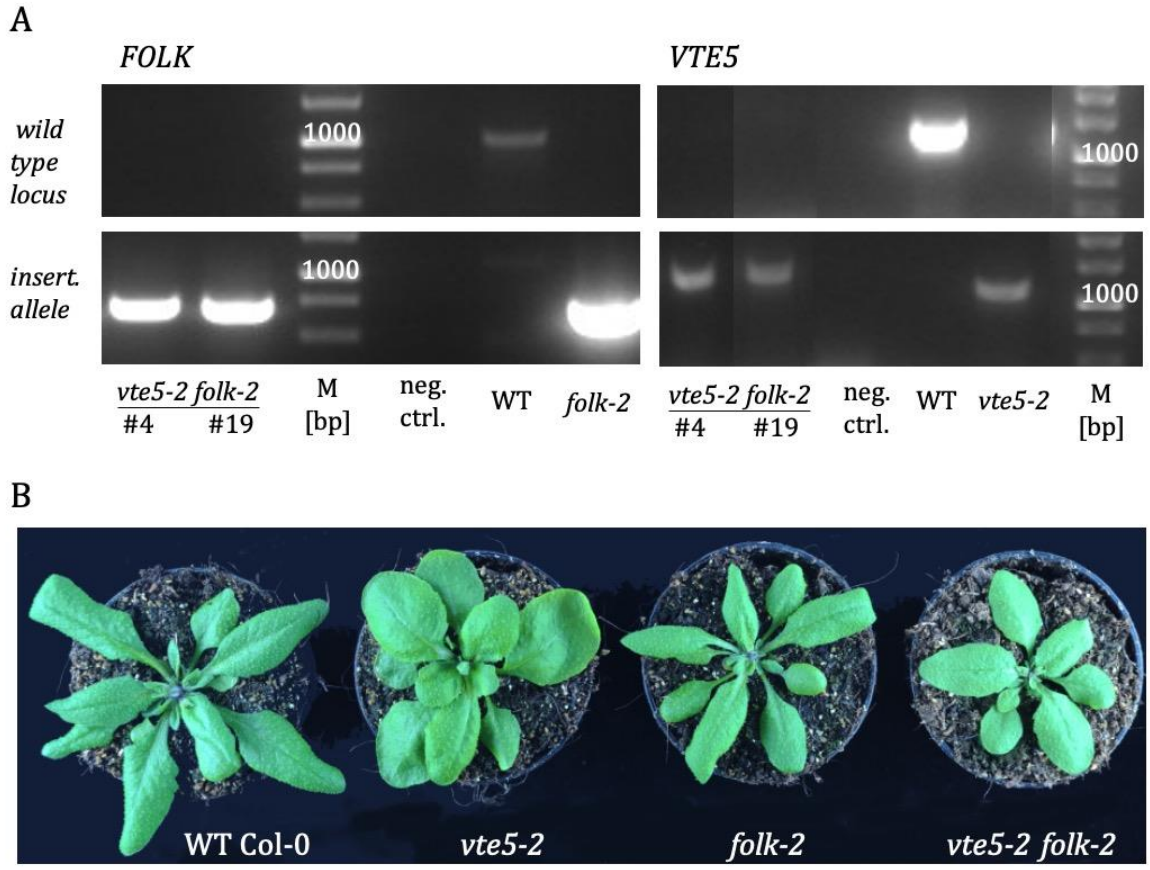

Figure 7 Genotype and phenotype analysis of double homozygous Arabidopsis *vte5-2 folk-2* mutant plants.

Double homozygous mutant plants, carrying a transposon insertion in *VTE5* and a T-DNA insertion in *FOLK*, were identified using PCR (A). For genotyping, primer combinations specific for the wild type gene and for the insertional allele (insert. allele) were used. The photo shows four-week-old homozygous single and double mutant plants (B). The *vte5-2, folk-2,* and *vte5-2 folk-2* mutant plants are viable and able to grow on soil. M= marker, neg. ctrl. = negative control (water without plant DNA).

3.1.2 Isoprenoid alcohol phosphates in leaves and seeds of the Arabidopsis mutants *vte5-2*, *folk-2,* and *vte5-2 folk-2*

The Arabidopsis isoprenoid kinase mutants *vte5-2* and *folk-2* were previously described to be impaired in the ability to phosphorylate phytol, geranylgeraniol, or farnesol. To test the impairment of isoprenoid alcohol kinase activity in the single null mutants, and the double mutant *vte5-2 folk-2*, the contents of phytyl-P, geranylgeranyl-P and farnesyl-P were quantified in seeds and leaves using LC MS/MS with a Q-Trap instrument. Isoprenoid alcohol phosphates were extracted from 20 mg of dry seeds or from 20 mg of leaves of four-week-old plants grown on MS medium supplemented with 1% sucrose. While the leaf isoprenoid alcohol phosphate values showed high variations

in several measurements, the isoprenoid alcohol phosphate contents in dry seeds were much more reproducible.

In leaves, a clear reduction of phytyl-P and phytyl-PP levels in the *vte5-2* and the *vte5-2 folk-2* lines by around 75% compared with the WT Col-0 was found. The *folk-2* leaves in contrast showed a non-significant increase in the phytyl-P content by about 60% compared with the WT level, accompanied with a non-significant decrease in phytyl-PP (Figure 8, A). Different to the leaf phytyl-P content, in seeds, the phytyl-P level was significantly reduced in all mutants in comparison to the WT Col-0 (Figure 8, B). Phytyl-P and phytyl-PP levels were significantly lower in *vte5-2* seeds. Phytyl-P was also significantly lower in *folk-2* and *vte5-2 folk-2* seeds, while the phytyl-PP level was lower in *folk-2* and significantly lower in *vte5-2 folk-2* in comparison to WT Col-0 level. Phytyl-P in *vte5-2* seeds was reduced by 15% in comparison to WT Col-0. In *folk-2* seeds, the phytyl-P level was reduced by 57% and in *vte5-2 folk-2* seeds by more than 90% (Figure 8, B).

The geranylgeranyl-P and geranylgeranyl-PP contents in *vte5-2* and *folk-2* leaves remained similar to WT with high standard deviations. The content of geranylgeranyl-P in *vte5-2 folk-2* was comparable to the WT Col-0, while the geranylgeranyl-PP level was lower than in the WT (Figure 8, C). In contrast to the leaves, significant differences in geranylgeranyl-P contents between the Col-0 WT seeds and the mutant seeds were found. Similar to the phytyl-P seed content, the geranylgeranyl-P content was significant lower in *vte5-2*, *folk-2,* and in *vte5-2 folk-2* seeds in comparison to Col-0 WT (Figure 8, D). The lowest geranylgeranyl-P content with only 15% of the Col-0 WT content was found in *folk-2* seeds. Seeds of *vte5-2* retained about 85% and *vte5-2 folk-2* about 45% of the WT content. No significant differences in geranylgeranyl-PP contents were found in seeds (Figure 8, D).

Analysis of farnesyl-P and farnesyl-PP showed that these analytes are rather low abundant in Arabidopsis (Figure 8, E and F). Quantification of farnesyl-P and farnesyl-PP did not reveal any significant differences between the Col-0 WT and the analyzed mutant leaves and seeds. In leaves, farnesyl-P was slightly increased in *vte5-2*, reduced in *folk-2* and similar to the WT Col-0 in *vte5-2 folk-2*. Farnesyl-PP contents in leaves were slightly but not significantly increased in *vte5-2* in comparison with the WT and increased by around 50% in *folk-2* and *vte5-2 folk-2.* In seeds, the farnesyl-P and farnesyl-PP contents were slightly higher with high standard deviations in all mutant lines in comparison to the Col-0 WT (Figure 8, F).

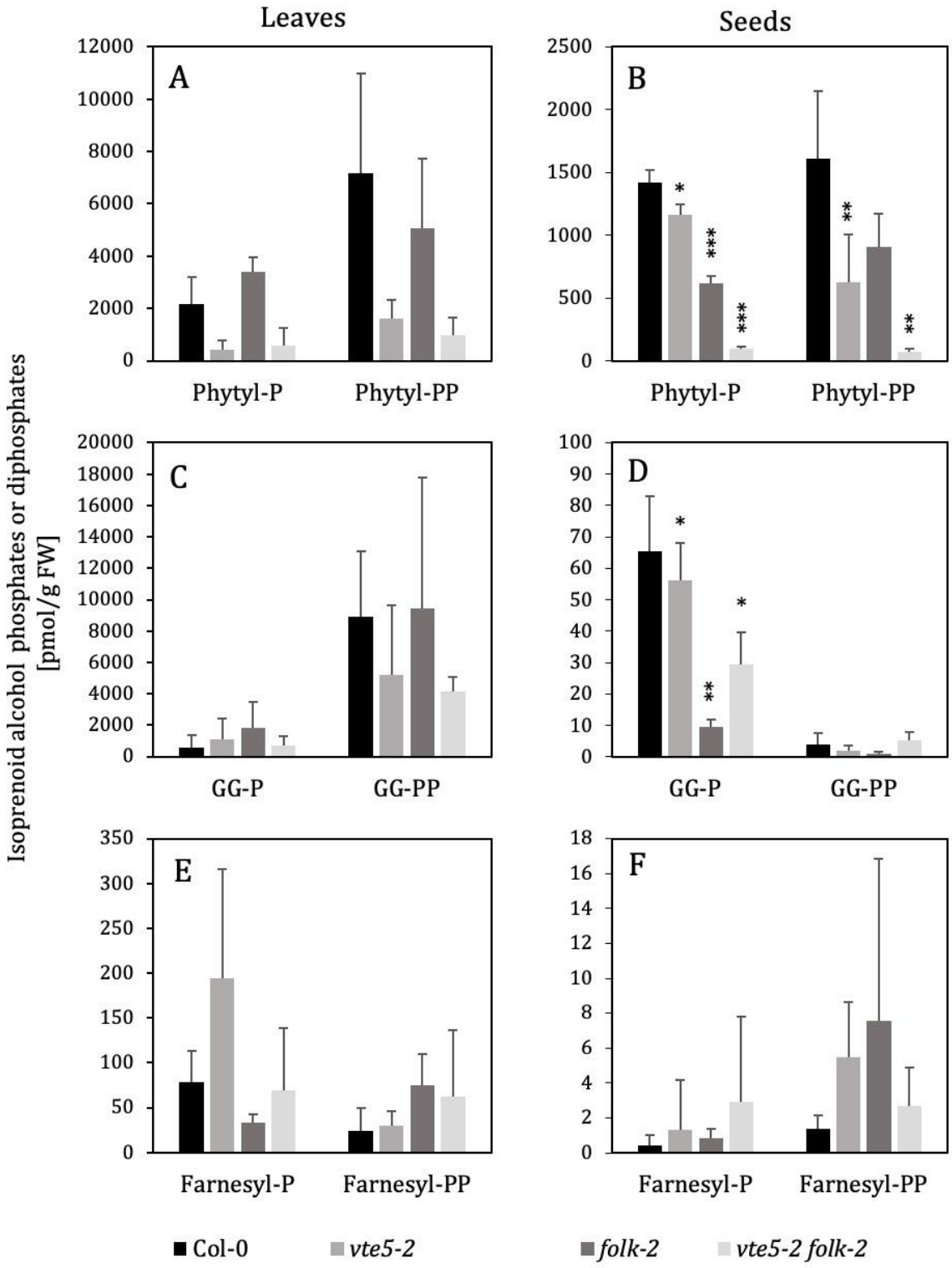

Figure 8 Isoprenoid alcohol phosphate contents in leaves and seeds of the Arabidopsis mutants *vte5-2*, *folk-2*, and *vte5-2 folk-2*.

Isoprenoid alcohol monophosphates (-P) and diphosphates (-PP) were extracted from leaves of 4-week-old Arabidopsis plants grown on MS medium (A, C and E) or from dry seeds (B, D and F). Phytyl phosphates (A and B), geranylgeranyl (GG) phosphates (C and D), and farnesyl phosphates (E and F) were analyzed with LC MS/MS with a Q-Trap instrument. Data represent the mean and SD of three to five replicates. Asterisks indicate significant differences to WT Col-0 (Student's t-test).

3.1.3 Isoprenoid alcohol phosphates in leaves of Arabidopsis *vte5-2*, *folk-2,* and *vte5-2 folk-2* lines after phytol, geranylgeraniol, or farnesol supplementation

As the isoprenoid alcohol phosphate contents in leaves showed high variations, experiments to increase the availability of phytol, geranylgeraniol, or farnesol for phosphorylation were performed. Arabidopsis seedlings were grown for three weeks on MS medium containing 1% sucrose. Afterward, seedlings were transferred for 24 h to liquid MES-KOH buffer supplemented with either 5 mM phytol (Figure 9, A), 5 mM geranylgeraniol (Figure 9, B), or 5 mM farnesol (Figure 9, C). After growth in the presence of phytol or geranylgeraniol, the seedlings were still green and were hardly stressed. In contrary, the seedlings grown in the presence of farnesol turned brown and the leaves started to get slushy. After treatment with the different alcohols, isoprenoid alcohol phosphates were extracted from WT Col-0 (background of *folk-2* mutant), WT Ds11 (*vte5-2* donor), *vte5-2*, *folk-2,* and *vte5-2 folk-2,* and analyzed by LC MS/MS with a Q-Trap instrument. The contents measured in plants after feeding were around 100-fold higher than in the four-week-old plants grown on MS medium (3.1.2).

After growth in the presence of phytol (Figure 9, A), the phytyl-P content was reduced by around 75% in *vte5-2* and *vte5-2 folk-2*, and by around 50% reduced in *folk-2* in comparison to WT Col-0. In comparison to the WT Ds11, phytyl-P level was highly significantly reduced in *vte5-2* and *vte5-2 folk-2.* After supplementation with geranylgeraniol (Figure 9, B), geranylgeranyl-P was highly significantly reduced in *folk-2* and *vte5-2 folk-2* in comparison to Col-0 while geranylgeranyl-P was increased in *vte5-2* and the WT Ds11 in comparison to Col-0. Still *vte5-2* had a reduced geranylgeranyl-P level in comparison to Ds11. After supplementation with farnesol (Figure 9, C), the farnesyl-P content was reduced by around 50% in Ds11, *vte5-2, folk-2,* and *vte5-2 folk-2* in comparison to Col-0. Taking into account that the seedlings supplemented with farnesol were highly stressed, the very low farnesyl-P contents observed, which were only slightly above background levels, did not allow to provide any conclusive results.

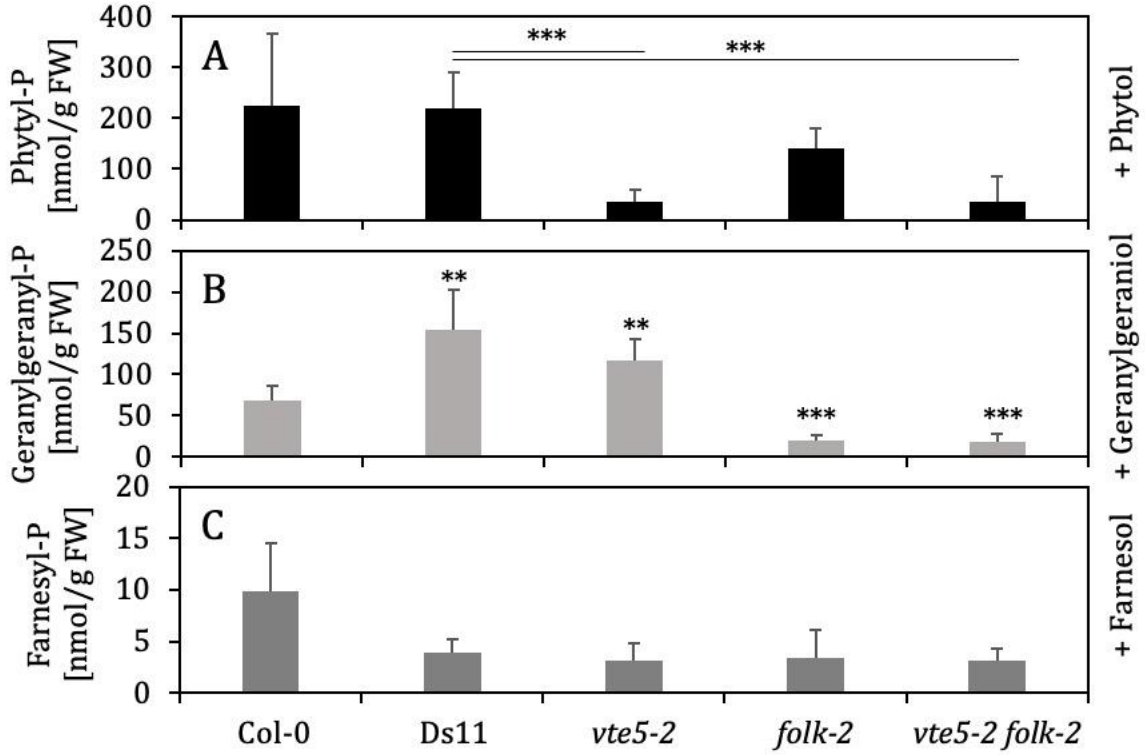

Figure 9 Leaf isoprenoid alcohol phosphates after supplementation of phytol, geranylgeraniol or farnesol measured by LC MS/MS with Q-Trap.

Isoprenoid alcohol monophosphates (-P) were measured by LC MS/MS with Q-Trap in leaves of three-week old Arabidopsis plants after growth in liquid culture supplemented with either 5 mM phytol (A), geranylgeraniol (B) or farnesol (C) for 24 h. Data represent the mean and SD of three to four replicates. Asterisks indicate significant differences to WT Col-0 (Student's t-test) or to WT Ds11 when underlined.

3.1.4 Phytol and geranylgeraniol accumulate in Arabidopsis *vte5-2 folk-2* mutant plants

Analysis of the isoprenoid alcohol phosphates in Arabidopsis *vte5-2, folk-2,* and *vte5-2 folk-2* showed reductions in the phytyl-P and geranylgeranyl-P contents in comparison to WT Col-0 or WT Ds11. The results of farnesyl-P analyses were inconclusive. To address the question if the block in isoprenoid alcohol kinase activity in *vte5-2*, *folk-2* and *vte5-2 folk-2* leads to a precursor accumulation, free phytol, geranylgeraniol, and farnesol were quantified in leaves from plants grown on soil without any isoprenoid alcohol supplementation (Figure 10, A and B). Additionally, seeds were analyzed for the content of free phytol (Figure 10, C). Isoprenoid alcohols were extracted and then silylated for GC-MS analysis.

Free phytol was significantly increased in *vte5-2*, *folk-2,* and also increased in *vte5-2 folk-2* leaves in comparison to the Col-0 WT. Interestingly, the free phytol content was also significantly higher in the leaves of WT Ds11 in comparison to Col-0 WT, while in the seeds, no significant differences in phytol contents between the Col-0

and the Ds11 WT lines were observed (Figure 10, C). The phytol content was significantly increased in the *vte5-2* and in *vte5-2 folk-2* seeds in comparison to Col-0. The amount of phytol in *folk-2* seeds was slightly higher but not significantly different to the WT Col-0.

Next to free phytol, also free farnesol and geranylgeraniol were analyzed in leaves. Free farnesol was not detectable in the leaves nor in seeds. This was presumably due to extremely low levels of farnesol in the plant extracts, because it was in principle possible to measure farnesol by GC-MS as shown by analysis of the farnesol standard. Free geranylgeraniol (Figure 10, B) was not detectable (n.d.) in Col-0, Ds11 and *vte5-2* leaves, while small amounts of free geranylgeraniol were detected in *folk-2* and in *vte5-2 folk-2* leaves. In comparison to the *folk-2* mutant, the *vte5-2 folk-2* mutant leaves contained highly significantly increased levels of free geranylgeraniol. The content of free geranylgeraniol in *vte5-2 folk-2* was around 42-fold higher than in *folk-2*.

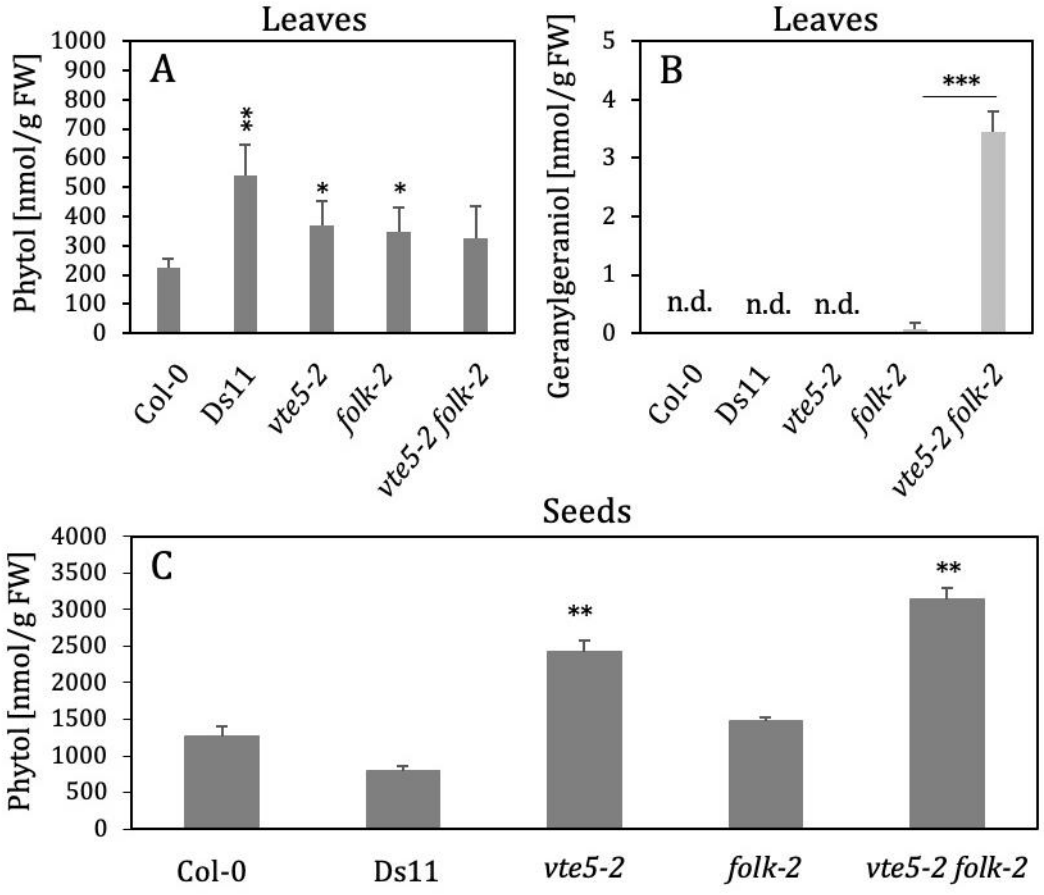

Figure 10 Free isoprenoid alcohol levels in Arabidopsis *vte5-2*, *folk-2,* and *vte5-2 folk-2*.

The free isoprenoid alcohols phytol, geranylgeraniol and farnesol were extracted from leaves (A and B), additionally phytol was extracted from dry seeds (C). Isoprenoid alcohols were analyzed by GC-MS after silylation. While phytol, geranylgeraniol, and farnesol standards could be detected by GC-MS, only phytol and geranylgeraniol but no farnesol were detectable in the leaves. Data represent the mean and SD of three to five replicates. Asterisks indicate significant differences to WT Col-0 (Student's t-test) or when underlined between the samples connected with the line.

3.1.5 Loss of Arabidopsis phytol kinase and farnesol kinase in the *vte5-2 folk-2* mutant has no impact on carotenoid and abscisic acid contents

Carotenoids are synthesized from two molecules of geranylgeranyl-PP. The first committed step of the carotenoid biosynthesis is the head-to-head condensation of two geranylgeranyl-PP molecules to form the C40 carotenoid phytoene (Cunningham and Gantt, 1998). To analyze the role of geranylgeraniol phosphorylation for the biosynthesis of carotenoids, the photosynthetic pigment content and composition were analyzed in the Arabidopsis *vte5-2*, *folk-2,* and *vte5-2 folk-2* mutants. Neoxanthin, violaxanthin, antheraxanthin, lutein, zeaxanthin and *β*-carotene together with chlorophyll a and b were determined by HPLC DAD measurements (Figure 11, B and C). Chlorophyll was spectrophotometrically analyzed in parallel according to Porra *et al.*, (1989) (Figure 11, A). Chlorophyll carries a phytyl-PP derived side chain. Previous *in vitro* studies showed, that geranylgeranyl-PP can be reduced to phytyl-PP and that also geranylgeranylated chlorophyll can be reduced to (phytyl)-chlorophyll by the reductase GGR (Keller *et al.*, 1998). If geranylgeraniol can be remobilized by phosphorylation via VTE5, FOLK, or both, for the biosynthesis of carotenoids or chlorophyll, reduced amounts of carotenoids or chlorophyll are expected in the respective Arabidopsis mutants *vte5-2*, *folk-2,* and *vte5-2 folk-2*. Spectrophotometric chlorophyll analysis revealed no significant differences between *vte5-2*, *folk-2* and *vte5-2 folk-2* in comparison to the Col-0 and Ds11 WT lines (Figure 11, A). Also, no significant differences in the composition of carotenoids could be observed by HPLC DAD measurements (Figure 11, B and C).

The mutation in *folk-2* is described to cause an abscisic acid (ABA) hypersensitive phenotype (Fitzpatrick *et al.*, 2011). Fitzpatrick *et al*. showed that exogenous ABA repressed *FOLK* gene expression in WT plants, and therefore the authors assumed a role for farnesol kinase in negative regulation of ABA signaling. The phytohormone ABA is a C15 sesquiterpene which is synthesized from the carotenoid zeaxanthin (Finkelstein and Rock, 2002). No significant differences in zeaxanthin levels were observed in *folk-2* nor in *vte5-2* or *vte5-2 folk-2*. Nevertheless, to answer the question if mutations in isoprenoid alcohol kinase activity have an impact on the level of ABA, ABA was quantified in leaves of *vte5-2*, *folk-2,* and *vte5-2 folk-2* according to Pan *et al.*, 2008. In agreement with the results of zeaxanthin measurements, no significant differences in the ABA contents were found in the mutant lines in comparison to the Col-0 and Ds11 WT lines (Figure 12). During LC MS/MS analysis of the phytohormone

ABA, also other phytohormones including gibberellic acid (GA), jasmonic acid (JA), the JA precursor 12-oxo-phytodienoic acid (OPDA), and salicylic acid (SA) were preliminarily quantified according to Pan *et al.*, 2008. No differences in the levels of OPDA, JA and SA could be observed in *vte5-2*, *folk-2*, and *vte5-2 folk-2* in comparison to the WT levels (data not shown). Measurements of gibberellic acid were not possible as GA could not be detected in any of the plant extracts.

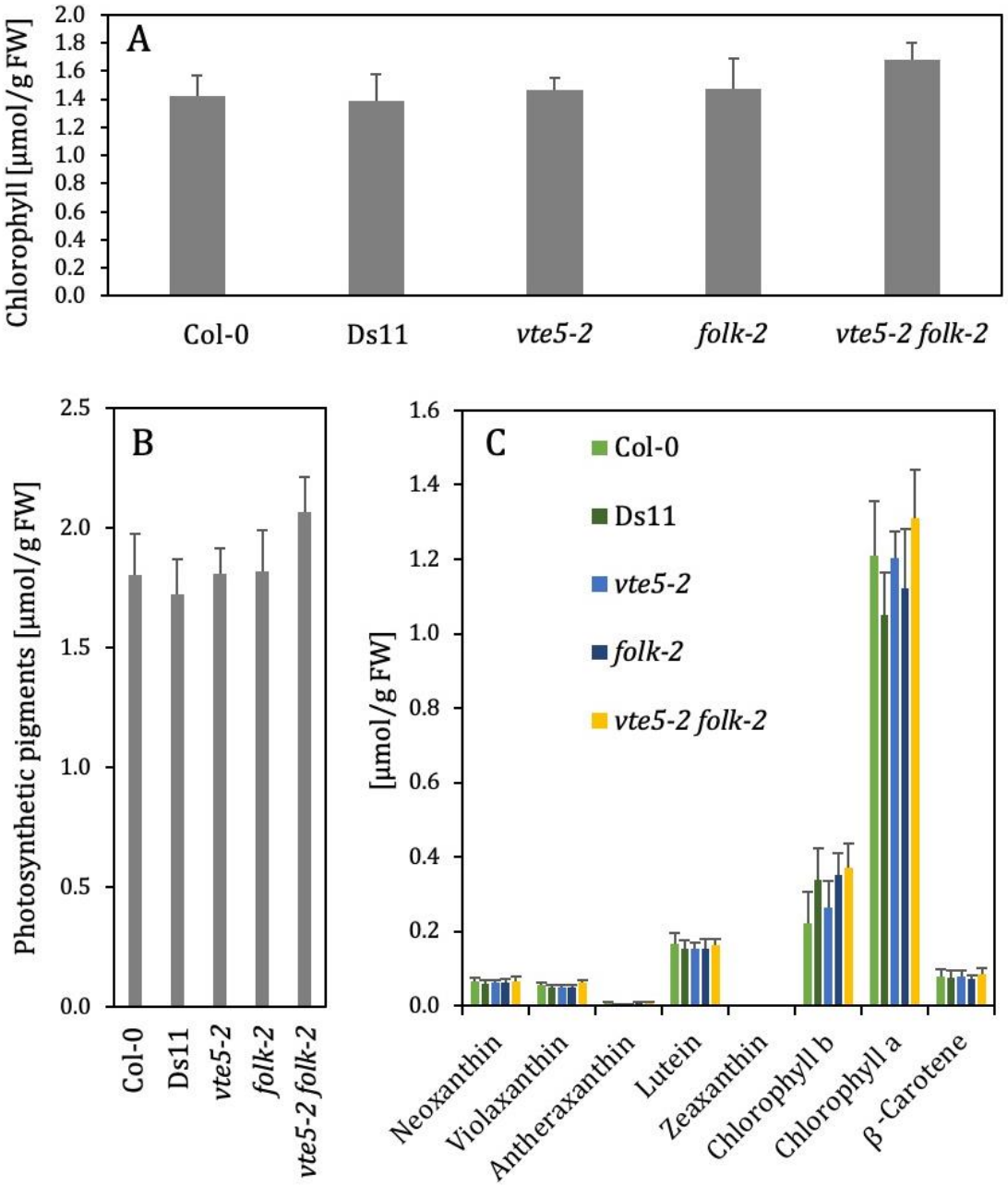

Figure 11 Photosynthetic pigments in *vte5-2*, *folk-2*, and *vte5-2 folk-2*.

Photosynthetic pigments were extracted from leaves of four-week-old Arabidopsis *vte5-2*, *folk-2, vte5-2 folk-2* plants together with the WT lines Col-0 and Ds11. Chlorophyll content (A) was measured spectrophotometrically following Porra *et al*. The total amount of photosynthetic pigments (B) and individual amounts of pigments (C) were determined by HPLC DAD. Data represent the mean and SD of five replicates.

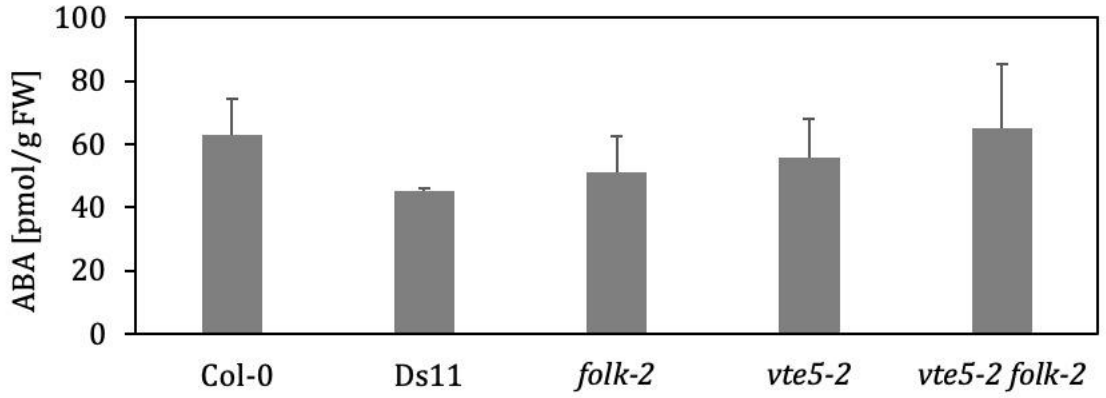

Figure 12 ABA contents in *vte5-2*, *folk-2,* and *vte5-2 folk-2.*

ABA was extracted from leaves of four-week-old Arabidopsis *vte5-2*, *folk-2,* and *vte5-2 folk-2* plants together with the WT Col-0 and Ds11. ABA was analyzed by LC MS/MS with Q-Trap according to Pan *et al.*, 2008. Data represent the mean and SD of five replicates.

3.1.6 Loss of Arabidopsis phytol kinase together with farnesol kinase in *vte5-2 folk-2* has a minor effect on free sterol content

Plants contain a complex mixture of sterols. While in humans, cholesterol is the major sterol, in plants cholesterol is only a minor component. The most abundant sterols in Arabidopsis are β-sitosterol followed by campesterol and stigmasterol (Benveniste, 2002). One of the initial steps of sterol biosynthesis is the formation of the C30 isoprenoid squalene. Squalene is formed by head-to-head condensation of two farnesyl-PP units derived from the cytosolic MVA pathway. As farnesyl-PP is the precursor for sterol biosynthesis, the role of farnesol phosphorylation for the biosynthesis of free sterols was investigated by measurement of the free sterols β-sitosterol, campesterol, stigmasterol and cholesterol. Arabidopsis *folk-2* mutants lack farnesol kinase activity, and therefore if farnesyl-P can be phosphorylated to farnesyl-PP, which might then be integrated into sterol biosynthesis, the content of free sterols in *folk-2* and *vte5-2 folk-2* might be reduced. To address this question, free sterols were extracted from leaves of four-week-old *vte5-2*, *folk-2*, and *vte5-2 folk-2* together with the WT lines Col-0 and Ds11, and after silylation analyzed by GC-MS. The total amount of free sterols (Figure 13, A) was similar in WT Col-0, WT Ds11, *vte5-2,* and *folk-2*. In the *vte5-2 folk-2* double mutant, the total amount of free sterols was significantly lower in comparison to the WT Col-0 and WT Ds11. The content of free sterols was reduced to around 78% of WT Col-0 level in *vte5-2 folk-2*. β-Sitosterol, campesterol and stigmasterol were each significantly reduced in *vte5-2 folk-2* to around 80%, 56% and 10%, respectively, of WT level (Figure 13, B, C and E). No significant differences in

cholesterol were observed. The single mutants *vte5-2* and *folk-2* showed no differences in the contents of free sterols in comparison to the WT controls.

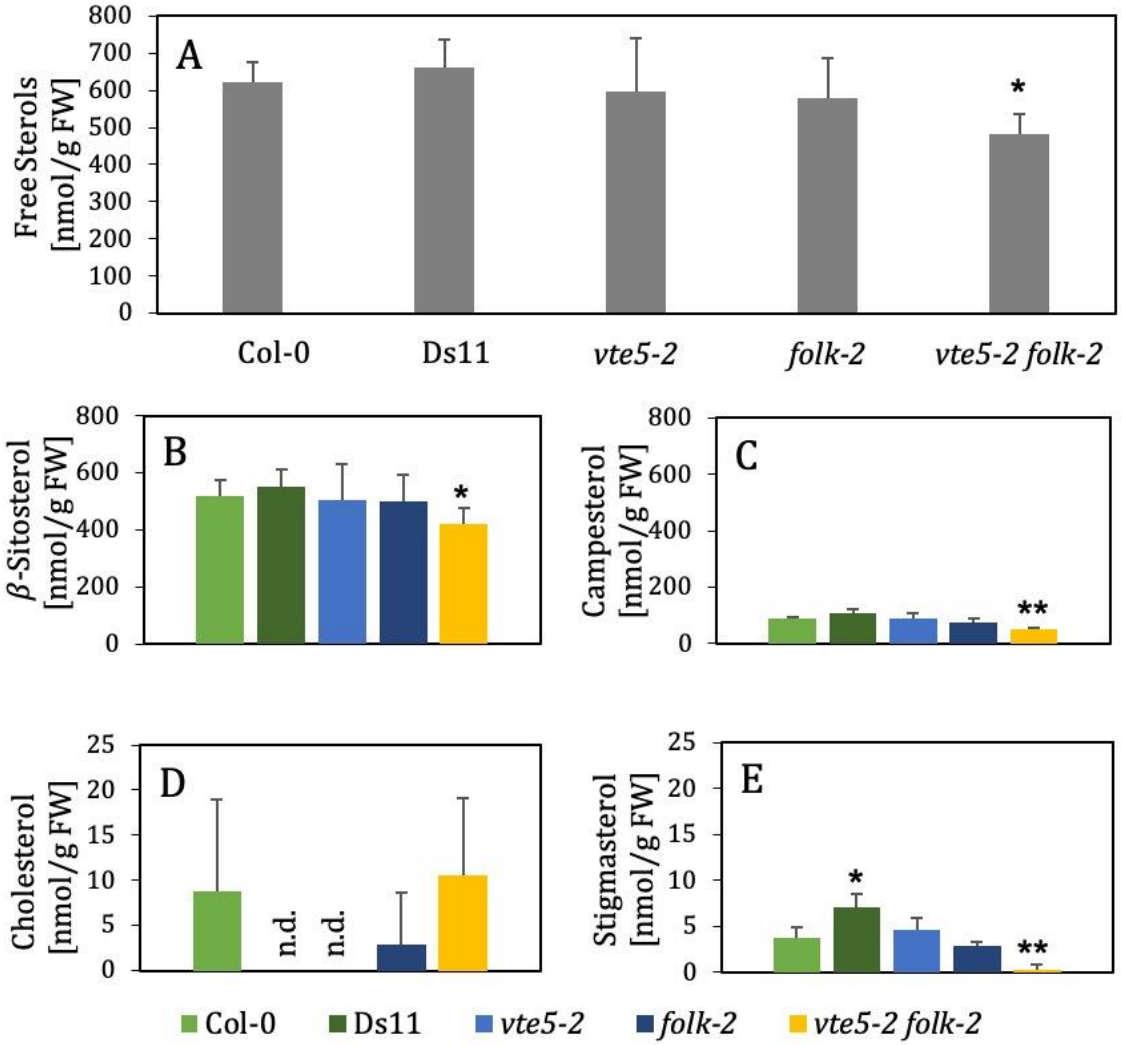

Figure 13 Free sterols in *vte5-2*, *folk-2*, and *vte5-2 folk-2*.

Free sterols were extracted from Arabidopsis *vte5-2, folk-2,* and *vte5-2 folk-2* leaves together with the WT Col-0 and Ds11 and analyzed by GC-MS. Total amount of free sterols (A) includes the sum of *β*-sitosterol (B), campesterol (C), cholesterol (D) and stigmasterol (E). Data represent the mean and SD of three replicates. Asterisks indicate significant differences to WT Col-0 (Student's t-test), (n.d. = not detected).

3.1.7 The defects of phytol kinase and farnesol kinase lead to tocopherol deficiency in the Arabidopsis *vte5-2 folk-2* mutant

Analysis of the isoprenoid alcohol phosphate contents in *vte5-2, folk-2,* and *vte5-2 folk-2* showed reductions of phytyl-P and phytyl-PP. In seeds, significant reductions in the amounts of phytyl-P were observed in all analyzed mutants. As previous studies showed that phytol phosphorylation is essential for the biosynthesis of tocopherol,

tocochromanols were extracted from leaves of four-week-old Arabidopsis *vte5-2*, *folk-2,* and *vte5-2 folk-2* plants together with the WT lines Col-0 and Ds11 (Figure 14, A). Additionally, tocochromanols were also extracted from dry seeds (Figure 14, B), and analyzed by HPLC FLD.

The sum of tocochromanols including *α*-, *β*-, *γ*-, *δ*-tocopherol and plastochromanol-8 (PC-8) was highly significantly reduced in *vte5-2 folk-2* leaves (Figure 14, A) and seeds (Figure 14, B) to nearly 0% of the WT Col-0 and Ds11. The *vte5-2* single mutant retained around 30% of WT Col-0 tocochromanol level in leaves and around 20% in seeds. No differences in the tocochromanol levels were found in the *folk-2* single mutant seeds and leaves in comparison to WT Col-0 and Ds11.

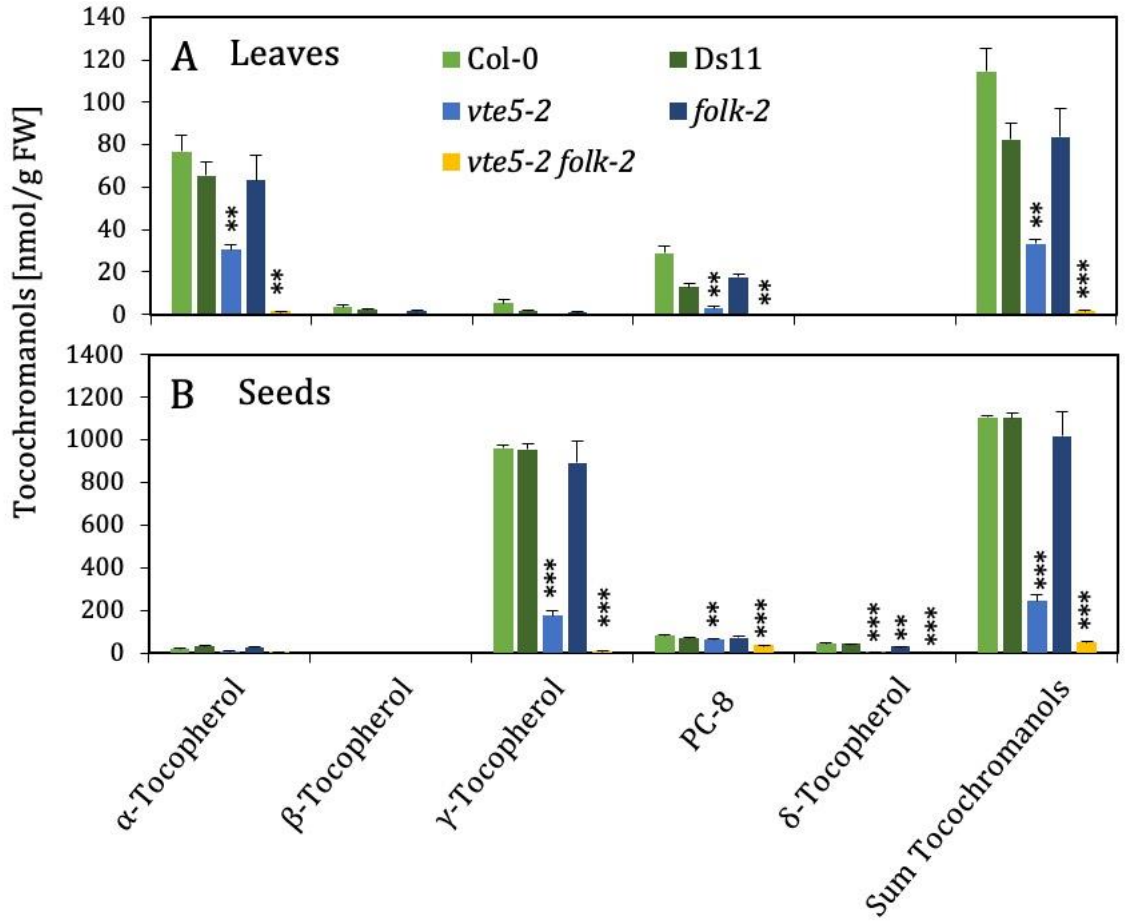

Figure 14 Tocochromanol contents in leaves and seeds of *vte5-2*, *folk-2,* and *vte5-2 folk-2.*

Tocochromanols were extracted from green leaves of four-week old plants (A) or from dried seeds (B) and measured by HPLC FLD. Data represent the mean and SD of five replicates. Asterisks indicate significant differences to WT Col-0 (Student's t-test).

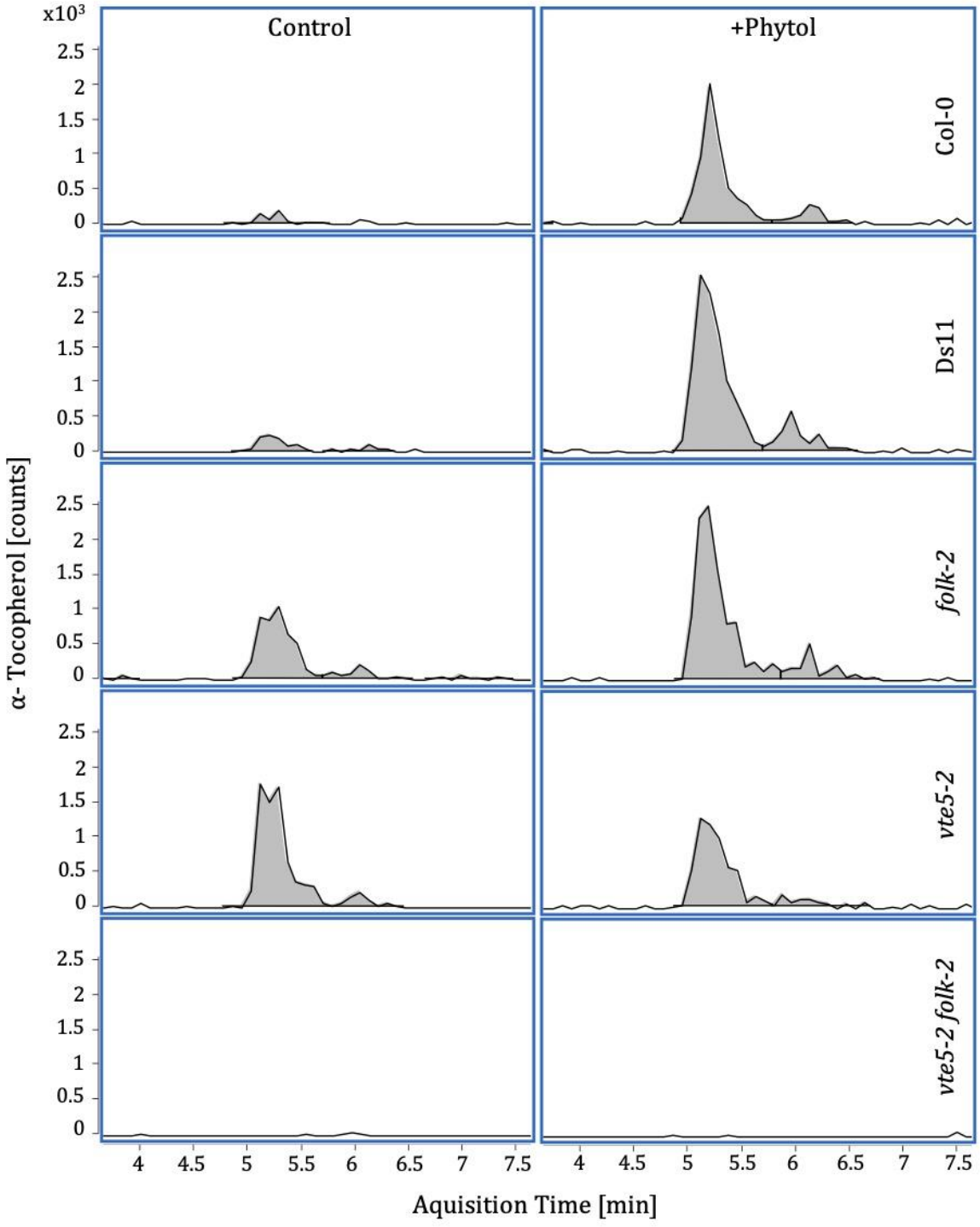

Figure 15 LC MS/MS analysis of *α*-tocopherol in *vte5-2*, *folk-2,* and *vte5-2 folk-2* mutants.

LC MS/MS analysis with Q-TOF of *α*-tocopherol in Arabidopsis leaves from three-week-old seedlings exposed to either 5 mM phytol (+Phytol) or without phytol (control) for 24 h. Representative chromatograms of product ion fragments are shown from the mass transition of *α*-tocopherol m/z 430.3811 to m/z 165.0916. Chromatograms are presented without normalization to fresh weight or internal standard.

During HPLC FLD analysis only small peaks for α-tocopherol were found in *vte5-2 folk-2* leaves. Therefore, it was unclear whether the double mutant leaves contain extremely low amounts of α-tocopherol, or whether they are completely devoid of α-tocopherol. To test whether the *vte5-2 folk-2* double mutant is completely tocopherol deficient, leaf extracts were analyzed by LC MS/MS using a Q-TOF instrument. To increase the precursor availability in the plants, seedlings were grown for 24 h in medium containing phytol. For this experiment, three-week-old seedlings were transferred for 24 h to liquid MES-KOH medium supplemented with 5 mM phytol (+Phytol) or without phytol (control) before the leaves were harvested. While the presence of α-tocopherol was confirmed in Col-0 WT, Ds11 WT, and in *vte5-2* and *folk-2* mutants, no α-tocopherol could be detected by MS/MS analysis in *vte5-2 folk-2* (Figure 15) with or without phytol supplementation. Therefore, the leaves of *vte5-2 folk-2* are absolutely devoid of tocopherol.

3.1.8 Loss of phytol kinase and farnesol kinase leads to a decrease in phylloquinone in Arabidopsis *vte5-2 folk-2*

Analysis of Arabidopsis phytol kinase (*vte5*) and phytyl-P kinase (*vte6*) mutants showed an essential role of phytol phosphorylation for the biosynthesis of tocopherol (vom Dorp *et al.*, 2015). A later study in 2017 showed in addition an essential role of phytyl-P kinase (VTE6) for the biosynthesis of phylloquinone (Wang *et al.*, 2017). As tocopherol biosynthesis in the *vte5-2 folk-2* double mutant line is severely affected, the relevance of FOLK and VTE5 for the biosynthesis of phylloquinone was analyzed. Leaves from four-week-old *vte5-2, folk-2*, *vte5-2 folk-2* lines together with their WT lines Col-0 and Ds11 were extracted and phylloquinone measured by HPLC FLD after post-column derivatization (Figure 16). While the phylloquinone content was increased in *vte5-2* by around 15% compared with the WT Col-0 and Ds11, phylloquinone was also slightly increased in *folk-2* in comparison to the WT lines. In contrast, the *vte5-2 folk-2* double mutant had a 60% reduced level of phylloquinone in comparison to the WT levels.

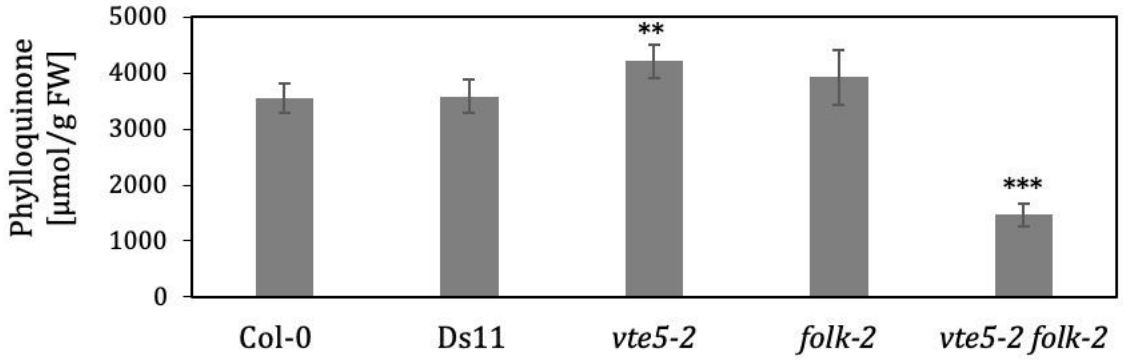

Figure 16 Phylloquinone contents in *vte5-2*, *folk-2*, and *vte5-2 folk-2* leaves.

Phylloquinone was extracted from leaves of four-week-old Arabidopsis *vte5-2*, *folk-2, vte5-2 folk-2* together with the WT lines Col-0 and Ds11 and measured by HPLC FLD after post-column reduction with Zn. Data represent the mean and SD of five replicates. Asterisks indicate significant differences to WT Col-0 (Student's t-test).

3.2 Further characterization of the tocopherol deficient Arabidopsis *vte5-2 folk-2* double mutant

3.2.1 Analysis of fatty acid isoprenoid alcohol esters in Arabidopsis *vte5-2*, *folk-2,* and *vte5-2 folk-2* mutants

Analysis of free isoprenoid alcohols in the Arabidopsis *vte5-2*, *folk-2,* and *vte5-2 folk-2* mutants showed the accumulation of free phytol in *vte5-2* and *folk-2* and in the double mutant *vte5-2 folk-2* (3.1.4). Interestingly in the double mutant also high amounts of free geranylgeraniol were detected in leaves which were not detectable in the WT Col-0, WT Ds11 or in *vte5-2*. In *folk-2* also small amounts of geranylgeraniol were found, but these amounts were much lower than the ones in the *vte5-2 folk-2* double mutant. As free isoprenoid alcohols, including phytol, geranylgeraniol and farnesol, are detrimental to membrane stability, these compounds are of low abundance under normal conditions. Previous studies on phytol metabolism in Arabidopsis showed, that free phytol can be esterified to fatty acid phytyl esters, which are less toxic than the free alcohols (Ischebeck *et al.*, 2006; vom Dorp *et al.*, 2015). To address the question if the accumulation of free phytol and geranylgeraniol observed in the Arabidopsis isoprenoid alcohol kinase mutants *vte5-2*, *folk-2,* and *vte5-2 folk-2* mutants results in an increased production of fatty acid isoprenoid alcohol esters, phytyl esters, geranylgeranyl esters and farnesyl esters were measured in leaves and seeds of the mutants together with the WT Col-0. Isoprenoid alcohol esters were analyzed by direct infusion MS/MS analysis with a Q-TOF instrument according to vom

Dorp (2015). The total amounts of leaf and seed isoprenoid alcohol esters (Figure 17) of the WT (Col-0) and the mutants *vte5-2*, *folk-2,* and *vte5-2 folk-2* were different. In leaves (Figure 17, A), the total amount of phytyl esters was reduced in *vte5-2* and *folk-2* but increased in *vte5-2 folk-2* in comparison to Col-0. Geranylgeranyl esters were very low abundant in Col-0 and even lower in *vte5-2* leaves. In the *folk-2* and the *vte5-2 folk-2* leaves, geranylgeranyl esters were significantly increased in comparison to Col-0. While the *folk-2* single mutant had around 5-fold more geranylgeranyl esters, the *vte5-2 folk-2* had 140-fold more geranylgeranyl esters than the Col-0 WT. Farnesyl esters were detectable in leaf extracts but were of very low abundance in all analyzed lines with no significant differences.

In dry seeds, the total amount of isoprenoid alcohol esters was much higher than in leaves. The total amount of phytyl esters was significantly increased in *vte5-2* and *vte5-2 folk-2* seeds in comparison to the Col-0 WT (Figure 17, B). No difference in phytyl ester content in *folk-2* was observed in comparison to Col-0. In contrast, *vte5-2* seeds had around 2-fold more phytyl esters and *vte5-2 folk-2* had 1.5-fold more phytyl esters in seeds than the Col-0 WT. Geranylgeranyl ester levels were significant higher in all mutant seeds in comparison to Col-0. Geranylgeranyl ester levels were 6-fold higher in *vte5-2* than the levels found in Col-0. In *folk-2,* geranylgeranyl esters were 22-fold higher and in *vte5-2 folk-2* the levels were even 50-fold higher than in Col-0. Farnesyl esters were also of very low abundance, but significantly more farnesyl esters were found in *folk-2* and *vte5-2 folk-2* seeds in comparison to the WT Col-0.

Analysis of the individual fatty acid composition of the esters showed, that the main fatty acid in phytyl esters in leaves was the 16:3 fatty acid (Figure 18, A). Interestingly, the *vte5-2 folk-2* double mutant showed less phytol esterification to 16:3 than the WT, but phytol was rather esterified also to 16:0, 18:3 and 20:3. These fatty acids were much less abundant in phytyl esters of WT Col-0 leaves. In seeds, phytol was mainly esterified to 18:2 and 18:3 followed by 16:3 and 16:0 fatty acids (Figure 19, A).

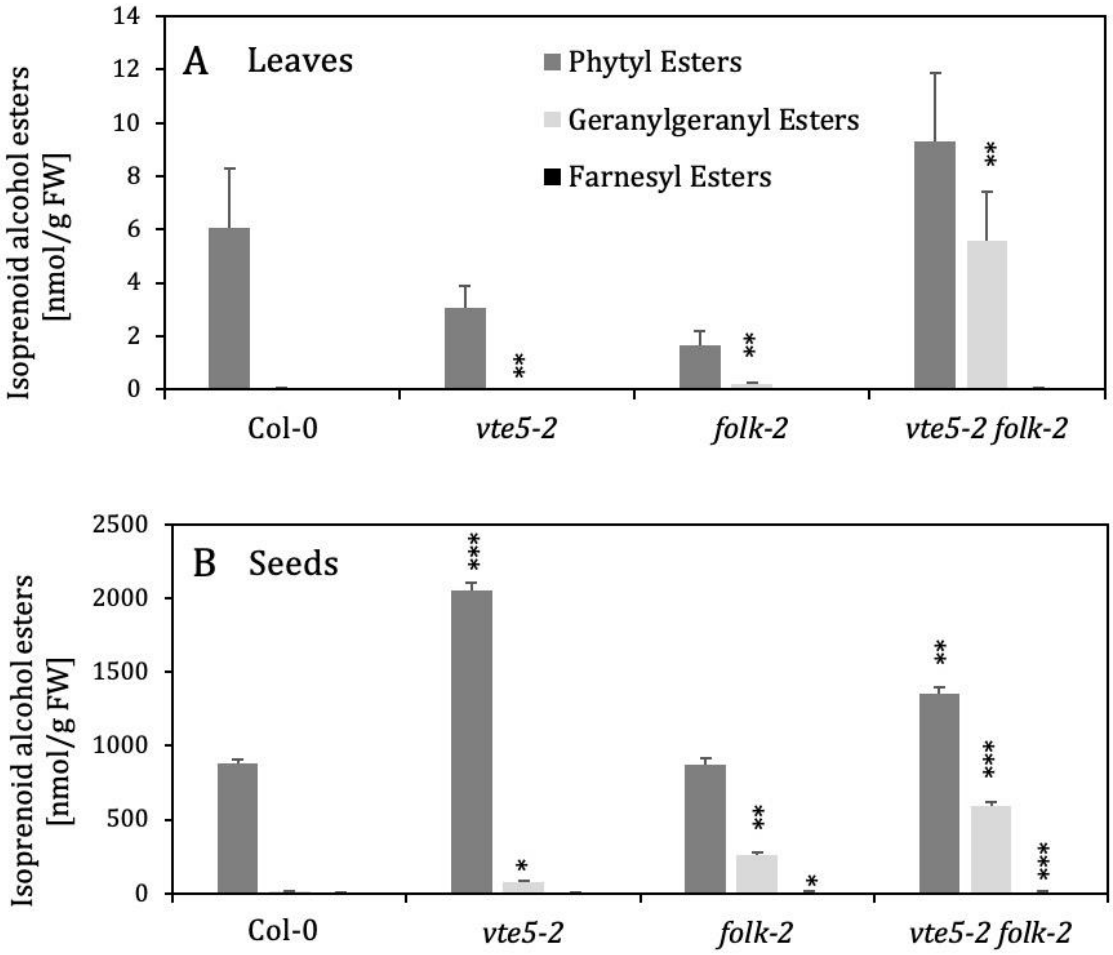

Figure 17 Total amount of fatty acid isoprenoid alcohol esters in Arabidopsis *vte5-2*, *folk-2,* and *vte5-2 folk-2* mutant leaves and seeds.

Fatty acid phytyl esters, geranylgeranyl esters, and farnesyl esters were determined by direct infusion Q-TOF MS/MS in leaves (A) from four-week-old Arabidopsis plants or from dry seeds (B). Data represent the mean and SD of three replicates. Asterisks indicate significant differences to the WT Col-0 (Student's t-test).

Geranylgeranyl esters (Figure 18 and Figure 19, B), which were highly abundant in *vte5-2 folk-2* leaves and seeds, were mainly esterified in the mutant leaves to 16:0 but also to 18:3 and 20:0. In seeds, the main fatty acids esterified to geranylgeraniol were 18:2 and 18:3. Farnesyl esters (Figure 18 and Figure 19, C), were very low abundant, but in the *vte5-2 folk-2* and *folk-2* mutant the levels were increased in leaves and seeds compared to the WT level. In leaves (Figure 18, C) of *vte5-2 folk-2,* the main fatty acid esterified to farnesol was 18:3 followed by 16:0, 16:3 and 20:0. In Col-0 leaves the main farnesyl esters were esterified with 20:0 followed by 16:3 fatty acid. In seeds of *vte5-2 folk-2* and *folk-2*, the main fatty acids esterified to farnesol were 18:2 and 18:3 in *vte5-2 folk-2* as well as in *folk-2*. In the Col-0 WT seeds hardly any 18:2 or 18:3

farnesyl esters were present. The main farnesyl esters found in Col-0 seeds were 16:3 followed by 20:0 (Figure 19, C).

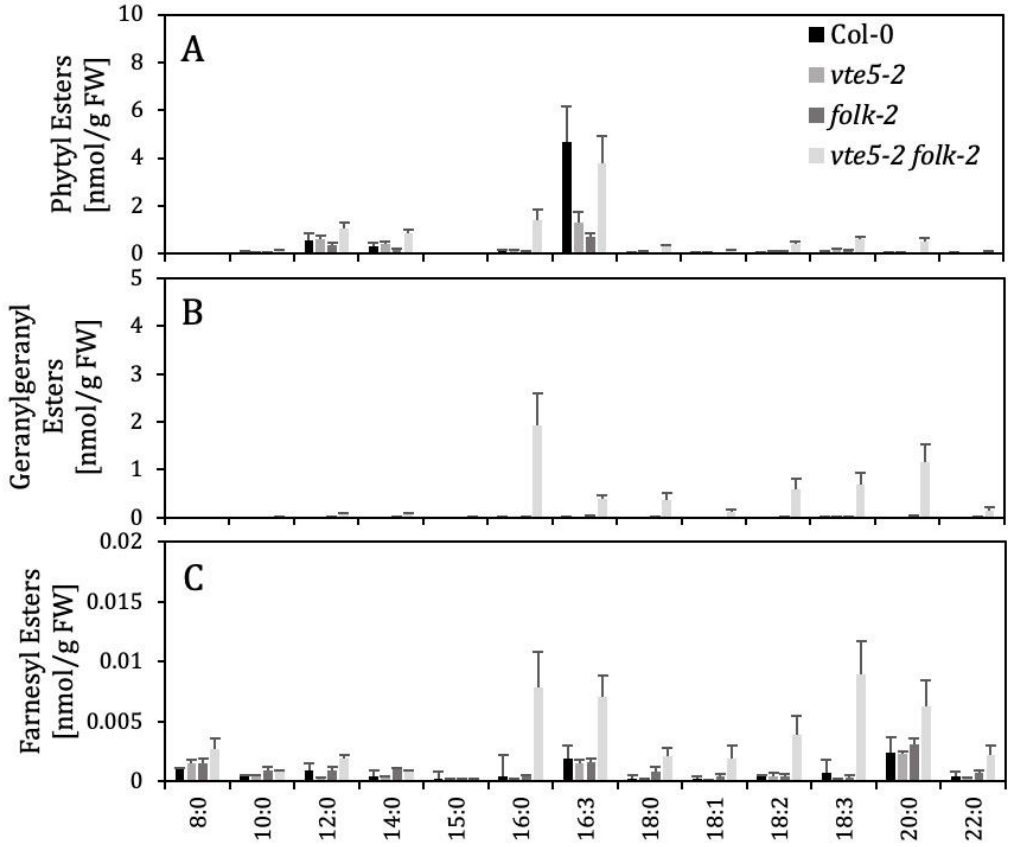

Figure 18 Fatty acid isoprenoid alcohol esters in Arabidopsis *vte5-2*, *folk-2*, and *vte5-2 folk-2* leaves.

Individual composition of fatty acid isoprenoid alcohol esters in Arabidopsis *vte5-2*, *folk-2*, and *vte5-2 folk-2* leaves in comparison to the WT Col-0. Fatty acid phytyl esters (A), and geranylgeranyl esters (B) and farnesyl esters (C) were determined by direct infusion Q-TOF MS/MS in leaves from four-week old Arabidopsis plants. Data represent the mean and SD of three replicates. Asterisks indicate significant differences to the WT Col-0 (Student's t-test).

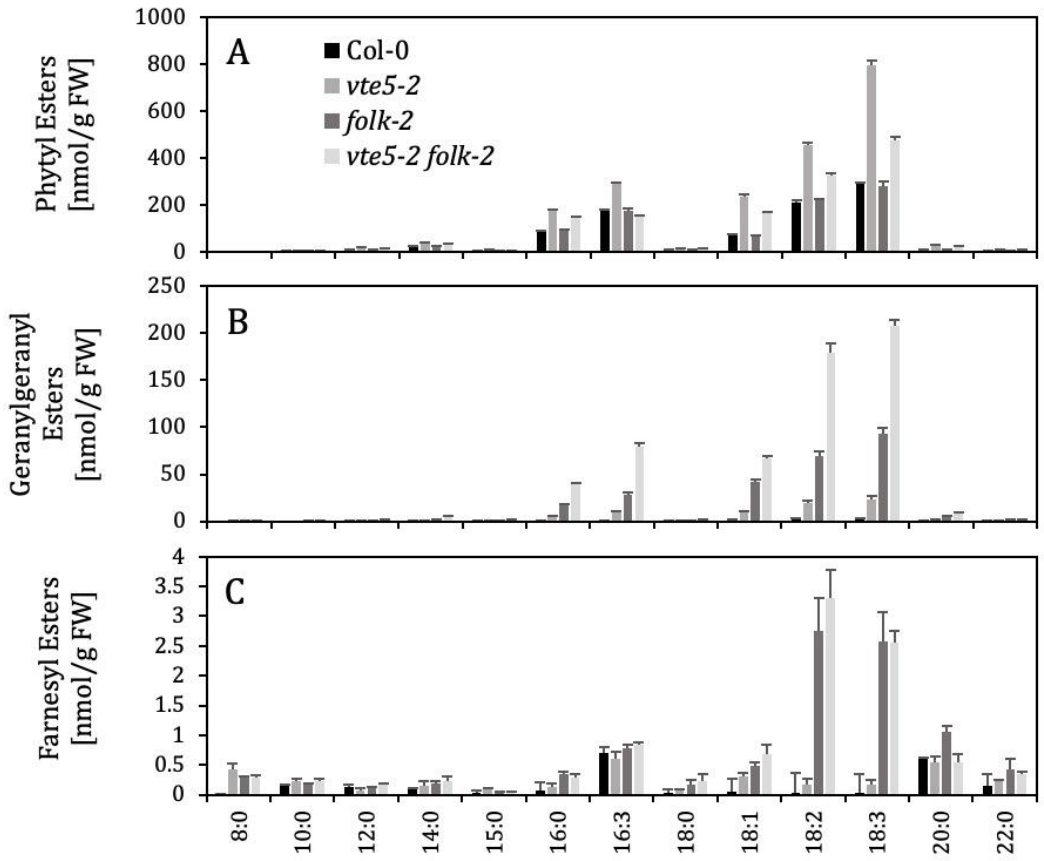

Figure 19 Fatty acid isoprenoid alcohol esters in Arabidopsis *vte5-2*, *folk-2,* and *vte5-2 folk-2* seeds.

Individual composition of fatty acid isoprenoid alcohol esters in Arabidopsis *vte5-2*, *folk-2,* and *vte5-2 folk-2* seeds in comparison to the WT Col-0. Fatty acid phytyl esters (A), and geranylgeranyl esters (B) and farnesyl esters (C) were determined by direct infusion Q-TOF MS/MS in dry seeds. Data represent the mean and SD of three replicates. Asterisks indicate significant differences to the WT Col-0 (Student's t-test).

3.2.2 Analysis of phytenal in Arabidopsis *vte5-2*, *folk-2,* and *vte5-2 folk-2* mutants

In plants, phytol can be converted into phytyl esters to decrease the amount of free phytol which is toxic. In mammals, phytol is degraded via α- and β-oxidation. It is possible, that plants like Arabidopsis harbor a phytol degradation pathway similar to mammals. As high amounts of free phytol were found in the leaves of *vte5-2*, *folk-2,* and *vte5-2 folk-2* mutants, it was possible that phytol degradation products might also accumulate. Phytenal, which is a known phytol degradation product in mammals, was therefore measured in leaves of *vte5-2*, *folk-2* and *vte5-2 folk-2* together with the WT lines Col-0 and Ds11. Phytenal was extracted from green leaves of four-week old Arabidopsis plants and derivatized as described in 2.6.9, and analyzed by LC MS/MS

analysis with a Q-Trap instrument. In agreement with the increased amounts of free phytol in *vte5-2* and *vte5-2 folk-2* leaves, significantly more phytenal was detected in *vte5-2* and *vte5-2 folk-2* in comparison to the Col-0 and Ds11 WT lines. Phytenal levels in *folk-2* were similar to the WT levels (Figure 20).

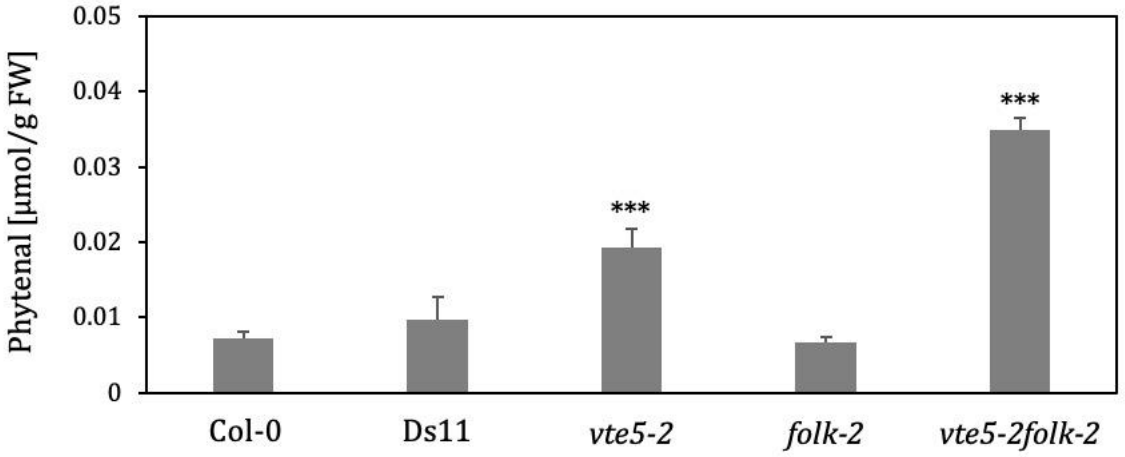

Figure 20 Phytenal in *vte5-2, folk-2,* and *vte5-2 folk-2* leaves.

Phytenal was extracted from leaves of four-week old Arabidopsis *vte5-2*, *folk-2,* and *vte5-2 folk-2* mutant plants together with the WT Col-0 and Ds11, derivatized and analyzed by LC MS/MS with Q-Trap. Data represent the mean and SD of five replicates. Asterisks indicate significant differences to the WT Col-0 (Student's t-test).

3.2.3 Phytyl lipid analysis in *vte5-2*, *folk-2,* and *vte5-2 folk-2* after nitrogen starvation

Abiotic stress, including nutrient starvation such as nitrogen deprivation, leads to the reorganization of many metabolic pathways to ensure survival of the plant. Under nitrogen deprivation, proteins are degraded to release nitrogen. Along with the degradation of proteins important for photosynthesis, large amounts of chlorophyll are degraded to reduce its phototoxic properties (Gaude *et al.*, 2007). When chlorophyll is degraded, high amounts of phytol are released. Previous studies showed, that upon different biotic and abiotic stresses, tocopherol is increased in plants. Especially high accumulation of tocopherol was observed in plants after nitrogen starvation (Gaude *et al.*, 2007; vom Dorp, 2015). This increase in tocopherol was later linked to the degradation of chlorophyll. Upon nitrogen starvation, chlorophyll is degraded and free phytol released. The free phytol is phosphorylated by VTE5 and VTE6 to enter the pathway of tocopherol synthesis (vom Dorp *et al.*, 2015). As Arabidopsis mutants with a defect in phytol kinase (*vte5-2*) still contain about 50% of WT tocopherol levels in leaves and about 20% in seeds, the question came up, whether the *vte5-2 folk-2* double

mutant, which is completely tocopherol deficient, shows stronger changes in phytol metabolism after stress treatment. Therefore, the double mutant *vte5-2 folk-2* together with the single mutants *vte5-2* and *folk-2* were analyzed after nitrogen starvation. Two-week-old Arabidopsis plants were transferred to nitrogen depleted medium (-N) or to nitrogen containing medium (+N) as control. After 12 days, when chlorophyll degradation was visible as chlorotic leaves of plants grown on -N medium, phytyl lipids including chlorophyll (Figure 21, A), phytol (Figure 21, B), tocopherol (Figure 21, C), and fatty acid isoprenoid alcohol esters (Figure 22) were analyzed.

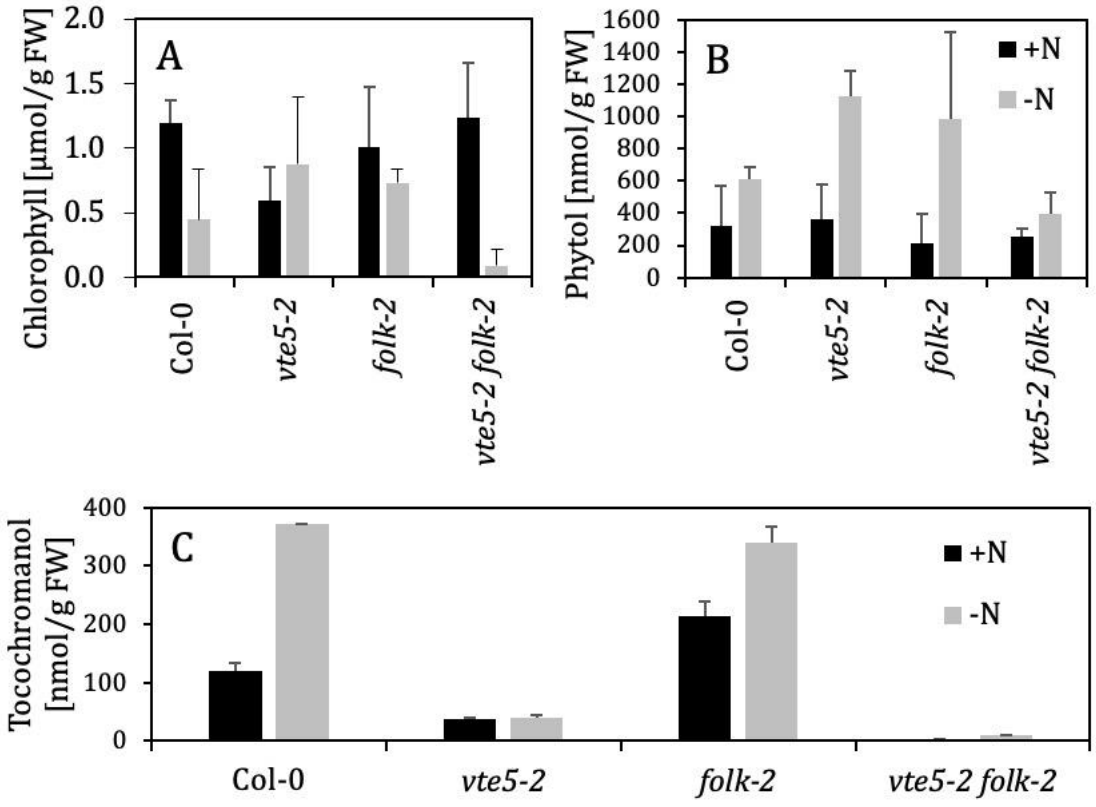

Figure 21 Chlorophyll, phytol, and tocochromanol contents in *vte5-2 folk-2* after nitrogen starvation.

Arabidopsis *vte5-2*, *folk-2,* and *vte5-2 folk-2* mutants were grown together with the Col-0 WT for two weeks on MS medium containing 1% sucrose. Afterward, plants were transferred for 12 days either to nitrogen deficient medium (-N) or to nitrogen containing medium (+N) as control. Chlorophyll (A) was determined by spectrophotometry, phytol (B) (after derivatization) by GC-MS and tocochromanol (C) was determined by HPLC FLD analysis. Data represent the mean and SD of three to five replicates.

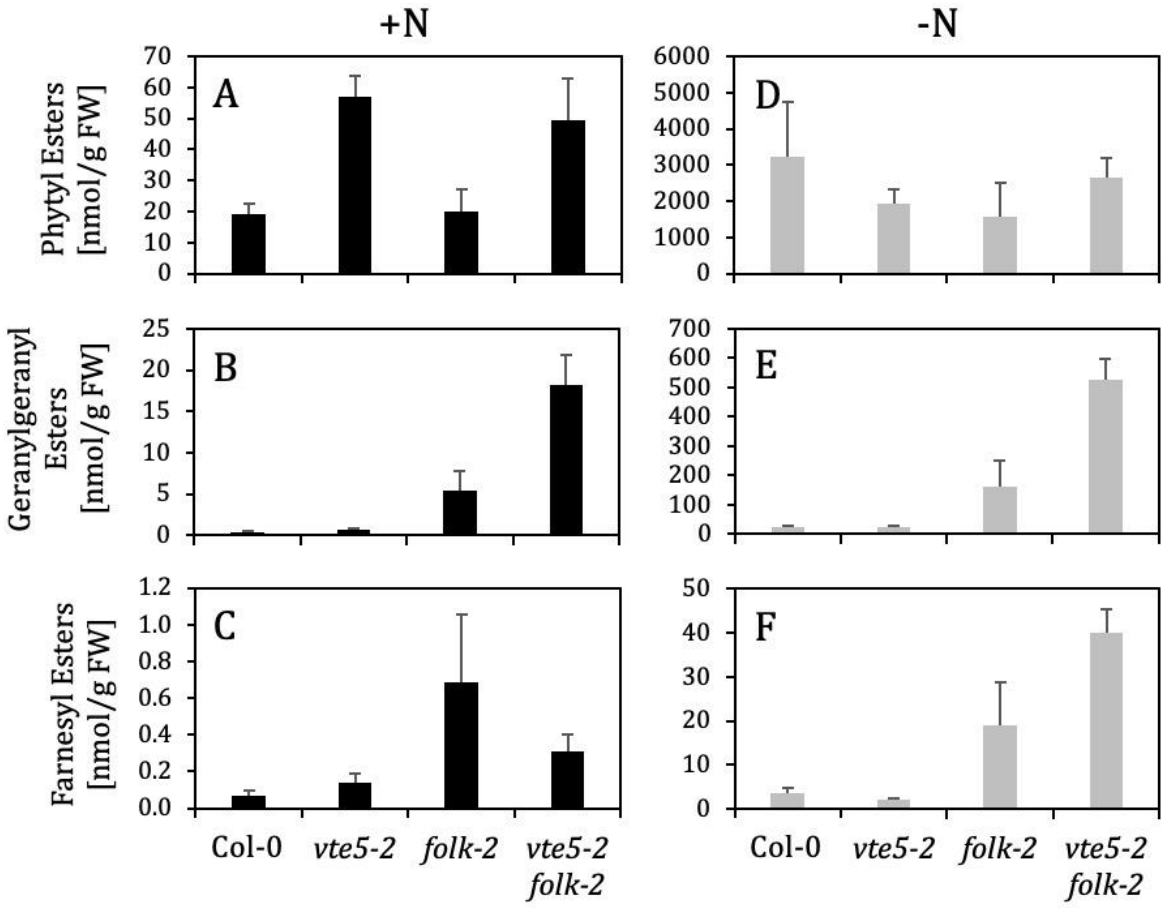

Figure 22 Isoprenoid alcohol ester contents in *vte5-2*, *folk-2* and *vte5-2 folk-2* leaves after nitrogen starvation.

Arabidopsis *vte5-2*, *folk-2,* and *vte5-2 folk-2* mutants were grown together with the Col-0 WT for two weeks on MS medium containing 1% sucrose. Afterward, plants were transferred for 12 days either to nitrogen deficient medium (-N) or to nitrogen containing medium (+N). Fatty acid isoprenoid alcohol esters were analyzed by direct infusion Q-TOF MS/MS. Data represent the mean and SD of three to five replicates.

The differences between the mutants and the Col-0 WT that were observed after growth on control medium (+N) were similar as observed before with plants growing on soil. No differences in growth were observed between the mutant plants and the WT lines when grown on nitrogen depleted medium.

While chlorophyll was decreased after nitrogen deprivation in Col-0, *folk-2,* and *vte5-2 folk-2*, chlorophyll was slightly higher in *vte5-2* with high standard deviation. The content of free phytol was increased upon nitrogen deprivation in all plants analyzed in comparison to the same line grown on nitrogen containing medium. Tocopherol levels were increased after nitrogen deprivation in Col-0 and *folk-2* but not in *vte5-2* nor in *vte5-2 folk-2* in comparison to the same line grown on nitrogen containing medium. Analysis of fatty acid isoprenoid alcohol esters showed a strong

increase of phytyl esters, geranylgeranyl esters as well as farnesyl esters upon nitrogen deprivation (Figure 22). While phytyl esters were highly increased after nitrogen deprivation in Col-0 as well as in all mutant lines, geranylgeranyl esters were highest in *vte5-2 folk-2* followed by *folk-2*. Similar to geranylgeranyl esters, farnesyl esters were strongly increased in *vte5-2 folk-2* followed by *folk-2* upon nitrogen deprivation.

3.2.4 The photosynthetic quantum yield of *vte5-2 folk-2* mutant plants is unaffected

Phylloquinone is required for photosystem I complex stability (Wang *et al.*, 2017). The Arabidopsis *vte5-2 folk-2* leaves showed a reduction in phylloquinone content to around 40% of the WT level (3.1.8). In addition, the leaves and seeds of *vte5-2 folk-2* mutant plants lack tocopherol (3.1.7). Tocopherols are important antioxidants able to prevent lipid oxidation in the thylakoid membrane. To analyze whether the decrease in phylloquinone or tocopherol affects the chloroplast architecture, the ultrastructure of *vte5-2*, *folk-2,* and *vte5-2 folk-2* chloroplasts was analyzed. Additionally, the photosynthetic quantum yield was determined in leaves by PAM fluorometry after exposure to different light intensities.

Chloroplast ultrastructure pictures were prepared by Dr. Michael Melzer (IPK Gatersleben) as described in 2.5.9. Analysis showed no visible alterations of the thylakoid membrane (Figure 23). Also, no visible alterations of plastoglobuli size or numbers were observed (data not shown).

Analysis of the photosynthetic quantum yield was performed by measurement of the chlorophyll fluorescence in leaves using PAM fluorometry. Plants were dark adapted for 1 h, and afterward exposed to a PAR of either 0 µmol/(s·m^2) photosynthetically active radiation (dark), 150 µmol/(s·m^2) (normal light), 500 or 900 µmol/(s·m^2) (high light). The photosynthetic quantum yield of photosystem II (YII) was calculated as described in section 2.5.8. The single mutant plants as well as the double mutant plants showed a similar photosynthetic quantum yield with no significant differences to their corresponding WT lines Col-0 and Ds11 under all light conditions (Figure 24).

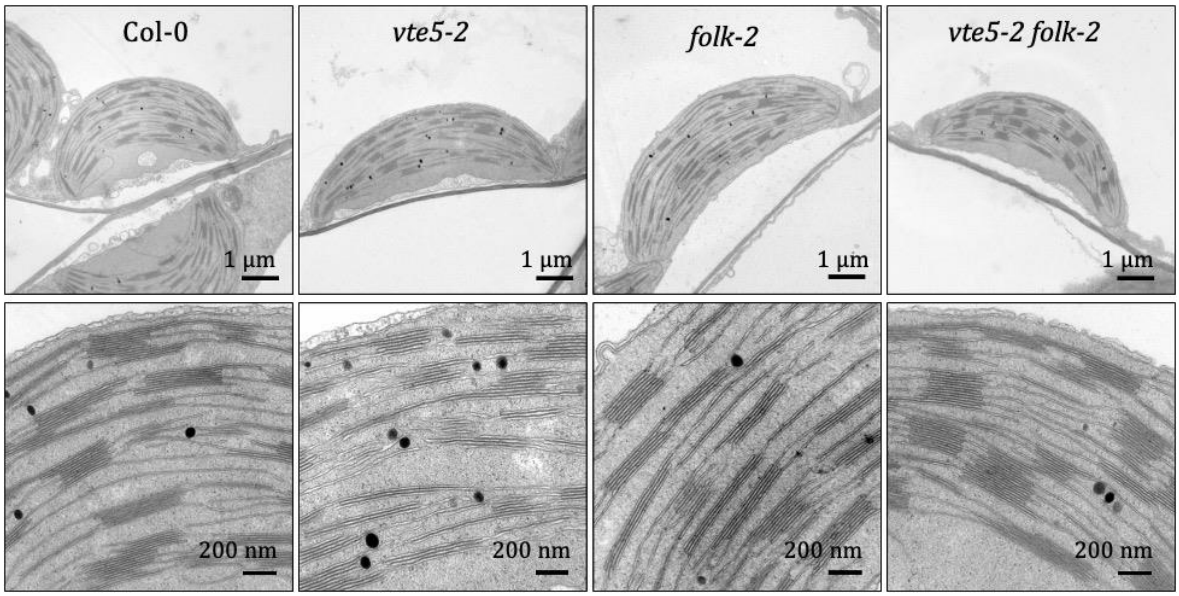

Figure 23 Chloroplast ultrastructure of *vte5-2*, *folk-2,* and *vte5-2 folk-2.*

Chloroplast ultrastructure was analyzed in leaves of four-week-old plants grown on soil by transmission electron microscope analysis. Plants were dark adapted before leaf cross sectioning. Cross sections were stained with methylene azur II stain, fixed by microwave assisted chemical fixation and spur resin. No differences in the chloroplast structure were observed in the mutant lines in comparison to the WT Col-0.

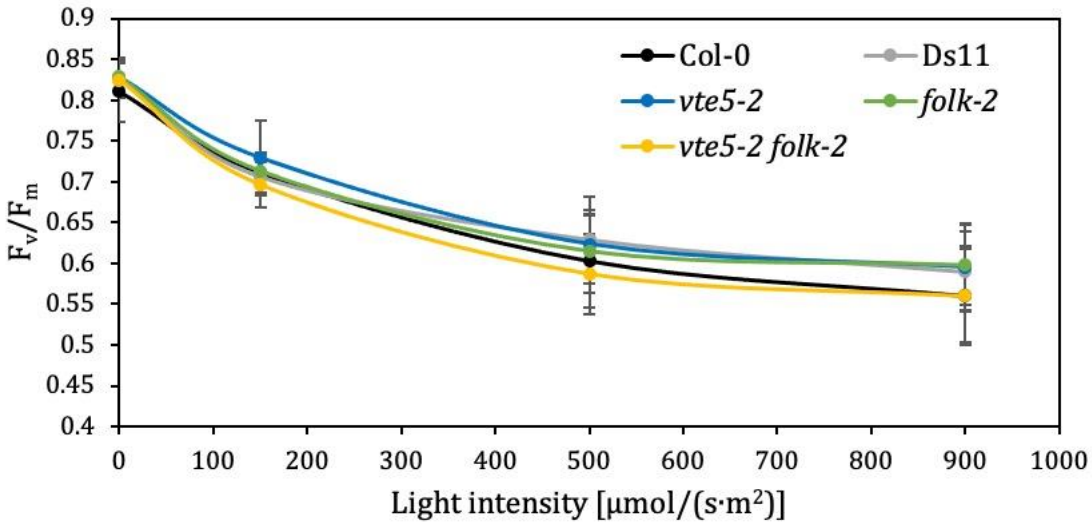

Figure 24 Photosynthetic quantum yield in *vte5-2*, *folk-2,* and *vte5-2 folk-2* leaves.

Photosynthetic quantum yield was measured in leaves of the Arabidopsis mutants *vte5-2, folk-2,* and *vte5-2 folk-2* together with the WT lines Col-0 and Ds11 by pulse amplified modulation (PAM). Plants were dark exposed for 1 h before the measurements and then exposed to the light conditions as indicated for 5 min each. Data represent the mean and SD of five plants per line and 10 measurements per plant and per radiation level.

3.2.5 Seed longevity is impaired in *vte5-2 folk-2*

Tocopherol was shown to be essential for seed germination after long seed storage periods. Tocopherol deficient Arabidopsis mutant seeds, including *vte1*, *vte2* and *vte6,* in common show a poor germination rate after a couple of months of storage (Sattler *et al.*, 2004; vom Dorp *et al.*, 2015). Sattler *et al*. employed a protocol for accelerated aging of Arabidopsis seeds. After incubation of seeds for 72 h at 40 °C, 100% humidity for accelerated aging, Sattler *et al*. could show that the germination rate of *vte1-1* and *vte2-1* seeds was compromised (Sattler *et al.*, 2004). To study whether the tocopherol deficient *vte5-2 folk-2* mutant also shows reduced seed longevity, *vte5-2*, *folk-2,* and *vte5-2 folk-2* seeds were aged according to Sattler *et al*., the germination rate determined, and compared to the respective WT Col-0 and Ds11 controls. While the germination rate of the untreated fresh seeds (about one month after harvesting, stored at 4 °C) (Figure 25, A) was similar in all analyzed mutants and the WT controls, the seed germination rate was significantly lower after four days of germination in the tocopherol deficient *vte5-2 folk-2* seeds after accelerated aging (Figure 25, B). The artificially aged *vte5-2 folk-2* seeds only reached a germination rate of 63%. After accelerated aging, the germination rates of *vte5-2* and of DS11 seeds were slightly, but not significantly lower in comparison to the same seeds without accelerated aging. Aged *vte5-2* and Ds11 seeds reached only a germination rate slightly above 90% five days after imbibition. The germination rate of the aged seeds of the *folk-2* mutant and of Col-0 remained unchanged in comparison to their untreated controls. Untreated seeds of these two lines reached 100% germination after two days and germination rate of aged seeds reached 100% after three days.

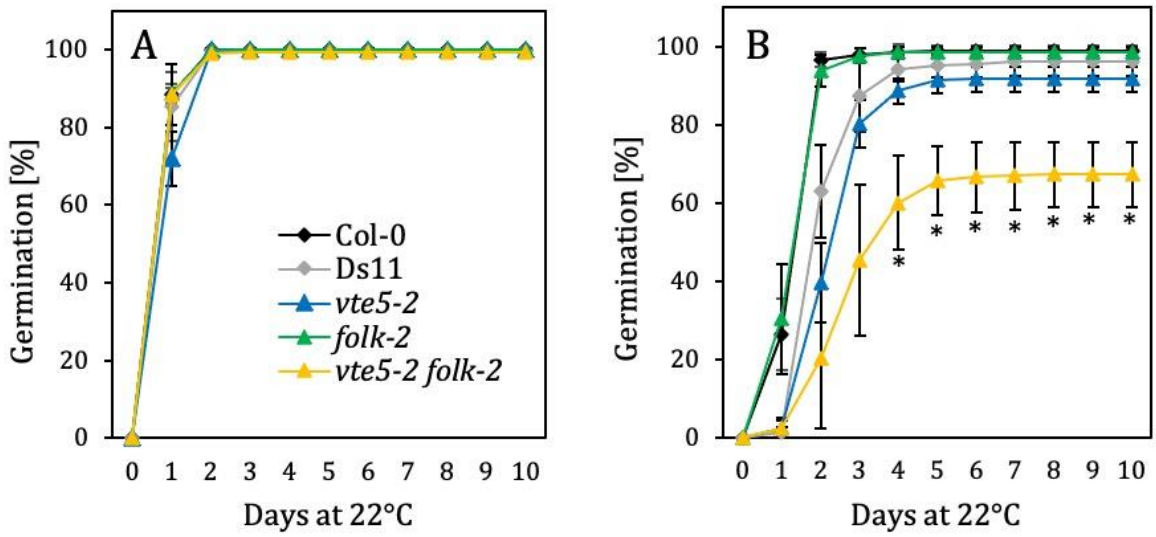

Figure 25 Seed germination rate of *vte5-2*, *folk-2*, and *vte5-2 folk-2* after accelerated aging.

Seed germination was analyzed in one-month old, dry seeds without treatment (stored at 4 °C) (A) and in dry seeds which were aged in accelerated manner according to Sattler *et al.* (2004) at 40 °C and 100% humidity for 72 h (B). Seeds were placed on wet filter papers and after one day of stratification, the germination rate was counted every day. The WT Col-0 (background of *folk-2)* and the WT Ds11 (donor line of *vte5-2*) were used as controls. While all seeds reached a germination rate of 100% after three days of germination without treatment (A), germination of seeds from the accelerated aging treatment (B) was partially impaired. Col-0 and *folk-2* seeds reached 98% germination after four days. The WT Ds11 and the *vte5-2* seeds only reached a germination rate slightly above 90% after four days. The *vte5-2 folk-2* seeds had a significantly reduced germination rate after four days and only reached a final germination rate of 67%. Data represent the mean and SD of 100±1 seeds analyzed from three different plants per line. Asterisks indicate significant differences to WT Col-0 (Student's t-test).

3.2.6 Supplementation of *vte5-2*, *folk-2,* and *vte5-2 folk-2* with homogentisate

While Arabidopsis only contains tocopherols under normal conditions, tocotrienols are high abundant in seeds of monocot plants. Previous attempts to increase the tocopherol content in Arabidopsis included the overexpression of tocopherol biosynthetic genes in leaves or seeds. The first committed step, the condensation of homogentisic acid (homogentisate, HGA) and phytyl-PP, was described to be a bottleneck reaction for tocopherol synthesis. Altering the HGA production in transgenic Arabidopsis demonstrated, that the HGA content is limiting for tocopherol synthesis (Stacey *et al.*, 2016; Mène-Saffrané and Pellaud, 2017). In addition, genetic engineering of HGA biosynthesis for enhanced HGA production, led to an increase in tocotrienol synthesis in Arabidopsis. This was unusual because Arabidopsis usually does not contain tocotrienol. To test, whether exogenous supplementation of HGA to plants can lead to HGA increase and stimulation of the tocopherol biosynthesis, Arabidopsis seedlings were grown on synthetic MS medium containing 5 mM HGA or lacking HGA (0 mM) as control. Afterward, tocochromanols

(including tocopherols, tocotrienols and PC-8) were extracted from leaves and analyzed by HPLC FLD. The total tocochromanol content was increased in Col-0 WT by around 50% after growth on HGA containing medium in comparison to the 0 mM HGA control (Figure 26). The tocochromanol content was unchanged in the Ds11 WT line and in the mutants *vte5-2*, *folk-2,* and *vte5-2 folk-2,* after growth on HGA containing medium.

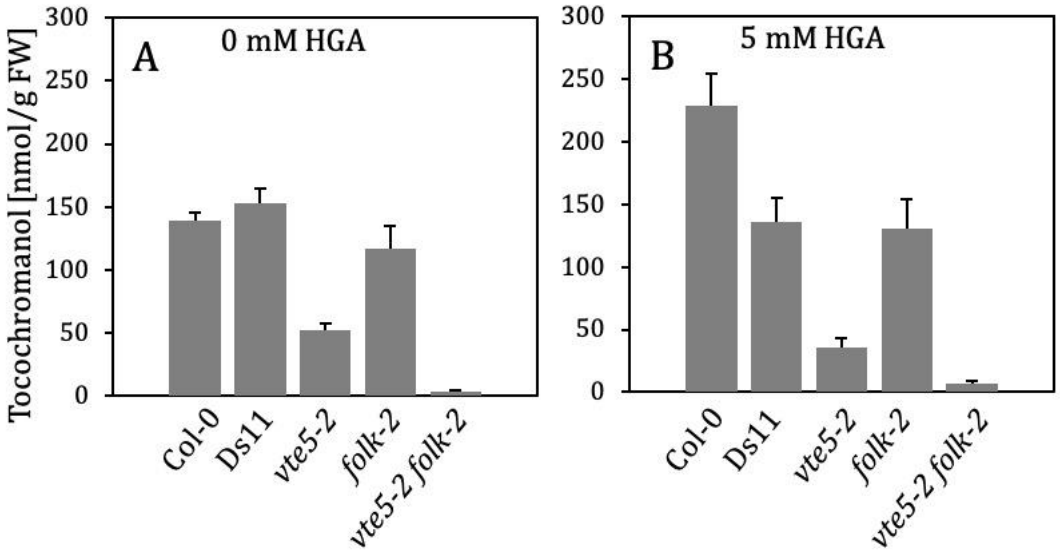

Figure 26 Tocochromanol content in WT Col-0, WT Ds11, *vte5-2, folk-2,* and *vte5-2 folk-2* after HGA supplementation

Arabidopsis WT Col-0, WT Ds11 and the mutants *vte5-2, folk-2,* and *vte5-2 folk-2* were grown on medium supplemented with 5 mM HGA (B) or without HGA (A). Plants were grown for two weeks on MS medium and afterward transferred to HGA containing MS medium for nine days. Tocochromanols (tocopherols, tocotrienols and PC-8) were extracted from leaves and analyzed by HPLC FLD. Data represent the mean and SD of five replicas.

Interestingly, in the leaf extracts from plants grown on HGA containing medium, small amounts of tocotrienols were detected. Tocotrienols are normally absent as Arabidopsis lacks a homogentisate geranylgeranyl transferase (HGGT) activity involved in tocotrienol synthesis in monocots. Tocotrienols are synthesized from HGA by attachment of the geranylgeranyl-PP side chain. After growth on HGA supplemented medium, minor amounts of α-tocotrienol were found in WT Col-0 plants (Figure 27) while other tocotrienols were not detected (n.d.). No tocotrienols were found in the Ds11 WT and small amounts of α-tocotrienol were found in *folk-2*. The phytol kinase mutant *vte5-2* which has reduced amounts of tocopherol, contained small amounts of α-tocotrienol and in addition, also γ-tocotrienol. The *vte5-2 folk-2* double mutant,

which is tocopherol deficient, contained small amounts of α-tocotrienol as well as γ-tocotrienol after supplementation with HGA in similar amounts as found in *vte5-2.* The presence of α-tocotrienol and γ-tocotrienol was confirmed by LC MS/MS analysis with a Q-Trap (appendix 7.4). LC MS/MS analysis of tocotrienols also revealed very low peaks for γ-tocotrienol (β- and γ-tocotrienol, because of their identical mass and very similar retention time they were not separable in LC MS/MS) in the Col-0 WT after supplementation with HGA.

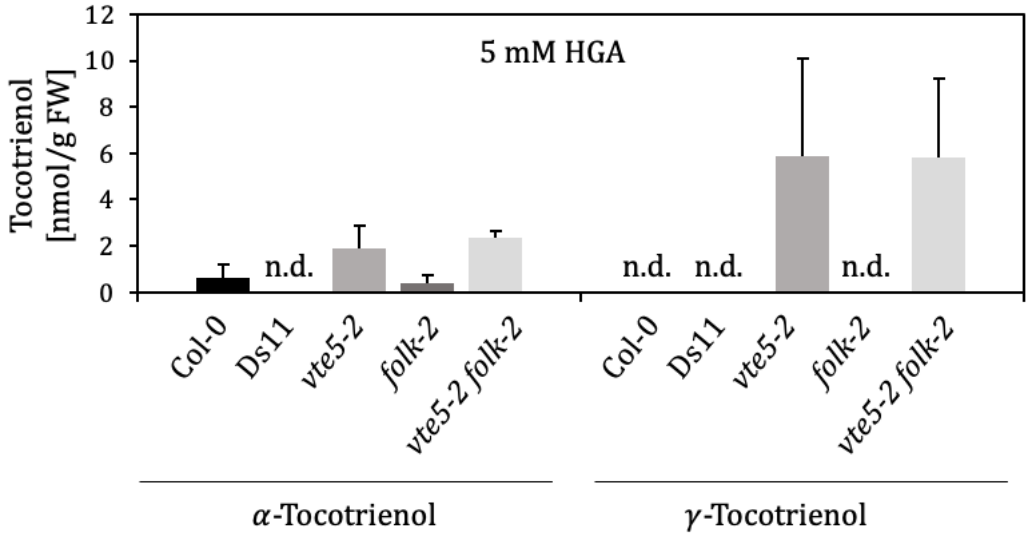

Figure 27 Tocotrienol content in Arabidopsis WT Col-0, WT Ds11, *vte5-2*, *folk-2* and *vte5-2 folk-2* seedlings after HGA supplementation measured by HPLC FLD.

Arabidopsis WT Col-0, WT Ds11 and the mutants *vte5-2*, *folk-2,* and *vte5-2 folk-2* were grown on medium either supplemented with 5 mM HGA (B) or without HGA (A). Plants were grown for two weeks on MS medium and afterwards transferred to HGA containing MS medium for nine days. Afterward tocotrienols were extracted from leaves and analyzed by HPLC FLD. Data represent the mean and SD of five replicas, (n.d. = not detected, β-tocotrienol and δ-tocotrienol were also not detected by HPLC FLD).

3.2.7 Subcellular localization of VTE5 and FOLK after transient transformation of *N. benthamiana* leaves

The subcellular localization of VTE5 and FOLK was analyzed to address the question, whether the two proteins are found in the chloroplast as expected from the impact of the *vte5* and *folk* mutations on phytyl lipids, which are localized to the chloroplast. Both protein sequences are predicted to carry a N-terminal transit peptide sequence presumably targeting the protein to chloroplast (according to the TargetP prediction program and SUBA4 database). The two cDNA sequences of VTE5 and FOLK were fused to the 5' end (N-terminus) of the fluorophore, enhanced GFP (eGFP). The

VTE5-eGFP and FOLK-eGFP fusion constructs were inserted into the binary vector pLH9000 with expression under the 35S promoter. The plasmids were transferred into *A. tumefaciens* cells and used for infiltration into *N. benthamiana* leaves and subsequent analysis with a confocal laser microscope (Figure 28).

For co-localization studies, the autofluorescence of chloroplasts was analyzed in parallel to the GFP signals. GFP signals were observed in the chloroplasts of *N. benthamiana* leaves transformed with the VTE5-eGFP or FOLK-eGFP constructs. The green GFP signal observed in chloroplasts could in principle be derived from chlorophyll autofluorescence with minor emission of light in the green range. This scenario was excluded by analysis of non-transformed neighboring cells which did not show any green fluorescent signal for chloroplasts (Figure 28, A, red arrows). Next to the chloroplast signals, strong GFP signals in small punctuate structures outside of the chloroplasts were detected (Figure 28, B, yellow arrows). To investigate the identity of this organelle, VTE5-eGFP and FOLK-eGFP constructs were co-infiltrated into the leaves with different organellar markers. After treatment of leaves with mitoTracker®, the mitochondria became visible. Co-infiltration with VTE5-eGFP or FOLK-eGFP showed no co-localization of mitochondria signals with the punctuated structures (data not shown). Next, VTE5-eGFP and FOLK-eGFP constructs were co-infiltrated in a 1:1 ratio with cells carrying either Man1-mCherry (Nebenführ *et al.*, 1999; Patwari *et al.*, 2019) localizing to the Golgi apparatus or cells carrying a CFP-SKL marker (Anna-Lena Falz, unpublished) specific for peroxisomes. No colocalization with Man1 in the Golgi was observed (data not shown), but co-infiltration with CFP-SKL revealed a clear colocalization with VTE5 and with FOLK in peroxisomes (Figure 29). It is interesting to mention that the chloroplast derived GFP signals became very weak, to not detectable, upon co-infiltration with the peroxisomal marker. SKL (Ser-Lys-Leu) represents the so-called peroxisome targeting type 1 (PTS1) sequence, which is a conserved tripeptide sequence located at the C-terminus of a majority of peroxisomal matrix proteins. Most proteins destined to the peroxisome matrix contain either a conserved peroxisome targeting type 1 (PTS1) or type 2 (PTS2) signal (Reumann *et al.*, 2007).

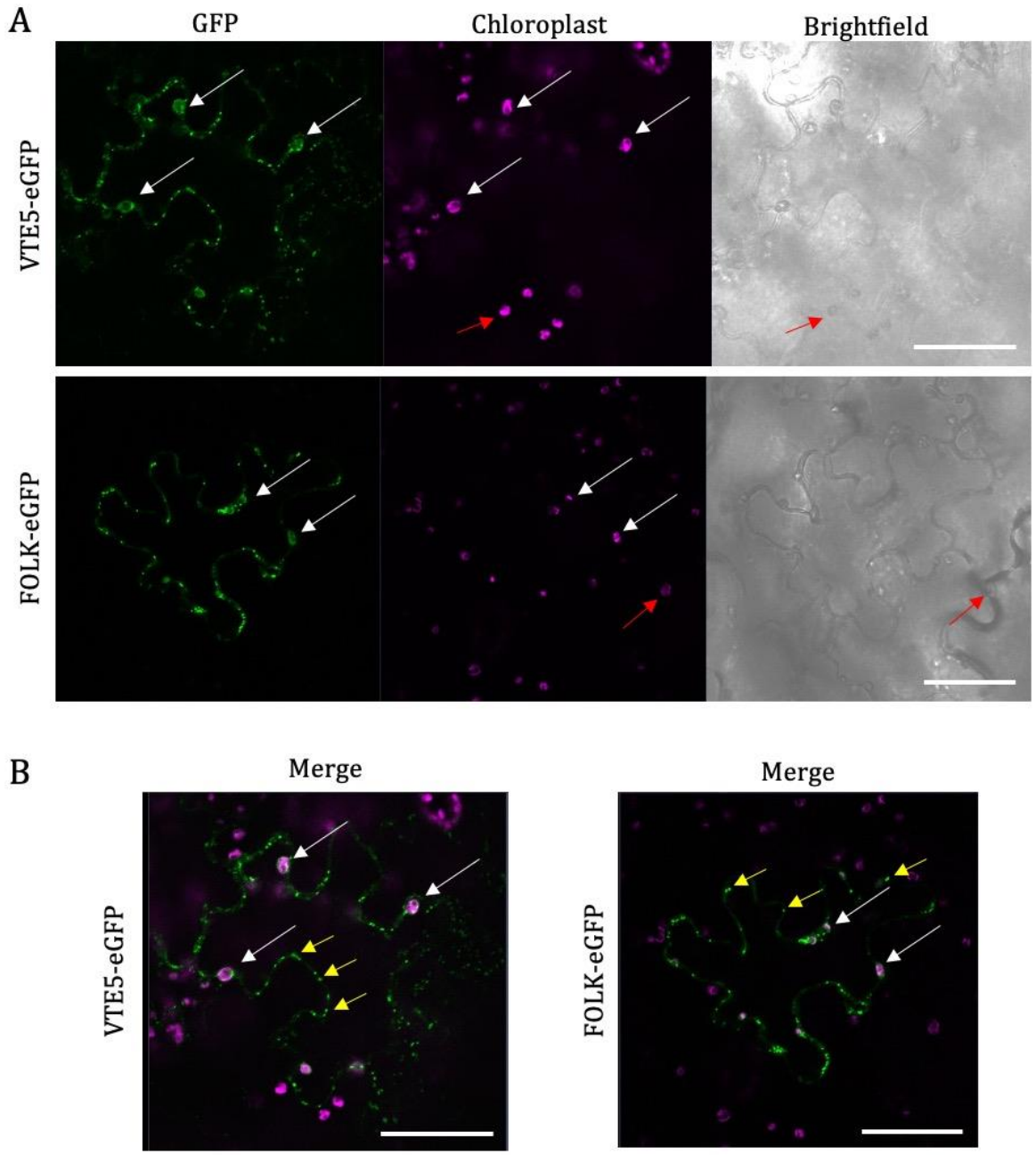

Figure 28 Subcellular localization of VTE5 and FOLK to chloroplasts.

Leaves from four to six-week-old *N. benthamiana* plants were infiltrated with *A. tumefaciens* carrying either the recombinant pLH900 35S-VTE5-eGFP (A, top) or pLH9000 35S-FOLK-eGFP (A, bottom). After three to four days of expression, leaves were analyzed for GFP signals (green) using a confocal laser scanning microscope (Zeiss LSM 780). Chloroplast autofluorescence (magenta) was used for chloroplast visualization. The GFP signals of both constructs were present in chloroplasts (white arrow). Chloroplast autofluorescence signals in the GFP channel were excluded by comparison to chloroplast signals in untransformed neighbouring cells (red arrow). In the merge of the GFP and the chloroplast channel (B), colocalization of the GFP signal and chloroplasts was visible (white arrow). Additional to the GFP signals in chloroplasts, also GFP signals in small punctuate structures (yellow arrows) were observed. Bar= 50 µm.

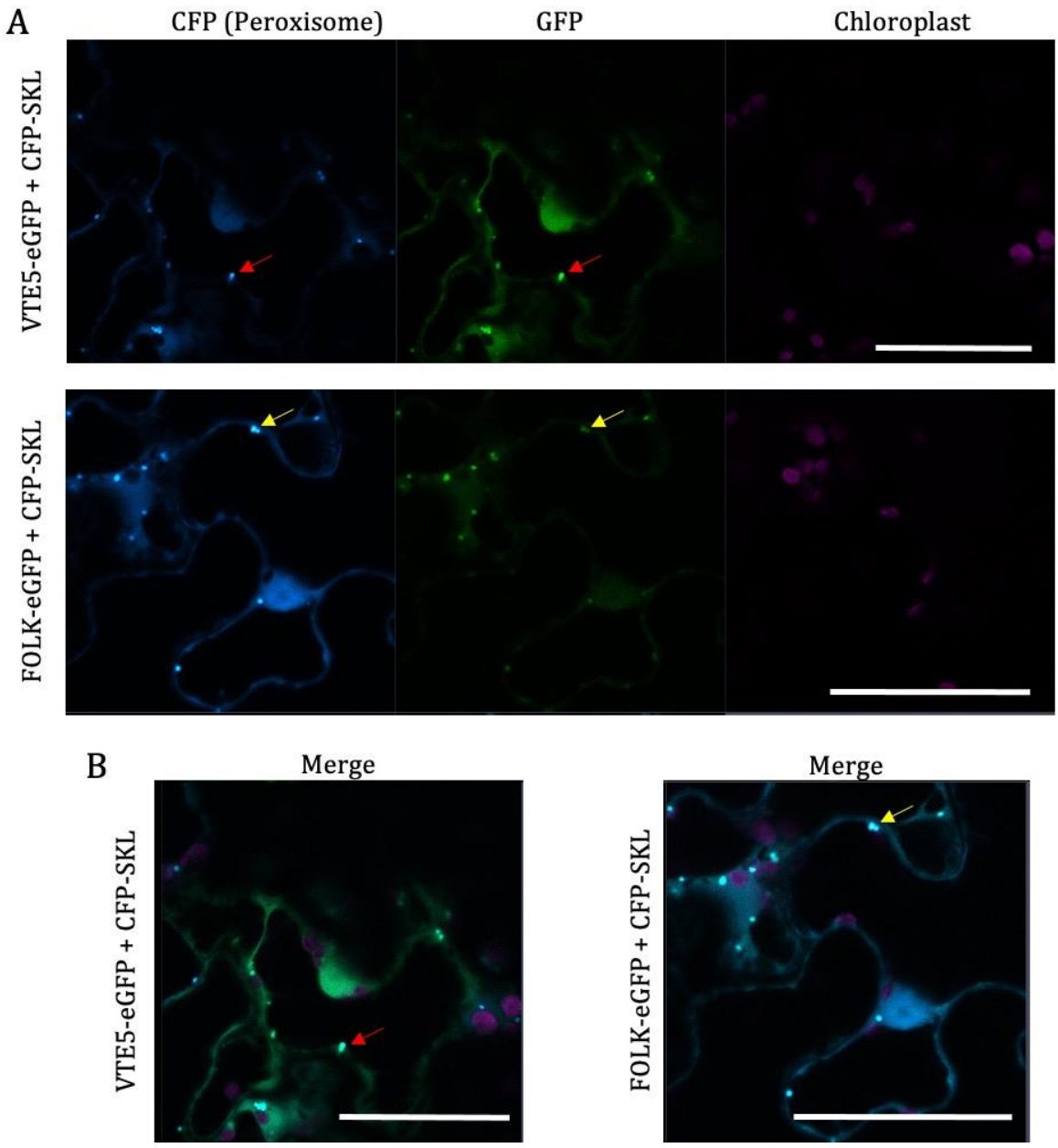

Figure 29 Subcellular localization of VTE5 and FOLK after co-infiltration with a peroxisome marker (CFP-SKL).

Leaves from four to six-week-old *N. benthamiana* plants were co-infiltrated with either recombinant pLH900 35S-VTE5-eGFP (A, top) or pLH9000 35S-FOLK-eGFP (A, bottom) together with *A. tumefaciens* carrying a recombinant peroxisome marker (CFP-SKL) construct with a CFP tag (blue). After three to four days of expression, leaves were analyzed for GFP signals (green) derived from either VTE5-eGFP or FOLK-eGFP and for CFP signals (blue) coming from the peroxisome CFP-SKL marker using a confocal laser scanning microscope (Zeiss LSM 780). Chloroplast autofluorescence (magenta) was used for chloroplast visualization. Punctuate signals for peroxisomes as well as for VTE5-eGFP (red arrows) and FOLK-eGFP (yellow arrows) were detected. In the merge of the GFP and CFP signals (B) a clear co-localization was observed between peroxisome signals and VTE5 as well as FOLK signals. Interestingly, no GFP signals in chloroplasts were detected in this experiment upon co-infiltration. In contrast, weak chloroplast signals were detected in addition to the punctuate signals when VTE5-eGFP or FOLK-eGFP were infiltrated without CFP-SKL (see Figure 28). Bar= 50 µm.

3.3 Substrate specificity of the two Arabidopsis isoprenoid alcohol kinases VTE5 and FOLK

Phytol from chlorophyll degradation can be remobilized in a salvage pathway by phosphorylation (vom Dorp *et al.*, 2015). The first committed step of this phosphorylation is catalyzed by the phytol kinase VTE5. The farnesol kinase FOLK is the only other isoprenoid alcohol kinase in Arabidopsis with a high sequence similarity to VTE5. FOLK was described to phosphorylate farnesol, and to a lesser extent geraniol and geranylgeraniol (Fitzpatrick *et al.*, 2011). As the analysis of Arabidopsis *vte5-2 folk-2* mutant plants revealed that they are completely tocopherol deficient, while the single mutant plants still contain tocopherol, the question was addressed whether FOLK possesses phytol kinase activity similar to VTE5. For this approach, Arabidopsis *FOLK* and *VTE5* full length coding sequences were cloned into the pETDuet-1 vector and heterologously expressed in *E. coli* Rosetta DE3 cells. As controls, either the empty pETDuet vector (ev) or the pETDuet GFP construct without kinase activity were used.

3.3.1 Substrate supplementation experiments after heterologous expression of VTE5 and FOLK in *E. coli*

To test whether the FOLK protein exhibits phytol kinase activity, in addition to farnesol, geranylgeraniol and geraniol kinase activities, *VTE5* and *FOLK* were heterologously expressed in *E. coli* as described in 2.5.6. After expression, protein production was analyzed by SDS PAGE. No differences between the protein extracts from cells expressing VTE5, FOLK, GFP or no expression (ev) were observed by SDS PAGE analysis followed by Coomassie staining (Appendix 7.5, Figure 39). The two recombinant proteins carry His-tags and therefore can be detected by Western blot, which is much more sensitive than protein staining. Western blot analysis of the proteins showed weak signals at the correct sizes of 33.1 and 33.2 kDa for VTE5 and FOLK His-tag fusion proteins, respectively, but the ev control also showed a band at around 33 kDa. In addition, smaller bands for VTE5 and FOLK at around 33 kDa were present which were absent from the ev sample (Appendix 7.5, Figure 39). Therefore, these bands presumably represent truncated forms of VTE5 or FOLK. The reason for the truncation remains unknown.

Nevertheless, recombinant *E. coli* cells were supplemented with either phytol, geranylgeraniol, or farnesol after inducing VTE5 or FOLK protein expression. Feeding of the recombinant *E. coli* cells was performed as described in 2.5.6. After induction of

protein expression cells were grown overnight at 16 °C. The next day the cultivation temperature was raised to 37 °C and either 5 mM phytol, geranylgeraniol, or farnesol were added as possible kinase substrates directly to the culture medium. Cells were cultivated in the presence of substrate for three hours, and afterward isoprenoid alcohol phosphates were extracted. LC MS/MS analysis showed clear differences between the extracts of cells expressing VTE5, FOLK or GFP (control) (Figure 30) in the presence of phytol, geranylgeraniol, or farnesol. In *E. coli* cells expressing VTE5, 40 mol% of phytyl-P (100% equals the sum of phytyl-p, phytyl-PP, geranylgeranyl-P, geranylgeranyl-PP, farnesyl-P and farnesyl-PP) were detected after phytol supplementation (+Phytol), while in the control cells (GFP), the phytyl-P content was around 1 mol% (Figure 30, A). 5 mol% of phytyl-P were detected in FOLK expressing cells, which is significantly more than in the GFP control (1 mol%). In the presence of geranylgeraniol (+Geranylgeraniol) (Figure 30, B), 40 mol% geranylgeranyl-P was observed in the VTE5 expressing cells and 90 mol% in the FOLK expressing cells, while in the GFP control geranylgeranyl-P was below 5 mol%. In the presence of farnesol (+Farnesol) (Figure 30, C), also more farnesyl-P was produced with VTE5 (60 mol%) and FOLK (40 mol%) in comparison to the GFP control. These results demonstrate that heterologous expression of *VTE5* and *FOLK* lead to the detection of kinase activities. Therefore, it can be concluded that the *E. coli* cells were able to express VTE5 and FOLK, albeit at low amounts and presumably in a truncated version, but in an enzymatically active form.

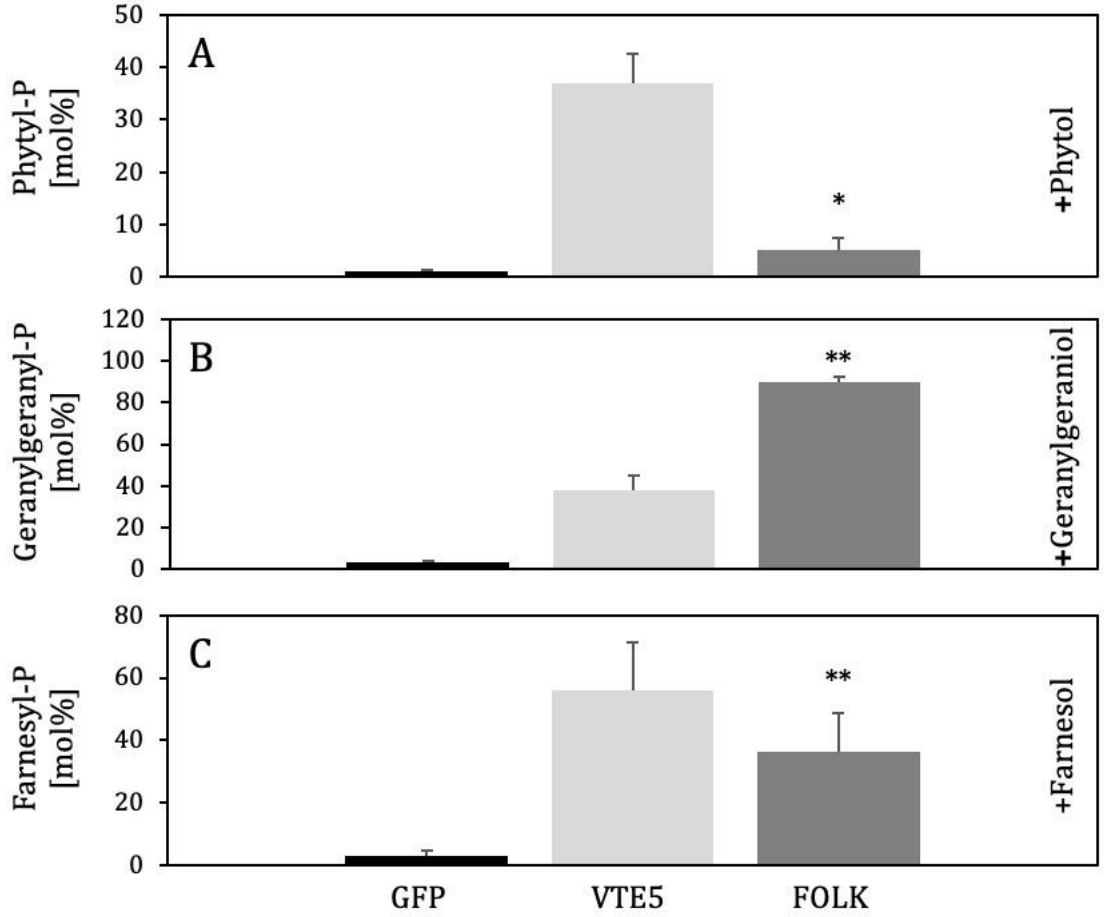

Figure 30 *E. coli* feeding experiments with phytol, geranylgeraniol, or farnesol after expression of VTE5 or FOLK.

Full length coding sequences of VTE5, FOLK, or GFP as control were expressed in *E. coli* Rosetta (DE3) cells. After induction of expression and 20 h cultivation at 16°C, cells were cultivated at 37°C in the presence of either 5 mM phytol (A), 5 mM geranylgeraniol (B) or 5 mM farnesol (C). The phosphorylation products phytyl-P, geranylgeranyl-P, or farnesyl-P were analyzed by LC MS/MS. Data represent the mean and SD of three replicates (n=2 for VTE5 + phytol).

3.3.2 Isoprenoid alcohol kinase assays after heterologous expression of VTE5 and FOLK in *E. coli*

To corroborate the results obtained by the substrate supplementation experiments (3.3.1) and to determine the substrate specificity in more detail, enzyme assays with protein isolated from *E. coli* were performed. Therefore, crude protein was isolated from cells after expression of VTE5, FOLK or the empty vector control (ev). Microsomal protein fractions were isolated by different centrifugation steps (2.5.6). Microsomal protein fractions were incubated with either 5 mM phytol, 5 mM geranylgeraniol, or 5 mM farnesol as potential kinase substrates for 30 min. As

phosphate donor, an equimolar mixture of ATP, CTP, GTP and UTP was added. Afterward, isoprenoid alcohol phosphates were isolated and analyzed by LC MS/MS. Significantly more phytyl-P, geranylgeranyl-P, and farnesyl-P were produced in assays of VTE5 with the respective isoprenoid alcohol substrates, in comparison to the ev control (Figure 31, A, C and E). While in the ev control, the phytyl-P, geranylgeranyl-P, and farnesyl-P content remained below 1 pmol per mg protein per minute, 72 pmol phytyl-P, 115 pmol geranylgeranyl-P and 224 pmol farnesyl-P per mg protein per minute were produced in the presence of VTE5 protein with the respective substrates.

In the assays with FOLK (Figure 31, B, D and F), kinase activity was around 10-times lower than in the assays with VTE5. Still, significant more farnesyl-P was produced in the presence of FOLK together with farnesol in comparison to the ev control (Figure 31, F). Around 20 pmol farnesyl-P were produced per mg protein per minute in the presence of FOLK, while it remained below 1 pmol per mg protein per minute in the ev control. Also more geranylgeranyl-P was produced (8 pmol per mg protein per minute) in the presence of FOLK in comparison to the ev control (Figure 31, D). In the assays with phytol, the kinase activity was very low, and no differences between the ev control and FOLK were observed (Figure 31, B). In summary, kinase activity was demonstrated for VTE5 and FOLK with significant differences to the ev control. While VTE5 showed kinase activity with phytol, geranylgeraniol, and farnesol, FOLK showed only a kinase activity with geranylgeraniol and farnesol but not with phytol.

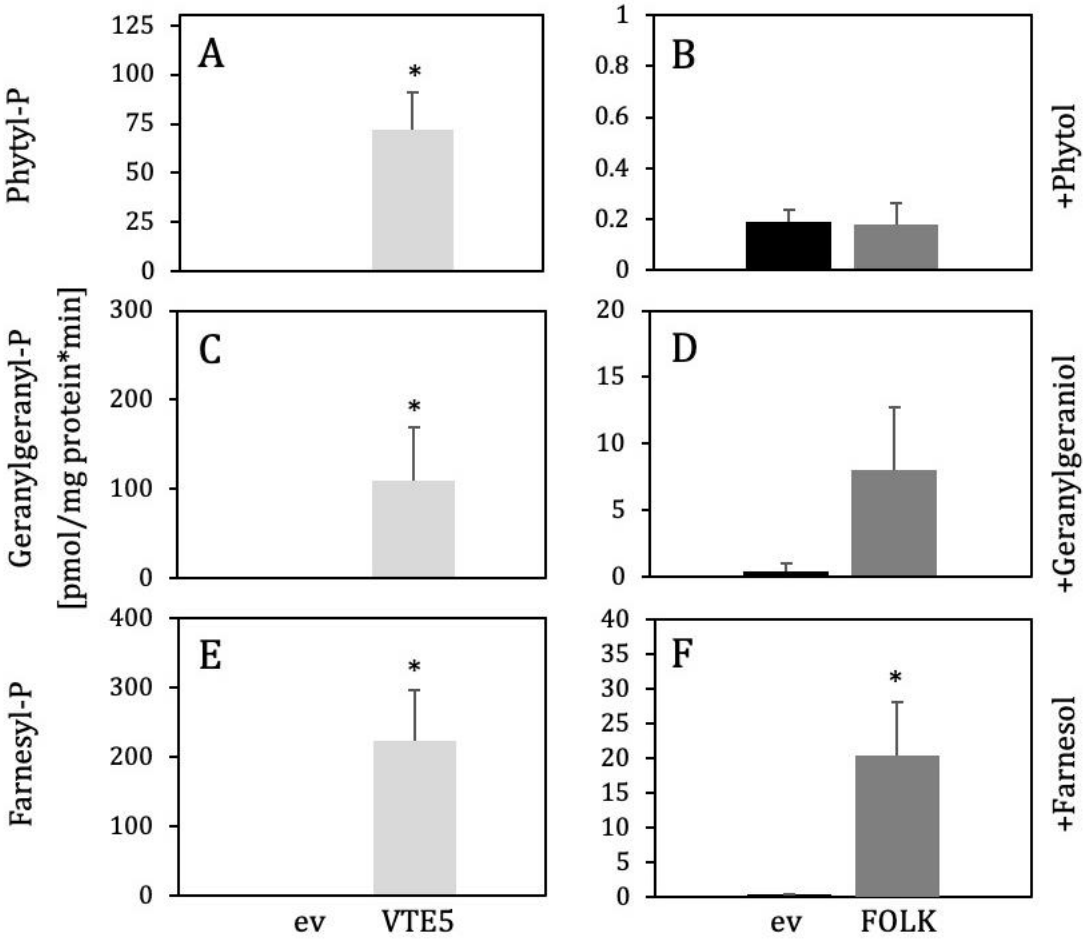

Figure 31 Isoprenoid alcohol kinase assays with VTE5 and FOLK proteins.

Isoprenoid alcohol kinase assays were performed with microsomal fractions of VTE5 (A, C, and E) and FOLK (B, D and F) proteins expressed in *E. coli* Rosetta (DE3) cells with pETDuet-1 constructs. Empty vector (ev) constructs were used as control. 5 mM of phytol (A and B), geranylgeraniol (C and D), or farnesol (E and F) together with an equimolar mixture of NTPs as phosphate donor were used as substrates. The monophosphate products phytyl-P (A and B), geranylgeranyl-P (B and C), and farnesyl-P (E and F) were analyzed by LC MS/MS with a Q-Trap instrument. VTE5 protein is able to convert all three substrates to the respective monophosphates. The FOLK protein only phosphorylates geranylgeraniol and farnesol while phosphorylation of phytol is similar to the ev control. Data represent the mean and SD of four replicates. Asterisks indicate significant differences to the empty vector (ev) control (Student's t-test).

3.4 The growth retardation of Arabidopsis *vte6-1* is independent from PAO-related chlorophyll breakdown and gibberellic acid availability

The Arabidopsis phytyl phosphate kinase (VTE6) was identified and characterized in 2015 by vom Dorp *et al.* (2015). Two independent Arabidopsis mutant lines (*vte6-1* and *vte6-2)* with transposon insertions in the first exon of At1g78620 (*VTE6*) represent null alleles as they lack *VTE6* mRNA as shown by RT-PCR expression analysis (vom Dorp *et al.*, 2015). Growth of Arabidopsis *vte6-1* and *vte6-2* is strongly

impaired. Plants are dwarf, do not develop mature leaves, and grow bushy. Additionally, plants are only viable on synthetic medium supplemented with sugar. The homozygous *vte6* mutant plants do not develop siliques and are therefore not able to produce seeds. The reason for this severe growth phenotype remained unclear. One hypothesis for the growth retardation is the accumulation of phytyl-P in *vte6-1* and *vte6-2*. Crossing of *vte6-1* with the *vte5-2* mutants lacking phytol kinase (*VTE5*) led to a reduction of phytyl-P accumulation and also partially rescued the severe growth phenotype. The *vte6-1 vte5-2* mutant plants were viable on soil but still dwarf and did not develop proper leaves nor siliques or seeds (vom Dorp *et al.*, 2015). It can be excluded that the lack of tocopherol in *vte6-1* and *vte6-2* is the reason for the severe growth phenotype, because other Arabidopsis mutants lacking tocopherol (*vte1, vte2*) are viable and grow similar as wild type plants (Porfirova *et al.*, 2002; Sattler *et al.*, 2004; Kanwischer *et al.*, 2005). Similarly, the *vte5-2 folk-2* double mutant generated in this study is tocopherol free but grows normally.

3.4.1 Generation and characterization of the *vte6-1 pao1* double mutant

To investigate the reason for the severe growth retardation of *vte6* mutant plants, heterozygous *vte6-1* plants were crossed with homozygous *pao1* plants. Due to a mutation in pheophorbide a oxygenase (PAO), the Arabidopsis *pao1* plants show a retarded degradation of chlorophyll (Pružinská *et al.*, 2003; Pružinská *et al.*, 2005). Therefore, during senescence e.g. induced via nitrogen deprivation, the *pao1* plants show a stay green phenotype because they retain most of their chlorophyll, while it is degraded in wild type under these conditions. Furthermore, *pao1* mutant plants show strongly suppressed accumulation of tocopherol during nitrogen deprivation, because no phytol for tocopherol synthesis is released from chlorophyll (vom Dorp *et al.*, 2015). These studies showed that the block of chlorophyll degradation in *pao1* has an effect on tocopherol content presumably due to impaired release of phytol that cannot be used for phosphorylation any more. To address the question, whether a block in chlorophyll degradation can alleviate the severe growth retardation in *vte6-1*, a double homozygous *vte6-1 pao1* mutant was generated by crossing heterozygous *vte6-1* plants with homozygous *pao1* plants. Double mutant plants were identified by genotyping PCR. While the *pao1* mutant plants do not show a growth defect under normal conditions, the *vte6-1* mutant plants are only viable on synthetic medium and are dwarf

and bushy. The double homozygous *vte6-1 pao1* are also dwarf, mainly bushy, and grow comparably to *vte6-1* (Figure 32). Nevertheless, some of the *vte6-1 pao1* plants were partially able to develop small leaves and even produced shoots but no siliques nor seeds (Figure 32, B).

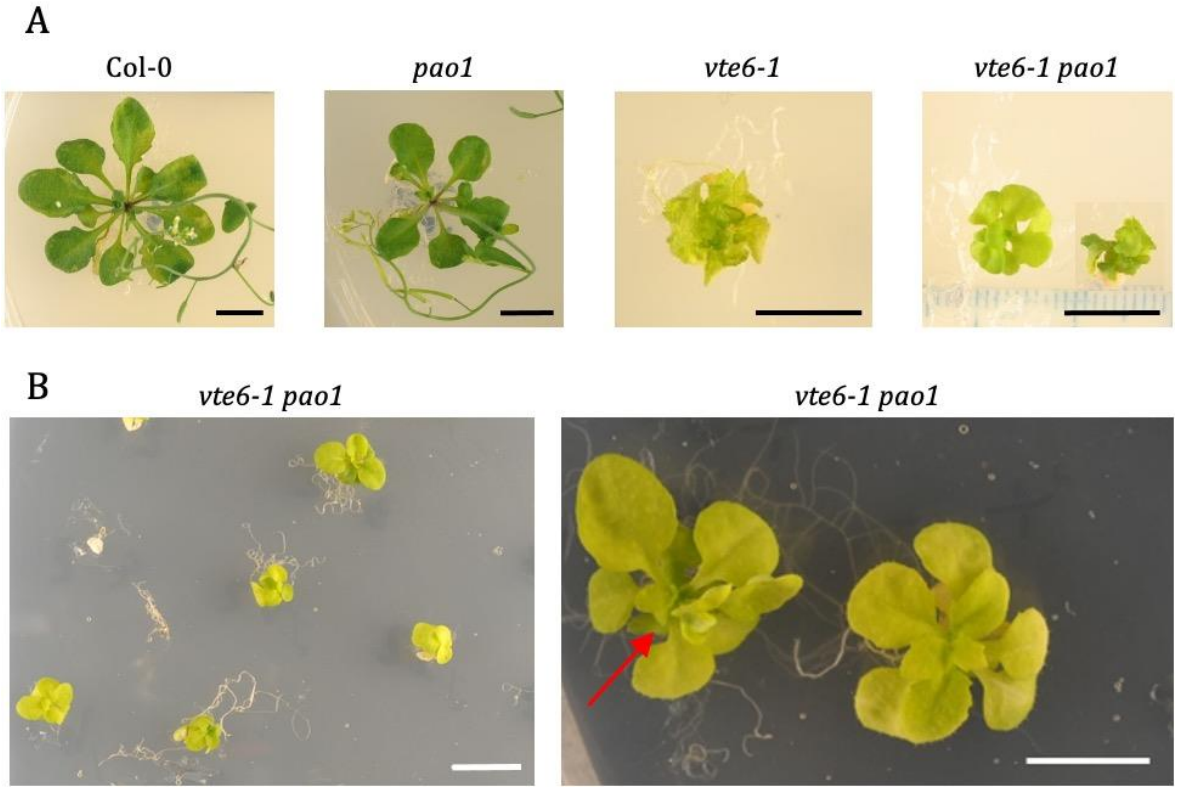

Figure 32 Phenotype of Arabidopsis *vte6-1 pao1* double mutant plants.

Growth of Arabidopsis Col-0, *pao1, vte6-1* and *vte6-1 pao1* (A). Plants are five-weeks old and were grown on MS medium supplemented with 1% sucrose. The *vte6-1 pao1* double mutant shows strongly retarded growth similar to *vte6-1*. The *vte6-1 pao-1* plants are dwarf and grow bushy but some plants developed slightly better (B). Only a few *vte6-1 pao1* plants were able to produce shoots (red arrow) but were not able to develop siliques nor seeds. Bar= 1 cm.

3.4.2 Supplementation of gibberellic acid to the growth medium of *vte6-1* plants

The phytohormone gibberellic acid (GA) is essential for growth and many developmental processes in plants. GA is for example required for leaf expansion, seed germination, and fruit ripening (Hooley, 1994). Several Arabidopsis mutants with a defect in GA biosynthesis or signal transduction processes are known. Interestingly, most of the mutants with a defective GA synthesis share a dwarf growth phenotype, which can be partially rescued by exogenous supplementation with GA (Koorneef *et al.*, 1985). GAs are tetracyclic diterpenoids synthesized from geranylgeranyl-PP. The geranylgeranyl-PP precursor could be derived from the chloroplast localized

isoprenoid MEP pathway. Alternatively, it is possible that geranylgeranyl-PP originates from phosphorylation of geranylgeraniol and geranylgeranyl-P, the last step might be catalyzed by VTE6. Therefore, it is possible that the mutation in the *vte6* plants causes GA deficiency, which in turn could be the origin for the severe growth retardation.

To test if *vte6-1* plants are impaired in GA synthesis, two-week-old seedlings of *vte6-1* and the respective WT (RIEKEN donor line No-0; Ds3) were transferred from MS medium supplemented with 1% sucrose to MS medium without sucrose and instead supplemented with 0 µM GA, 10 µM GA or 100 µM GA (GA3, Olchemin). Growth of *vte6-1* was documented for eight days. No changes in the growth retardation of *vte6-1* were detected (Figure 33). Also, no differences in growth of the plants between the different concentrations of GA were observed. While the WT plants increased in size by a factor of approximately two on all plates during the eight days of growth, the *vte6-1* plants remained small and bushy on control plates without GA (0 µM GA) and on plates supplemented with 10 µM GA or 100 µM GA.

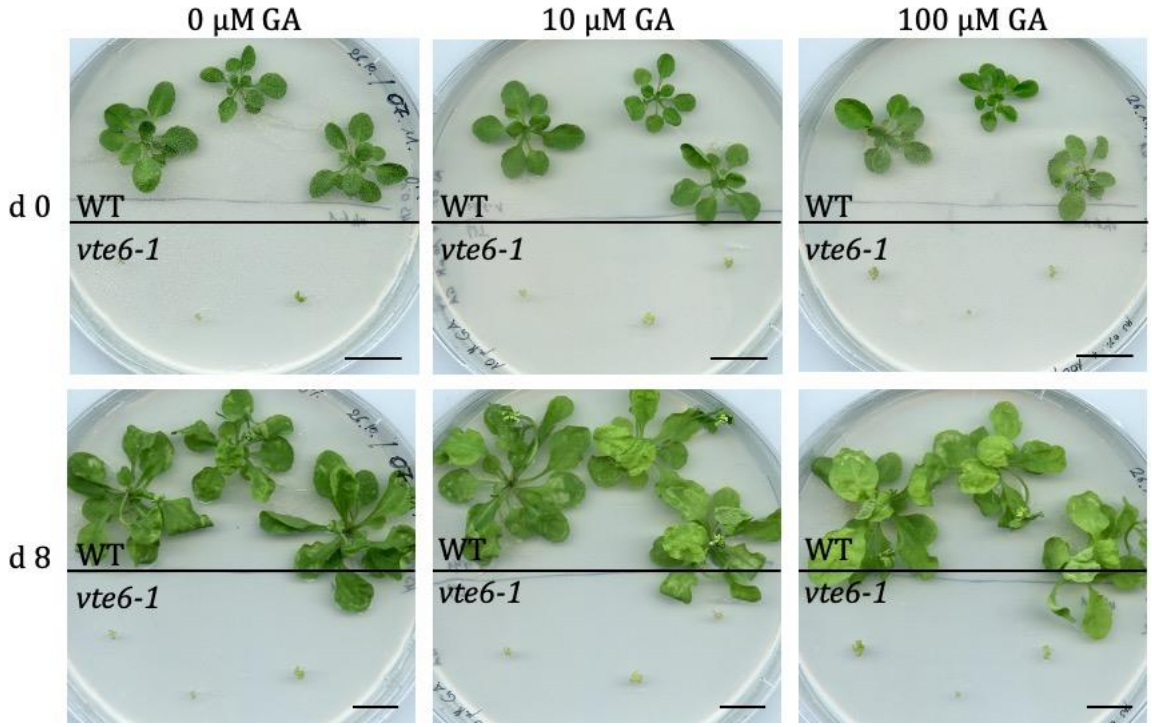

Figure 33 Supplementation of gibberellic acid (GA) to Arabidopsis *vte6-1*.

Arabidopsis *vte6-1* mutant plants were grown together with their respective WT control (No-0, Ds3) for two weeks on MS medium supplemented with 1% sucrose. Afterward, plants were transferred to fresh MS plates (d 0) without sucrose and either supplemented with 10 µM GA (GA3 from Olchemin), 100 µM GA or 0 µM GA as control. Plants were further cultivated under these conditions for eight days. After eight days (d 8) no differences in the plant growth could be observed for WT and *vte6-1* between the different GA concentrations. Bar= 2 cm.

4 Discussion

Plant metabolism includes the synthesis of metabolites important for plant survival during normal or abiotic and biotic stress conditions. Basic building blocks for biomolecules are derived from biosynthetic precursors, e.g. from central metabolism, fatty acid synthesis or isoprenoid synthesis. Isoprenoid alcohol phosphates are important precursors for the biosynthesis of essential compounds in plants, including photosynthetic pigments, some phytohormones, sterols, tocopherol (vitamin E), and phylloquinone (vitamin K1). Isoprenoid alcohol phosphates can be synthesized in plants *de novo* via the cytosolic MVA or the plastidial MEP pathway. Further they can be produced in salvage pathways by phosphorylation of free isoprenoid alcohols. In the last years, analysis of phytol metabolism showed that the free isoprenoid alcohol phytol, released during chlorophyll degradation, can be remobilized by phosphorylation for the biosynthesis of tocopherols (vitamin E) and phylloquinone (vitamin K1). Remobilization of phytol in Arabidopsis is catalyzed by two enzymes, phytol kinase (VTE5) and phytyl-P kinase (VTE6). While Arabidopsis *vte6* null mutants are tocopherol deficient, *vte5* mutant plants still contain reduced amounts of tocopherol in leaves and seeds. In Arabidopsis, only one homologous gene with high sequence similarity to *VTE5* at the deduced amino acid level was identified (Valentin *et al.*, 2006). The respective gene was later designated *FOLK* for farnesol kinase (Fitzpatrick *et al.*, 2011). FOLK was characterized to phosphorylate free farnesol, geraniol and geranylgeraniol. A putative phytol kinase activity was not addressed so far. In this work, the Arabidopsis isoprenoid alcohol kinases VTE5 and FOLK were analyzed. The roles of phytol, farnesol, and geranylgeraniol phosphorylation for the biosynthesis of tocopherol, phylloquinone, sterols, photosynthetic pigments including chlorophyll, and phytohormones were investigated. Furthermore, tocopherol deficient Arabidopsis insertion lines, impaired in isoprenoid alcohol phosphorylation, were characterized concerning growth and development as well as for their isoprenoid lipid composition.

4.1 The role of VTE5 and FOLK during isoprenoid alcohol phosphorylation

The possibility to measure isoprenoid alcohol phosphates by LC MS/MS in plant extracts is a crucial advantage for investigating the role of isoprenoid alcohol kinases in plant metabolism. Phytyl-P, phytyl-PP, geranylgeranyl-P, and geranylgeranyl-PP measurements by LC-MS/MS were previously developed by Dr. Katharina Gutbrod (vom Dorp, 2015). The existing analytical method was used and adapted for the additional analysis of farnesyl-phosphates next to phytyl- and geranylgeranyl-phosphates. The two Arabidopsis mutants *vte5-2* and *folk-2* lacking phytol kinase and farnesol kinase activity were crossed, and a *vte5-2 folk-2* double mutant was generated. The *vte5-2 folk-2* double mutant is viable and develops normally. Measurements of isoprenoid alcohol phosphates in leaf and seed extracts showed that the single and double mutant plants are impaired in isoprenoid alcohol phosphorylation. Most drastic alterations were observed in phytyl-phosphates and geranylgeranyl-phosphates. Analysis of farnesyl-phosphates remained inconclusive due to their low abundance in the plant extracts.

Phytyl-P was reduced in *vte5-2* and *vte5-2 folk-2* leaves and significantly reduced in *vte5-2*, *folk-2,* and *vte5-2 folk-2* seeds (Figure 8). Geranylgeranyl-P was unchanged in leaves but also significantly reduced in *vte5-2*, *folk-2,* and *vte5-2 folk-2* seeds. Therefore, all mutants had reduced phytyl-P and geranylgeranyl-P values suggesting for the first time that the two enzymes are involved in the phosphorylation of the isoprenoid alcohols phytol and geranylgeraniol *in planta*. Nevertheless, the isoprenoid alcohol monophosphates were not completely absent from the mutant plants. Further, the monophosphates need to be phosphorylated once more to the respective diphosphates to serve as activated precursors for biosynthetic pathways. The phytyl-PP levels are reduced in all mutants, with the strongest reduction observed in the *vte5-2 folk-2* double mutant. On the contrary, the geranylgeranyl-PP content is not significantly lower in the mutant leaves and seeds than in the WT. Presumably, the *de novo* synthesized pool of geranylgeranyl-PP is much higher than the geranylgeranyl-PP content synthesized by phosphorylation from geranylgeranyl-P.

In agreement with the measurements of isoprenoid alcohol phosphates, the free isoprenoid alcohols (measured by GC-MS) were clearly increased (Figure 10), indicating that *vte5-2*, *folk-2*, and *vte5-2 folk-2* are impaired in the ability to phosphorylate isoprenoid alcohols. Phytol was significantly increased and

accumulated in *vte5-2*, *folk-2*, and *vte5-2 folk-2*. Additionally, free geranylgeraniol was detected in *folk-2* and in even higher levels in *vte5-2 folk-2*, but it was absent from WT and *vte5-2.* Free farnesol could not be detected in any of the plant extracts.

Free phytol can be esterified to fatty acid phytyl esters to remove the free alcohol from the metabolism, because it is toxic for the plant in high amounts (Ischebeck *et al.*, 2006; Gaude *et al.*, 2007; Lippold *et al.*, 2012; vom Dorp, 2015). Fatty acid isoprenoid alcohol esters were measured by direct infusion MS/MS according to the previously described method for phytyl ester measurements (vom Dorp, 2015). Next to phytyl esters, geranylgeranyl esters and farnesyl esters were measured (Figure 17). The results showed for the first time, that next to phytyl esters also geranylgeranyl and farnesyl esters are present in Arabidopsis. While phytyl esters have been described in many plants, including Arabidopsis, mosses, algae, and others (Krauß and Vetter, 2018), geranylgeranyl esters and farnesyl esters are so far only barely known. Geranylgeranyl esters were described, for example, in the moss *Polytrichum commune*. The content of geranylgeranyl esters found in spores of this moss was about seven times lower than the content of phytyl esters. The geranylgeranyl esters were identified as components of the steryl and wax ester fraction of *Polytrichum commune* spores (Liljenberg and Karunen, 1978). In the work described here, geranylgeranyl ester levels detected were 50-times lower in leaves and nearly 1000-times lower in seeds than the phytyl esters in Arabidopsis WT. In contrast, in the *vte5-2 folk-2* double mutant, phytyl esters were also more abundant than geranylgeranyl esters, but the levels of geranylgeranyl esters strongly accumulated almost reaching WT phytyl ester levels. Farnesyl esters are barely described but were for example identified in the microalgae *Botryococcus branii* (Inoue *et al.*, 1994). Farnesyl esters were so far not described in Arabidopsis, and the function of geranylgeranyl and farnesyl esters remains unknown. Similar to the hypothesis that phytyl esters can serve as an intermediate sink of phytol, geranylgeranyl esters and farnesyl esters could represent sinks for the intermediate storage of geranylgeraniol or farnesol, respectively. In 2014, Nagel *et al.* overexpressed isoprenyl diphosphate synthases in spruce which lead to the accumulation of geranylgeranyl-PP and geranylgeranyl esters. Insect herbivore survival was significantly lower on these overexpression lines, and therefore, geranylgeranyl esters might function in plant defense.

Analysis of the composition of fatty acids esterified to the isoprenoid alcohols showed that the main fatty acid esterified to phytol was 16:3 in leaves and 18:3 in

seeds. Similar results were observed in previous studies (Gaude *et al.*, 2007) and the fatty acid composition correlates with a high abundance of 16:3 and 18:3 fatty acids found in Arabidopsis monogalactosyl and digalactosyl diacylglycerol (MGDG and DGDG). The galactolipids MGDG and DGDG are major structural components of photosynthetic membranes in chloroplasts (Dörmann *et al.*, 1995; Jarvis *et al.*, 2000). Geranylgeranyl esters, which were highly abundant in *vte5-2 folk-2* leaves, were mainly esterified to 16:0 but also to 20:0, followed by 18:3 and 18:2. The 20:0 fatty acid is of low abundance under normal conditions. Measurements of lipid membrane components such as MGDG and DGDG and of phospholipids in the *vte5-2 folk-2* mutant would be interesting to investigate if these mutants show differences in the fatty acid composition of these lipids.

4.2 The salvage pathway of isoprenoid alcohol phosphorylation via VTE5 and FOLK plays a minor role for geranylgeranyl-PP and farnesyl-PP dependent metabolites

The Arabidopsis mutants *vte5-2, folk-2,* and *vte5-2 folk-2* are impaired in their ability to phosphorylate phytol, geranylgeraniol, and farnesol. Phytyl-PP gives rise to the side chains of tocopherol, phylloquinone, and chlorophyll. Geranylgeranyl-PP is part of the biosynthetic pathway of carotenoids and some phytohormones, including abscisic acid (ABA) and gibberellic acid (GA). Further, two molecules of farnesyl-PP form squalene, the precursor of sterol biosynthesis.

4.2.1 Chlorophyll, carotenoids, and phytohormone biosynthesis are unaffected in *vte5-2 folk-2*

Geranylgeraniol and geranylgeranyl esters accumulate to high amounts in *folk-2* and *vte5-2 folk-2*. In Arabidopsis, geranylgeranyl-chlorophyll is the precursor for (phytyl-) chlorophyll synthesis. The double bonds of geranylgeranyl-chlorophyll are reduced to yield chlorophyll in Arabidopsis by the geranylgeranyl reductase (GGR). Measurements of photosynthetic pigments showed no differences in chlorophyll levels nor in chlorophyll composition in *vte5-2 folk-2* (Figure 11), suggesting that these enzymes are not involved in chlorophyll biosynthesis. Arabidopsis *ggr* mutants are unable to reduce the geranylgeranyl side chain in geranylgeranyl chlorophyll to the respective phytyl chain. These plants accumulate geranylgeranyl chlorophyll, which is under normal conditions of only very low abundance. The *ggr* mutant plants have a

very strong growth retardation and are pale yellow (Tanaka *et al.*, 1999). This demonstrates that the geranylgeranylated form of chlorophyll is reduced very quickly to the photosynthetic active phytylated form of chlorophyll. If geranylgeranyl-PP for chlorophyll biosynthesis is derived from phosphorylation of geranylgeraniol instead of from *de novo* synthesized geranylgeranyl-PP, a block in geranylgeraniol phosphorylation could reduce the accumulation of geranylgeranyl chlorophyll. A block in geranylgeraniol phosphorylation could be achieved by the introduction of the *vte5-2 folk-2* mutation in a *ggr* background. Nevertheless, the fact that with a complete lack of GGR, the geranylgeranyl group cannot be reduced to the respective phytyl moiety, this triple mutant is probably not viable as more biosynthetic pathways next to the chlorophyll biosynthesis may be affected.

Similar to the findings that the chlorophyll content remains unchanged in *vte5-2*, *folk-2,* and *vte5-2 folk-2,* no changes in the levels of carotenoids were identified (Figure 11). Carotenoids are C40 tetraterpenes formed from two molecules of geranylgeranyl-PP. As geranylgeranyl-PP can also be synthesized *de novo*, and the levels of geranylgeranyl-PP were not significantly reduced in the analyzed mutants, photosynthetic pigment biosynthesis is presumably not dependent on geranylgeraniol phosphorylation via VTE5 and FOLK.

The phytohormone ABA is synthesized from the carotenoid zeaxanthin. Arabidopsis *folk* mutants were shown to have an ABA-hypersensitive phenotype, and FOLK is hypothesized to be involved in ABA signaling (Fitzpatrick *et al.*, 2011). Measurements of ABA in non-stressed plants showed no differences in the ABA content in *vte5-2, folk-2,* and *vte5-2 folk-2* plants in comparison to the WT (Figure 12). This result underlines the suggestion that FOLK and VTE5 are not involved in carotenoid biosynthesis and are therefore also not altering ABA content. In plants, ABA levels are maintained at rather low levels under normal conditions but can be strongly increased upon stress (Xiong and Zhu, 2003). Therefore, stress experiments in which the ABA levels are increased could show different results that were so far not observable due to low ABA levels in all analyzed plants.

4.2.2 The content of sterols is slightly reduced in *vte5-2 folk-2*

Sterols are synthesized from the C30 isoprenoid alcohol phosphate squalene. Squalene is formed by condensation of two molecules of farnesyl-PP. The Arabidopsis

farnesol kinase (FOLK) is able to phosphorylate farnesol to farnesyl-P, but also the phytol kinase (VTE5) showed activity with farnesol as a substrate (Figure 31). Analysis of the most abundant sterols found in Arabidopsis, *β*-sitosterol, campesterol, and stigmasterol (Benveniste, 2002) showed a reduction of these sterols only in the double mutant *vte5-2 folk-2,* while the contents in the respective single mutant plants were not affected (Figure 13). Sterols are important components of cell membranes. In plants, campesterol is the precursor of the steroid hormones, the brassinosteroids (He *et al.*, 2003). Brassinosteroids are, for example, important for the regulation of cell expansion and morphogenesis. Plants with low brassinosteroid content are mainly dwarf (Altmann, 1998). The *vte5-2 folk-2* double mutant has no obvious growth phenotype. Therefore, the reduced campesterol content does presumably not lead to a decreased brassinosteroid level. In addition to reduced campesterol, *β*-sitosterol and stigmasterol levels were reduced in *vte5-2 folk-2*. Nevertheless, they were not completely absent. Measurements of farnesyl-P and farnesyl-PP contents in leaf extracts were inconclusive, because the amounts were extremely low. Therefore, farnesyl phosphorylation catalyzed by VTE5 and FOLK could contribute minor amounts of substrates for the sterol biosynthesis, but farnesyl-PP from *de novo* synthesis presumably is the main substrate for sterol biosynthesis. As sterol biosynthesis is located in the cytosol, this contribution would need further regulatory reactions ensuring either the presence of VTE5 and FOLK in the cytosol or an exchange of farnesyl-P or farnesyl-PP between different organelle compartments. In this regard it is interesting to note that VTE5 and FOLK were not only localized to the chloroplast, but also in addition to the peroxisome. It is possible that the peroxisomal localization of VTE5 and FOLK might be linked to metabolic pathways outside the chloroplast, possibly involving sterol synthesis in the cytosol.

Taken together, the sterol biosynthesis which depends on farnesyl-PP in the cytosol is slightly affected by the loss of farnesol kinase (FOLK) and phytol kinase (VTE5). On the other hand, the direct metabolites dependent on geranylgeranyl-PP in the chloroplasts, including chlorophyll and photosynthetic pigments were not affected by the loss of VTE5 and FOLK. In Arabidopsis, geranylgeranyl-PP is synthesized *de novo* by the cytosolic MVA pathway, and inside plastids by the MEP pathway from farnesyl-PP catalyzed by GERANYLGERANYL SYNTHASE11 (GGPS). Twelve paralogous *GGPPS* genes (*GGPPS1–GGPPS12*) exist in the genome of Arabidopsis. GGPS11 is the only synthase localized in plastids (Lange and Ghassemian, 2003). Arabidopsis mutants

with a defect in GGPS11 are not viable, and knockdown mutants of this enzyme have reduced levels of chlorophylls, tocopherols, plastoquinone, and tocopherols (Ruiz-Sola *et al.*, 2016). Interestingly, analysis of the other GGPS proteins did not show reductions in these compounds, strengthening the idea that the isoprenoid alcohol phosphate pools are strictly separated between the cytosol and the plastids. This assumption is also interesting in regard to the finding that *vte5-2 folk-2* plants are tocopherol deficient, and tocopherol biosynthesis is located inside of chloroplasts.

4.3 The Arabidopsis farnesol kinase FOLK is involved in tocopherol and phylloquinone biosynthesis but only shows minor phytol kinase activity

Tocopherols carry a phytyl-PP derived side chain. The phytyl-P kinase VTE6 phosphorylates phytyl-P to phytyl-PP. Arabidopsis *vte6* mutant plants are completely deficient in tocopherol and phylloquinone (vom Dorp *et al.*, 2015; Wang *et al.*, 2017). The VTE6 substrate phytyl-P can be synthesized by phosphorylation of phytol catalyzed by the phytol kinase VTE5 (Valentin *et al.*, 2006). The Arabidopsis *vte5-1* and *vte5-2* mutants still contain reduced levels of tocopherols in seeds and leaves (Valentin *et al.*, 2006; vom Dorp *et al.*, 2015). In this work, *vte5-2* mutants were crossed with *folk-2* mutants, which are deficient in farnesol kinase and geranylgeraniol kinase activity. The *vte5-2 folk-2* double mutant completely lacks tocopherols, while the *vte5-2* single mutant has reduced tocopherol levels, and the *folk-2* mutant has similar tocopherol levels as the WT (Figure 14). Additionally, phylloquinone levels are reduced by 60% in *vte5-2 folk-2* leaves compared to the WT, while the respective single mutants have no decrease in phylloquinone (Figure 16). Therefore, FOLK and VTE5 are together involved in the production of phytyl-PP for tocopherol as well as phylloquinone biosynthesis. However, while tocopherol synthesis fully depends on phytyl-P produced by VTE5 and FOLK, an additional pool of phytyl-P or phytyl-PP must exist for phylloquinone synthesis.

FOLK represents the only homologous gene to *VTE5* in Arabidopsis (Valentin *et al.*, 2006; Fitzpatrick *et al.*, 2011; vom Dorp, 2015). FOLK harbors farnesol kinase activity as confirmed by enzyme assays, and in addition shows activity with geranylgeraniol and geraniol, albeit to a lower extent (Fitzpatrick *et al.*, 2011). Isoprenoid alcohol kinases were often shown to be able to accept several substrates. A geranylgeraniol kinase and a geranylgeranyl-P kinase in the archaebacterium

Sulfolobus acidocaldarius was identified in 1996 (Ohnuma *et al.*, 1996) and linked to the salvage pathway of ether-linked lipids. Next to geranylgeraniol (C20), the enzyme was also active to a lower extent with farnesol (C15), hexaprenol (C30), and octaprenol (C40) but not with geraniol (C10) or undecaprenol (C55).

The biosynthesis of tocopherol depends on phytyl-PP from phytol phosphorylation. As shown in this work, enzyme assays with recombinant FOLK protein did not reveal any phytol kinase activity for FOLK, but only confirmed the already described farnesol and geranylgeraniol kinase activities (Figure 31). In the contrary, enzyme assays with VTE5 showed activity with phytol, farnesol, and geranylgeraniol. Nevertheless, supplementation experiments, where phytol was directly added to the growth medium of *E. coli* cells expressing *FOLK*, showed a slight but significant increase in phytyl-P. Taken into account that the overall activity of FOLK in the enzyme assays was around 10-fold lower than the activity of VTE5, a minor phytol kinase activity could be present, but the activity was too low to distinguish it from the empty vector control. Attempts to perform enzyme assays with other VTE proteins expressed in *E. coli* also caused difficulties. The VTE2 protein from Arabidopsis, for example, showed only 3% of the activity of the VTE2 homolog from *Synechocystis* after expression in *E. coli* (Collakova and DellaPenna, 2001). Next to a possible phytol kinase activity of FOLK found in the supplementation experiments, also the analysis of the *folk-2* mutant plants indicated a possible phytol kinase activity of FOLK. For example, supplementation of phytol to *folk-2* plants resulted in lower phytyl-P levels as in the WT plants. Also, phytyl-P levels were significantly lower in *folk*-2 seeds in comparison to WT seeds.

To conclude, VTE5, together with FOLK are important for the biosynthesis of tocopherol and phylloquinone. Both of these quinone lipids carry phytyl-PP derived side chains. VTE5 is mostly active with phytol and shows low activity with geranylgeraniol. In contrast, FOLK shows considerably activity with geranylgeraniol, but the activity with phytol is low or even not existing according to the performed enzymatic assays with phytol as substrate. Therefore, next to phytol phosphorylation also geranylgeraniol phosphorylation could be important for the biosynthesis of tocopherol and phylloquinone.

Two scenarios could be hypothesized for the role of FOLK in the biosynthesis of tocopherol and phylloquinone. First, FOLK could be able to phosphorylate phytol in small amounts, but this low activity could not be detected by the enzyme assays

performed here. In this scenario, the activity of FOLK with geranylgeraniol would not be relevant. Second, FOLK catalyzes the phosphorylation of geranylgeraniol to geranylgeranyl-P, which could then be reduced to phytyl-P by the geranylgeranyl reductase (GGR). Here it is possible that geranylgeranyl-P is directly reduced to phytyl-P, or geranylgeranyl-P could be first phosphorylated, possibly by VTE6, to geranylgeranyl-PP, which is then reduced to phytyl-PP by GGR. In both scenarios, the levels of phytyl-PP are strongly reduced in leaves and seeds of *vte5-2 folk-2,* in agreement with the data shown in Figure 8. In contrast to phytyl-PP, the level of geranylgeranyl-PP in *vte5-2 folk-2* leaves is only partially reduced and it seems to be unaltered in the seeds (Figure 8). It is reasonable to assume that geranylgeranyl-PP still found in *vte5-2 folk-2* is derived from the plastidial *de novo* isoprenoid synthesis trough the MEP pathway. This *de novo* synthesized geranylgeranyl-PP can be used for the synthesis of chlorophyll, carotenoids, ABA, and after reduction to phytyl-PP, give rise to the small amount of phylloquinone synthesized in *vte5-2 folk-2*. The *de novo* pool of geranylgeranyl-PP cannot be employed for tocopherol production after reduction to phytyl-PP. Presumably, the largest fraction of phylloquinone is also derived from phytyl-PP derived from isoprenoid alcohol phosphorylation but the reason why this pool cannot be employed for tocopherol biosynthesis remains unknown.

Possibly two separate pools of geranylgeranyl-PP (and phytyl-PP derived from it) exist in chloroplasts: one pool of geranylgeranyl-PP/phytyl-PP (C20-PP) derived from *de novo* synthesis, and a second pool derived from phytol phosphorylation. This second, kinase-derived C20-PP pool is absolutely required for tocopherol synthesis. Tocopherol synthesis cannot be performed using phytyl-PP derived from the *de novo* geranylgeranyl-PP pool. On the other hand, the *de novo* geranylgeranyl-PP pool can be used for phylloquinone synthesis (after reduction to phytyl-PP), albeit to a lower extent (Figure 34). However, the *de novo* geranylgeranyl-PP pool is fully sufficient to maintain a normal level chlorophyll and carotenoid synthesis.

4.4 Characterization of *vte5-2 folk-2*

4.4.1 The tocopherol deficient *vte5-2 folk-2* mutant shows reduced seed longevity, but photosynthetic activity is unaffected

Tocopherol deficiency is often accompanied by alterations of seed longevity. Several low tocopherol mutants of Arabidopsis, including *vte1, vte2,* and *vte6,* show a reduced germination rate after several months of seed storage (Sattler *et al.*, 2004; vom Dorp *et al.*, 2015). The tocopherol deficient *vte5-2 folk-2* mutant characterized here also shows reduced seed longevity (Figure 25). Seeds from *vte5-2*, *folk-2*, and *vte5-2 folk2* plants were artificially aged according to previous accelerated seed aging experiments performed with *vte1* and *vte2* (Sattler *et al.*, 2004). While the *vte5-2 folk-2* double mutant seeds had a significantly reduced germination rate after accelerated aging treatment, the *vte5-2* seeds showed a slightly reduced germination rate, and the *folk-2* seeds showed a similar germination rate as the WT. This result correlates with the tocopherol levels found in the leaves and seeds of the respective mutants. Tocopherols are antioxidants, scavenge reactive oxygen species, and prevent lipid oxidation. While the *folk-2* plants have the same levels of tocopherol as the WT, the tocopherol levels in *vte5-2* are reduced, and the *vte5-2 folk-2* double mutant completely lacks tocopherol. Nevertheless, accelerated aging of the tocopherol deficient mutants *vte1-1* and *vte2-1* resulted in much more severe alterations in the germination rate. In the accelerated aged *vte1-1* and *vte2-1* seeds, Sattler *et al.* showed that the germination rate was decreased nearly down to 0%. In the present work, the germination rate of the *vte5-2 folk-2* seeds was less reduced to approximately 60%. Differences with the experiments performed by Sattler *et al.* (2004) could be due to a slightly different experimental setup or due to differences in the genotypes.

Photosynthetic quantum yield was unaffected in the *vte5-2*, *folk-2*, and *vte5-2 folk-2* mutant plants. In addition, the levels of photosynthetic pigments were unchanged, and the chloroplast ultrastructures were not changed. Therefore, FOLK, and VTE5 activity presumably is not important for structural integrity of the chloroplasts and for overall photosynthesis even though phylloquinone is reduced in the *vte5-2 folk-2* double mutant. Phylloquinone is required for the stability of photosystem I (Wang *et al.*, 2017). In addition to the photosystem I, phylloquinone is found in plastoglobules (Lohmann *et al.*, 2006). The phylloquinone levels are reduced to around 40% of the WT level in the *vte5-2 folk-2* double mutant. Therefore,

phylloquinone is not completely absent. It is possible that the plastoglobules of *vte5-2 folk-2* are preferentially depleted from phylloquinone, and the remaining phylloquinone might be localized to the thylakoids and might be sufficient to maintain photosystem I stability. In addition, all mutant plants show healthy green leaves comparable to the WT plants, and they behave similarly to the WT leaves after high light stress, supporting the conclusion that overall photosynthesis is not affected by the loss of phytol and farnesol kinase activity.

4.4.2 HGA supplementation leads to tocotrienol production in Arabidopsis WT Col-0 and in the tocopherol deficient *vte5-2 folk-2* mutant

Arabidopsis plants contain tocopherols and do not produce tocotrienols. While tocopherols carry a phytyl-PP derived side chain, tocotrienols carry a geranylgeranyl-PP derived side chain. Tocotrienols are, for example, highly abundant in monocot seeds and are synthesized from homogentisate (HGA) to which a geranylgeranyl-PP side chain is attached by homogentisate geranylgeranyl transferase (HGGT) (Cahoon *et al.*, 2003; Yang *et al.*, 2011). Overexpression of p-hydroxyphenolpyruvate dioxygenase (HPPD), the enzyme catalyzing the last step of HGA biosynthesis, leads to an increase in tocopherol levels, presumably by increasing the precursor availability of HGA (Tsegaye *et al.*, 2002). In the present work, HGA supplementation resulted in an increased tocopherol production, but also to a low production of tocotrienols in Arabidopsis Col-0 WT leaves (Figure 26 and Figure 27). Tocotrienols were also found in *vte5-2* leaves after HGA supplementation, but the tocopherol content remained unchanged in comparison to the *vte5-2* plants grown without HGA supplementation. Interestingly, also the tocopherol deficient *vte5-2 folk-2* produced small amounts of tocotrienols, while tocopherols were still absent after HGA supplementation.

Arabidopsis only contains a homogentisate phytyl transferase (HPT) gene, but is devoid of a homogentisate geranylgeranyl transferase (HGGT). HPT was shown to be specific for phytyl-PP with a nine times higher activity for phytyl-PP compared with geranylgeranyl-PP (Collakova and DellaPenna, 2001; Yang *et al.*, 2011; Zhang *et al.*, 2013). On the other hand, barley HGGT was six times more active with geranylgeranyl-PP than with phytyl-PP (Yang *et al.*, 2011). Nevertheless, if HGA strongly accumulates in Arabidopsis after HGA supplementation, it might be possible that the weak activity of HPT with geranylgeranyl-PP could result in tocotrienol production. As also small amounts of tocotrienols were found in *vte5-2 folk-2,* the question comes up where the

respective geranylgeranyl-PP comes from. Either a third, so far unknown isoprenoid alcohol kinase could be present in Arabidopsis, or geranylgeranyl-PP from *de novo* synthesis could be used for tocotrienol production. However, the *de novo* synthesized geranylgeranyl-PP is not reduced to phytyl-PP and employed for tocopherol biosynthesis, as shown in the mutants *vte5-2 folk-2* and *vte6*. It is likely that phytyl-PP and/or geranylgeranyl-PP from phosphorylation rather than from the *de novo* synthesized pool of geranylgeranyl-PP is employed for tocopherol and phylloquinone biosynthesis, and *de novo* synthesized geranylgeranyl-PP/phytyl-PP can in part be used for phylloquinone and tocotrienol but not for tocopherol synthesis (Figure 34).

4.4.3 VTE5 and FOLK are localized in chloroplasts and peroxisomes

Localization studies of VTE5 and FOLK fusion proteins with fluorescent tags using transient expression in *N. benthamiana* leaves indicated that the two proteins are targeted to chloroplasts and peroxisomes(Figure 28 and Figure 29). The peroxisome localization is unexpected as no peroxisomal target sequences can be found in VTE5 and FOLK (according to the TargetP prediction program and the SUBA4 database). On the contrary, the chloroplast localization is in line with the predicted localization of VTE5 and FOLK. Also, VTE5 was previously identified in proteome analyses of Arabidopsis chloroplasts by mass spectrometry (Zybailov *et al.*, 2008). The biosynthesis of tocopherol is localized in the chloroplast. The activities of enzymes of tocopherol biosynthesis, VTE2, VTE3, and VTE4, were confirmed in isolated subfractions of spinach chloroplasts (Soll *et al.*, 1980). The tocopherol cyclase (VTE1) was localized in plastoglobules of plastids (Vidi *et al.*, 2006), and YFP-VTE6 fusion constructs were found in chloroplasts of transformed plant protoplasts (vom Dorp *et al.*, 2015). The chloroplast localization of VTE5 and FOLK is in agreement with their function in tocopherol biosynthesis.

In addition, VTE5-eGFP and FOLK-eGFP fluorescence signals were found in punctuate structures. Co-infiltration with the peroxisomal CFP-SKL marker (PTS1 marker) showed that the punctuated structures are peroxisomes. Interestingly, the chloroplast signals observed in the analysis without a CFP-SKL marker were not present anymore after co-infiltration of VTE5-eGFP or FOLK-eGFP with the peroxisome marker. Neither in VTE5 nor in FOLK, peroxisome targeting signals of type 1 (PTS1) or of type2 (PTS2) can be found. PTS1 is represented by nine major tripeptide sequences

at the C-terminus, and PTS2 is represented by two major nonapeptide sequences at the N-terminus (Reumann, 2004). Both types of PTS are considered robust indicators for the peroxisomal localization of unknown proteins. Nevertheless, it was shown that CFP-PTS1 fluorophore fusion constructs can cause problems during peroxisome targeting analysis in transient plant expression systems (Falter *et al.*, 2019). Yellow fluorescent protein (YFP) fusion constructs were found in peroxisomes, but only upon co-infiltration with the peroxisome marker CFP-PTS1. It is assumed that non-monomer GFP-variants have a weak heterodimerization ability with CFP-PTS1 and therefore, can enter peroxisomes via piggy-back import (Falter *et al.*, 2019). Co-expression experiments with monomeric *Cerulean-PTS1* (Cer-PTS1) did not show this piggy-back import. Therefore, co-infiltration of VTE5-eGFP or FOLK-eGFP with Cer-PTS1 instead of co-infiltration with CFP-SKL could help to avoid binding to and piggy-back transport with CFP-SKL. Nevertheless, the punctuate signals, which were later identified as peroxisomes were always present in infiltrated leaves even if no CFP-SKL was co-infiltrated. Therefore, the peroxisomal localization of VTE5-eGFP and FOLK-eGFP is independent of the positive control CFP-SKL. The last steps of isoprenoid *de novo* synthesis of the cytosolic MVA pathway are localized to peroxisomes (Simkin *et al.*, 2011; Clastre *et al.*, 2011). It is possible that isoprenoid alcohol kinases contribute to isoprenoid alcohol-phosphate and -diphosphate synthesis inside peroxisomes, in addition to the *de novo* synthesis of isoprenoid diphosphates via mevalonate. This would reveal a so far unknown role of isoprenoid alcohol phosphorylation outside of chloroplasts. It is interesting to mention that also the enzymes catalyzing the last steps of the biosynthesis of the phylloquinone head group precursor (1,4-dihydroxy-2-naphthoate) are localized to peroxisomes (Babujee *et al.*, 2010). It is possible that that the phytyl side chain might already be attached to the head group inside the peroxisome (Figure 35). In this case, the VTE5 and FOLK proteins could be involved in phytyl-PP synthesis in peroxisomes. However, the enzyme catalyzing the attachment of the phytyl side chain to 1,4-dihydroxy-2-naphthoate is again localized to chloroplasts, the main localization of phylloquinone biosynthesis.

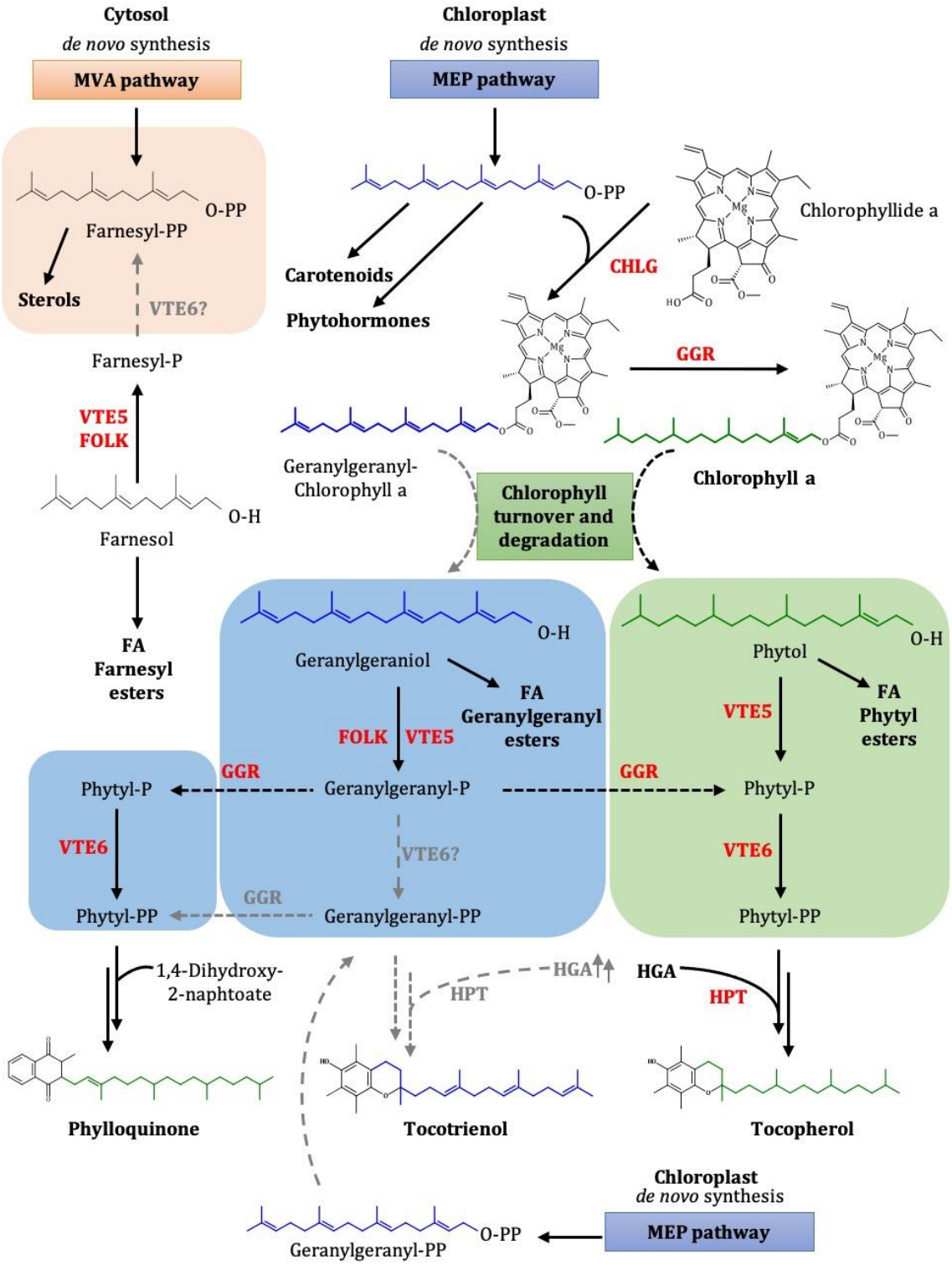

Figure 34 The role of the salvage pathway of isoprenoid alcohol phosphorylation catalyzed by VTE5 and FOLK.

The Arabidopsis farnesol kinase (FOLK) is the only homolog to the phytol kinase (VTE5). While VTE5 can phosphorylate phytol, geranylgeraniol, and farnesol, FOLK mainly phosphorylates geranylgeraniol and farnesol. Arabidopsis *vte5-2 folk-2* mutant plants are tocopherol deficient and contain reduced amounts of phylloquinone. Therefore, FOLK contributes to the biosynthesis pathway of tocopherol and phylloquinone, presumably via geranylgeraniol phosphorylation. Presumably different pools of isoprenoid phosphates are used for tocopherol and phylloquinone biosynthesis. Tocotrienols are only formed in Arabidopsis if HGA is available in excess amounts. Grey arrows indicate hypothesized pathways.

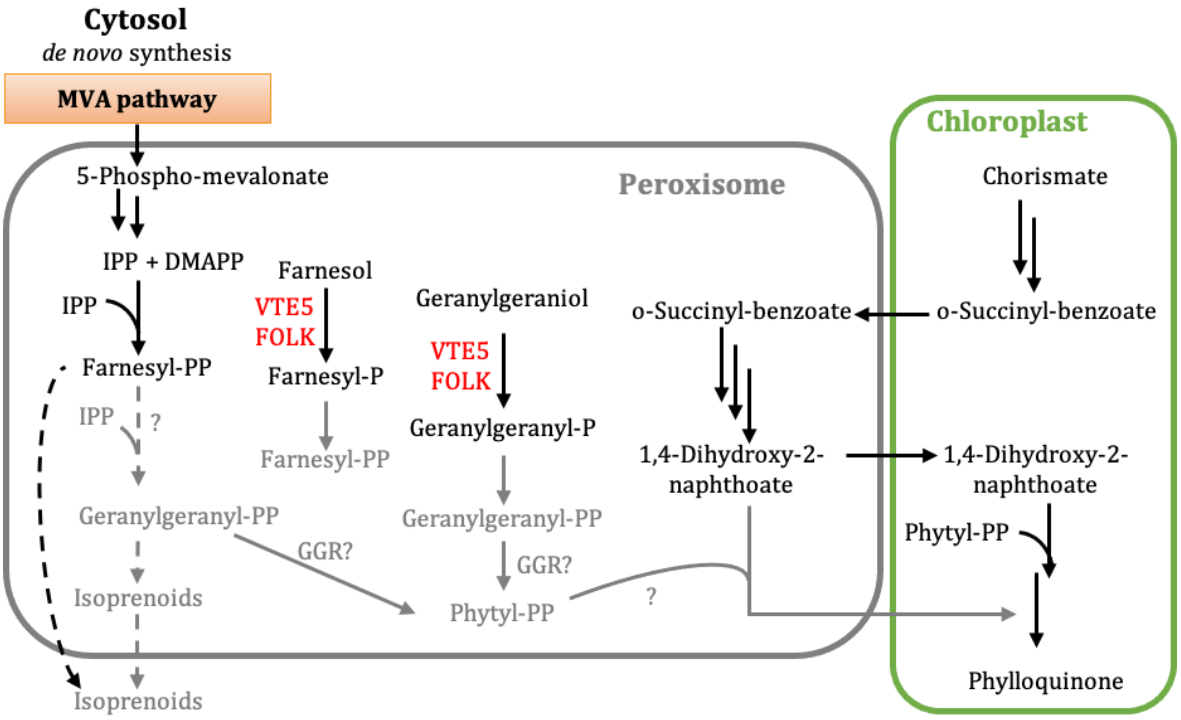

Figure 35 Hypothesized role of VTE5 an FOLK in peroxisomes.

Transient localization studies indicated a peroxisomal localization of VTE5 and FOLK. Both enzymes are able to phosphorylate geranylgeraniol and farnesol to the respective isoprenoid alcohol monophosphates. Isoprenoid *de novo* synthesis by the mevalonate (MVA) pathway is mainly located to the cytosol but recent studies showed that the last steps leading to the formation of farnesyl-PP are located in the peroxisomes. Phylloquinone, which consists of a naphthoate head group to which a phytyl-PP side chain is attached, is synthesized in chloroplasts, but three enzymes catalyzing the last steps of the head group synthesis of phylloquinone (1,4-dihydroxy-2-naphtoate) were shown to be present in peroxisomes. As the Arabidopsis *vte5-2 folk-2* mutant has reduced phylloquinone levels, it can be hypothesized that the peroxisomal localization of these proteins is linked to phylloquinone synthesis. Figure modified and adapted after Clastre *et al.*, 2011 and Gutbrod *et al.*, 2019. Grey arrows indicate hypothesized pathways.

4.5 The retarded growth of the *vte6-1* mutant

The tocopherol deficient Arabidopsis mutant lines *vte6-1* and *vte6-2* were characterized in 2015 (vom Dorp *et al.*, 2015). While the phytyl lipid content of these plants, which have a defect in phytyl-P kinase activity, is severely impaired, they also have a very drastic growth phenotype. The *vte6-1* and *vte6-2* seedlings are only viable on synthetic medium supplemented with sucrose, show dwarfed growth, and are bushy with pale green leaves. Supplementation with the growth hormone gibberellic acid (GA) did not change the retarded growth of *vte6-1* (Figure 33). Measurements of GA in the *vte6* mutant plants have not been performed so far. GA measurements would reveal if GA availability in the *vte6* mutant plants is decreased. It can be excluded that tocopherol deficiency is the reason for the decreased growth as other tocopherol

deficient Arabidopsis mutants grow normally (*vte1, vte2, vte5-2 folk-2*) (Porfirova *et al.*, 2002; Bergmüller *et al.*, 2003; this work).

Due to their defective phytyl-P kinase activity, *vte6* plants accumulate phytyl-P in leaves, which might be detrimental for plant growth and development. The assumption that this increase in phytyl-P could cause the drastic growth phenotype of *vte6* plants was supported by the analysis of Arabidopsis *vte5-2 vte6-1* double mutant plants lacking phytol kinase together with phytyl-P kinase. In this double mutant, phytyl-P does not accumulate any more due to the additional lack of phytol kinase activity. In the double mutant, the growth phenotype was not completely rescued, but seedlings showed slightly improved growth.

In the work presented here, a mutation in pheophorbide a oxygenase (PAO) (*pao1*), which is a key enzyme in chlorophyll degradation, was introduced into the *vte6-1* background by a crossing of the respective single mutant plants. Similar to the *vte5-2 vte6-1* mutants, the retarded growth in *vte6-1 pao1* mutant plants was not rescued, but some plants started to develop shoots (Figure 32). Nevertheless, no siliques or seeds were produced, and the leaves of *vte6-1 pao1* remained small and bushy. The *pao1* mutant plants are strongly impaired in chlorophyll degradation. The hydrolysis of the phytyl moiety of chlorophyll takes place in an upstream reaction of PAO but is blocked in the *pao1* mutant and no free phytol is released from chlorophyll in *pao1* (Pružinská *et al.*, 2005; Aubry *et al.*, 2008; Liu and Guo, 2013). Further it was shown that in *pao1* plants, tocopherol levels are not increased upon chlorotic stress. This proves that the *pao1* mutation leads to a defective phytol phosphorylation pathway similar as found in *vte5-2 vte6-1.* Quantification of phytol, phytyl-P and phytyl-PP in vt*e6-1 pao1* should be performed to show if these compounds accumulate less in the double mutant in comparison to the *vte6-1* single mutant. Less accumulation of phytyl-P could lead to the slightly better growth of *vte6-1 pao1,* similar as previously described for *vte5-2 vte6-1.* Nevertheless, the *vte6-1 pao1* and *vte5-2 vte6* mutant plants still have a strong retardation in growth. Therefore, next to phytyl-P accumulation, presumably additional problems are causing the strong growth defect of *vte6-1* which still need to be identified.

5 Summary

The isoprenoid alcohol phytol can be phosphorylated in Arabidopsis to phytyl-phosphate (phytyl-P) by the phytol kinase (VTE5) and further to phytyl-diphosphate (phytyl-PP) by the phytyl phosphate kinase (VTE6). Phytyl-PP derived from phytol phosphorylation enters the biosynthesis of tocopherol and phylloquinone. Arabidopsis phytol kinase mutant plants (*vte5*) still contain reduced levels of tocopherol, while phytyl phosphate kinase mutant plants (*vte6*) are tocopherol deficient. One homolog of *VTE5* in Arabidopsis was identified and later designated *FOLK* for farnesol kinase. FOLK is able to phosphorylate farnesol, geraniol, and geranylgeraniol. In this work, the role of phytol, geranylgeraniol, and farnesol phosphorylation, for the biosynthesis of different metabolites including tocopherol (vitamin E) and phylloquinone (vitamin K1), was investigated in Arabidopsis *vte5-2*, *folk-2,* and vte5-2 *folk-2* mutant plants.

Phytyl-P and geranylgeranyl-P levels are reduced, while phytol accumulates in *vte5-2* and *vte5-2 folk-2.* Geranylgeraniol accumulates in *folk-2* and *vte5-2 folk-2.* The *vte5-2* single mutant shows reduced tocopherol levels, while the *folk-2* single mutant plants have similar tocopherol levels as the WT. The phylloquinone levels are similar to the WT in *vte5-2* and in *folk-2*. The *vte5-2 folk-2* double mutant plants are tocopherol deficient and have a reduced content of phylloquinone in comparison to the WT. Therefore, the farnesol kinase (FOLK) and the phytol kinase (VTE5) are involved in tocopherol and phylloquinone biosynthesis. Enzyme assays with recombinant proteins expressed in *E. coli* revealed that VTE5 is able to phosphorylate phytol, geranylgeraniol, and farnesol, while FOLK only phosphorylated geranylgeraniol and farnesol but not phytol. Geranylgeranyl-PP is the precursor for the biosynthesis of chlorophyll and carotenoids. The contents of chlorophyll and carotenoids were not altered in the mutants indicating that VTE5 and FOLK are not required for the biosynthesis of these compounds. The sterol content was slightly reduced in the *vte5-2 folk-2* double mutant suggesting that farnesol phosphorylation by VTE5 and FOLK contributes to sterol synthesis.

Arabidopsis mutant plants lacking phytyl phosphate kinase (VTE6) activity show a strong growth retardation. The decreased growth of *vte6-1* could not be rescued by supplementation with gibberellic acid. Arabidopsis *vte6* mutants were described to accumulate phytyl-P and phytol derived from chlorophyll degradation. Accumulation

of phytyl-P might be detrimental for plant growth and therefore cause the severe growth phenotype. The introduction of the *pao1* mutation, affected in chlorophyll degradation, into the *vte6-1* background did not rescue the retarded growth of *vte6-1*. The *vte6-1 pao1* plants were still only viable on synthetic medium supplemented with sucrose. Nevertheless, some plants grew slightly better and developed shoots but no siliques nor seeds.

In conclusion, Arabidopsis farnesol kinase FOLK and the phytol kinase VTE5 are involved in the biosynthesis of tocopherol and phylloquinone. Tocopherol and phylloquinone synthesis depends on the availability of phytyl-PP. However, the recombinant FOLK protein does not show *in vitro* phytol kinase activity. Presumably, the geranylgeraniol kinase activity of FOLK contributes to tocopherol and phylloquinone biosynthesis. This shows the important role of geranylgeraniol phosphorylation next to phytol phosphorylation for tocopherol and phylloquinone biosynthesis in Arabidopsis.

6 References

Altmann, T. (1998) A tale of dwarfs and drugs: brassinosteroids to the rescue. *Trends in Genetics*. **14**(12), 490–495.

Aubry, S., Mani, J., Hörtensteiner, S. (2008) Stay-green protein, defective in Mendel's green cotyledon mutant, acts independent and upstream of pheophorbide a oxygenase in the chlorophyll catabolic pathway. *Plant Molecular Biology*. **67**(3), 243–256.

Babujee, L., Wurtz, V., Ma, C., Lueder, F., Soni, P., van Dorsselaer, A., Reumann, S. (2010) The proteome map of spinach leaf peroxisomes indicates partial compartmentalization of phylloquinone (vitamin K1) biosynthesis in plant peroxisomes. *Journal of Experimental Botany*. **61**(5), 1441–1453.

Basset, G.J., Latimer, S., Fatihi, A., Block, E.S. and A. (2017) Phylloquinone (vitamin K1): Occurrence, biosynthesis and functions. *Mini-Reviews in Medicinal Chemistry*. **17**(12), 1028–1038.

Benveniste, P. (2002) Sterol metabolism. *The Arabidopsis Book*. **1**, e0004–e0004.

Bergmüller, E., Porfirova, S., Dörmann, P. (2003) Characterization of an Arabidopsis mutant deficient in γ-tocopherol methyltransferase. *Plant Molecular Biology*. **52**(6), 1181–1190.

Booth, S.L., Sadowski, J. (1997) Determination of phylloquinone in foods by high-performance liquid chromatography. In *Methods in Enzymology*. Academic Press, pp. 446–456.

Cahoon, E.B., Hall, S.E., Ripp, K.G., Ganzke, T.S., Hitz, W.D., Coughlan, S.J. (2003) Metabolic redesign of vitamin E biosynthesis in plants for tocotrienol production and increased antioxidant content. *Nature Biotechnology*. **21**(9), 1082–1087.

Calisto, B.M., Perez-Gil, J., Bergua, M., Querol-Audi, J., Fita, I., Imperial, S. (2007) Biosynthesis of isoprenoids in plants: Structure of the 2C-methyl-d-erithrytol 2,4-cyclodiphosphate synthase from Arabidopsis thaliana. Comparison with the bacterial enzymes. *Protein Science*. **16**(9), 2082–2088.

Carrie, C., Murcha, M.W., Millar, A.H., Smith, S.M., Whelan, J. (2007) Nine 3-ketoacyl-CoA thiolases (KATs) and acetoacetyl-CoA thiolases (ACATs) encoded by five genes in Arabidopsis thaliana are targeted either to peroxisomes or cytosol but not to mitochondria. *Plant Molecular Biology*. **63**(1), 97–108.

Clastre, M., Papon, N., Courdavault, V., Giglioli-Guivarc'h, N., St-Pierre, B., Simkin, A.J. (2011) Subcellular evidence for the involvement of peroxisomes in plant isoprenoid biosynthesis. *Plant Signaling & Behavior*. **6**(12), 2044–2046.

Collakova, E., DellaPenna, D. (2001) Isolation and functional analysis of homogentisate phytyltransferase from Synechocystis sp. PCC 6803 and Arabidopsis. *Plant Physiology*. **127**(3), 1113–1124.

Cunningham, F.X., Gantt, E. (1998) Genes and enzymes of carotenoid biosynthesis in plants. *Annual Review of Plant Physiology and Plant Molecular Biology*. **49**(1), 557–583.

Dörmann, P., Hoffmann-Benning, S., Balbo, I., Benning, C. (1995) Isolation and characterization of an Arabidopsis mutant deficient in the thylakoid lipid digalactosyl diacylglycerol. *The Plant Cell*. **7**(11), 1801–1810.

vom Dorp, K. (2015) *Phytol and tocopherol metabolism in Arabidopsis thaliana*. PhD thesis, University of Bonn, Germany.

vom Dorp, K., Hölzl, G., Plohmann, C., Eisenhut, M., Abraham, M., Weber, A.P.M., Hanson, A.D., Dörmann, P. (2015) Remobilization of phytol from chlorophyll degradation is essential for tocopherol synthesis and growth of Arabidopsis. *The Plant Cell*. **27**(10), 2846–2859.

Durr, I.F., Rudney, H. (1960) The reduction of β-Hydroxy-β-methylglutaryl coenzyme A to mevalonic acid. *Journal of Biological Chemistry*. **235**(9), 2572–2578.

Falter, C., Thu, N.B.A., Pokhrel, S., Reumann, S. (2019) New guidelines for fluorophore application in peroxisome targeting analyses in transient plant expression systems. *Journal of Integrative Plant Biology*. **61**(7), 884–899.

Ferguson, J.J., Durr, I.F., Rudney, H. (1959) The biosynthesis of mevalonic acid. *Proceedings of the National Academy of Sciences of the United States of America*. **45**(4), 499–504.

Finkelstein, R.R., Rock, C.D. (2002) Abscisic acid biosynthesis and response. *The Arabidopsis Book*. **1**, e0058–e0058.

Fitzpatrick, A.H., Bhandari, J., Crowell, D.N. (2011) Farnesol kinase is involved in farnesol metabolism, ABA signaling and flower development in Arabidopsis. *The Plant Journal*. **66**(6), 1078–1088.

Fleming, I. (1967) Absolute configuration and the structure of chlorophyll. *Nature*. **216**(5111), 151–152.

Forman, B.M., Goode, E., Chen, J., Oro, A.E., Bradley, D.J., Perlmann, T., Noonan, D.J., Burka, L.T., McMorris, T., Lamph, W.W., Evans, R.M., Weinberger, C. (1995) Identification of a nuclear receptor that is activated by farnesol metabolites. *Cell*. **81**(5), 687–693.

Gaude, N., Bréhélin, C., Tischendorf, G., Kessler, F., Dörmann, P. (2007) Nitrogen deficiency in Arabidopsis affects galactolipid composition and gene expression and results in accumulation of fatty acid phytyl esters. *The Plant Journal*. **49**(4), 729–739.

Gupta, R., Chakrabarty, S.K. (2013) Gibberellic acid in plant: still a mystery unresolved. *Plant Signaling & Behavior*. **8**(9), e25504.

Gutbrod, K., Romer, J., Dörmann, P. (2019) Phytol metabolism in plants. *Progress in Lipid Research*. **74**, 1–17.

Hartmann, M.-A. (1998) Plant sterols and the membrane environment. *Trends in Plant Science*. **3**(5), 170–175.

He, J.-X., Fujioka, S., Li, T.-C., Kang, S.G., Seto, H., Takatsuto, S., Yoshida, S., Jang, J.-C. (2003) Sterols regulate development and gene expression in Arabidopsis. *Plant Physiology*. **131**(3), 1258–1269.

Hooley, R. (1994) Gibberellins: perception, transduction and responses. *Plant Molecular Biology*. **26**(5), 1529–1555.

Hörtensteiner, S. (2013) Update on the biochemistry of chlorophyll breakdown. *Plant Molecular Biology*. **82**(6), 505–517.

Hsieh, M.-H., Goodman, H.M. (2005) The Arabidopsis IspH homolog is involved in the plastid nonmevalonate pathway of isoprenoid biosynthesis. *Plant Physiology*. **138**(2), 641–653.

Inoue, H., Korenaga, T., Sagami, H., Koyama, T., Sugiyama, H., Ogura, K. (1994) Formation of farnesyl oleate and three other farnesyl fatty acid esters by cell-free extracts from Botryococcus braunii B race. *Phytochemistry*. **36**(5), 1203–1207.

Ischebeck, T., Zbierzak, A.M., Kanwischer, M., Dörmann, P. (2006) A salvage pathway for phytol metabolism in Arabidopsis. *The Journal of Biological Chemistry*. **281**(5), 2470–7.

Jarvis, P., Dörmann, P., Peto, C.A., Lutes, J., Benning, C., Chory, J. (2000) Galactolipid deficiency and abnormal chloroplast development in the Arabidopsis MGD synthase 1 mutant. *Proceedings of the National Academy of Sciences of the United States of America*. **97**(14), 8175–8179.

Jeffry S.W., Mantoura R.F.C., W.S.W. (1997) *Phytoplankton pigments in oceanography: guidelines to modern methods*. UNESCO Publishing: Paris. ISBN 92-3-103275-5. 661 pp.

Joo, C.N., Park, C.E., Kramer, J.K.G., Kates, M. (1973) Synthesis and acid hydrolysis of monophosphate and pyrophosphate esters of phytanol and phytol. *Canadian Journal of Biochemistry*. **51**(11), 1527–1536.

Kanwischer, M. (2007) *Phytol aus dem Chlorophyllabbau ist limitierend für die Tocopherol (Vitamin E)-Synthese*. PhD thesis, University of Potsdam (MPI, Golm), Germany.

Kanwischer, M., Porfirova, S., Bergmüller, E., Dörmann, P. (2005) Alterations in tocopherol cyclase activity in transgenic and mutant plants of Arabidopsis affect tocopherol content, tocopherol composition, and oxidative stress. *Plant Physiology*. **137**(2), 713–723.

Katz, J.J., Norris, J.R. (1973) Chlorophyll and light energy transduction in photosynthesis. In D. R. A. O. SANADI & L. B. T.-C. T. in B. PACKER, eds. *Current Topics in Bioenergetics*. Elsevier, pp. 41–75.

Keller, Y., Bouvier, F., d'Harlingue, A., Camara, B. (1998) Metabolic compartmentation of plastid prenyllipid biosynthesis. *European Journal of Biochemistry*. **251**(1-2), 413–417.

Kellogg, B.A., Poulter, C.D. (1997) Chain elongation in the isoprenoid biosynthetic pathway. *Current Opinion in Chemical Biology*. **1**(4), 570–578.

Koorneef, M., Elgersma, A., Hanhart, C.J., van Loenen-Martinet, E.P., van Rijn, L., Zeevaart, J.A.D. (1985) A gibberellin insensitive mutant of Arabidopsis thaliana. *Physiologia Plantarum*. **65**(1), 33–39.

Krauß, S., Vetter, W. (2018) Phytol and phytyl fatty acid esters: Occurrence, concentrations, and relevance. *European Journal of Lipid Science and Technology*. **120**(7), 1700387.

Kreszies, V. (2019) *ABA-dependent and -independent regulation of tocopherol (vitamin E) biosynthesis in response to abiotic stress in Arabidopsis*. PhD thesis, University of Bonn, Germany.

Lange, B.M., Ghassemian, M. (2003) Genome organization in Arabidopsis thaliana: a survey for genes involved in isoprenoid and chlorophyll metabolism. *Plant Molecular Biology*. **51**(6), 925–948.

Lichtenthaler, H.K. (1999) The 1-deoxy-D-xylulose-5-phospate pathway of isoprenoid biosynthesis in plants. *Annual Review of Plant Physiology and Plant Molecular Biology*. **50**(1), 47–65.

Lichtenthaler, H.K., Rohmer, M., Schwender, J. (1997) Two independent biochemical pathways for isopentenyl diphosphate and isoprenoid biosynthesis in higher plants. *Physiologia Plantarum*. **101**(3), 643–652.

Liljenberg, C., Karunen, P. (1978) Changes in the content of phytyl and geranylgeranyl esters of germinating Polytrichum commune spores. *Physiologia Plantarum*. **44**(4), 369–372.

Lippold, F., vom Dorp, K., Abraham, M., Hölzl, G., Wewer, V., Yilmaz, J.L., Lager, I., Montandon, C., Besagni, C., Kessler, F., Stymne, S., Dörmann, P. (2012) Fatty acid phytyl ester synthesis in chloroplasts of Arabidopsis. *The Plant Cell*. **24**(5), 2001–2014.

Liu, F., Guo, F.-Q. (2013) Nitric oxide deficiency accelerates chlorophyll breakdown and stability loss of thylakoid membranes during dark-induced leaf senescence in Arabidopsis. *PLOS ONE*. **8**(2), e56345.

Lohmann, A., Schöttler, M.A., Bréhélin, C., Kessler, F., Bock, R., Cahoon, E.B., Dörmann, P. (2006) Deficiency in phylloquinone (vitamin K1) methylation affects prenyl quinone distribution, photosystem I abundance, and anthocyanin accumulation in the Arabidopsis AtmenG mutant. *Journal of Biological Chemistry*. **281**(52), 40461–40472.

Mène-Saffrané, L. (2018) Vitamin E biosynthesis and its regulation in plants. *Antioxidants*. **7**(2).

Mène-Saffrané, L., Pellaud, S. (2017) Current strategies for vitamin E biofortification of crops. *Current Opinion in Biotechnology*. **44**, 189–197.

Murashige, T., Skoog, F. (1962) A revised medium for rapid growth and bio assays with tobacco tissue cultures. *Physiologia Plantarum*. **15**, 473–497.

Nagel, R., Berasategui, A., Paetz, C., Gershenzon, J., Schmidt, A. (2014) Overexpression of an isoprenyl diphosphate synthase in Spruce leads to unexpected terpene diversion products that function in plant defense. *Plant Physiology*. **164**(2), 555–569.

Nebenführ, A., Gallagher, L.A., Dunahay, T.G., Frohlick, J.A., Mazurkiewicz, A.M., Meehl, J.B., Staehelin, L.A. (1999) Stop-and-Go movements of plant golgi stacks are mediated by the acto-myosin system. *Plant Physiology*. **121**(4), 1127–1141.

Ohnuma, S., Watanabe, M., Nishino, T. (1996) Identification and characterization of geranylgeraniol kinase and geranylgeranyl phosphate kinase from the Archaebacterium sulfolobus acidocaldariu. *The Journal of Biochemistry*. **119**(3), 541–547.

Oostende, C. van, Widhalm, J.R., Basset, G.J.C. (2008) Detection and quantification of vitamin K1 quinol in leaf tissues. *Phytochemistry*. **69**(13), 2457–2462.

Pan, X., Welti, R., Wang, X. (2008) Simultaneous quantification of major phytohormones and related compounds in crude plant extracts by liquid chromatography–electrospray tandem mass spectrometry. *Phytochemistry*. **69**(8), 1773–1781.

Patwari, P., Salewski, V., Gutbrod, K., Kreszies, T., Dresen-Scholz, B., Peisker, H., Steiner, U., Meyer, A.J., Schreiber, L., Dörmann, P. (2019) Surface wax esters contribute to drought tolerance in Arabidopsis. *The Plant Journal*. **98**(4), 727–744.

Porfirova, S., Bergmüller, E., Tropf, S., Lemke, R., Dörmann, P. (2002) Isolation of an Arabidopsis mutant lacking vitamin E and identification of a cyclase essential for all tocopherol biosynthesis. *Proceedings of the National Academy of Sciences of the United States of America*. **99**(19), 12495–12500.

Porra, R.J., Thompson, W.A., Kriedemann, P.E. (1989) Determination of accurate extinction coefficients and simultaneous equations for assaying chlorophylls a and b extracted with four different solvents. *Lipids and Lipid Metabolism*. **975**, 384–394.

Pružinská, A., Tanner, G., Anders, I., Roca, M., Hörtensteiner, S. (2003) Chlorophyll breakdown: Pheophorbide a oxygenase is a Rieske-type iron–sulfur protein, encoded by the accelerated cell death 1 gene. *Proceedings of the National Academy of Sciences of the United States of America*. **100**(25), 15259–15264.

Pružinská, A., Tanner, G., Aubry, S., Anders, I., Moser, S., Müller, T., Ongania, K.-H., Kräutler, B., Youn, J.-Y., Liljegren, S.J., Hörtensteiner, S. (2005) Chlorophyll breakdown in senescent Arabidopsis leaves. Characterization of chlorophyll catabolites and of chlorophyll catabolic enzymes involved in the degreening reaction. *Plant Physiology*. **139**(1), 52–63.

Reumann, S. (2013) Biosynthesis of vitamin K1 (phylloquinone) by plant peroxisomes and its integration into signaling molecule synthesis pathways. In L. A. del Río, ed. *Peroxisomes and their key role in cellular signaling and metabolism. Subcellular Biochemistry, vol 69.* Dordrecht: Springer, pp. 213–229.

Reumann, S. (2004) Specification of the peroxisome targeting signals type 1 and type 2 of plant peroxisomes by bioinformatics analyses. *Plant Physiology*. **135**(2), 783–800.

Reumann, S., Babujee, L., Ma, C., Wienkoop, S., Siemsen, T., Antonicelli, G.E., Rasche, N., Lüder, F., Weckwerth, W., Jahn, O. (2007) Proteome analysis of Arabidopsis leaf peroxisomes reveals novel targeting peptides, metabolic pathways, and defense mechanisms. *The Plant Cell*. **19**(10), 3170–3193.

Rohmer, M. (1999) The discovery of a mevalonate-independent pathway for isoprenoid biosynthesis in bacteria, algae and higher plants. *Natural Product Reports*. **16**(5), 565–574.

Ruiz-Sola, M.Á., Coman, D., Beck, G., Barja, M.V., Colinas, M., Graf, A., Welsch, R., Rütimann, P., Bühlmann, P., Bigler, L., Gruissem, W., Rodríguez-Concepción, M., Vranová, E. (2016) Arabidopsis GERANYLGERANYL DIPHOSPHATE SYNTHASE 11 is a hub isozyme required for the production of most photosynthesis-related isoprenoids. *New Phytologist*. **209**(1), 252–264.

Sattler, S.E., Cahoon, E.B., Coughlan, S.J., DellaPenna, D. (2003) Characterization of tocopherol cyclases from higher plants and cyanobacteria. Evolutionary implications for tocopherol synthesis and function. *Plant Physiology*. **132**(4), 2184–2195.

Sattler, S.E., Gilliland, L.U., Magallanes-Lundback, M., Pollard, M., DellaPenna, D. (2004) Vitamin E is essential for seed longevity and for preventing lipid peroxidation during germination. *The Plant Cell*. **16**(6), 1419–1432.

Schaeffer, A., Bronner, R., Benveniste, P., Schaller, H. (2001) The ratio of campesterol to sitosterol that modulates growth in Arabidopsis is controlled by STEROL METHYLTRANSFERASE 2;1. *The Plant Journal*. **25**(6), 605–615.

Schaller, H., Bouvier-Navé, P., Benveniste, P. (1998) Overexpression of an Arabidopsis cDNA encoding a sterol-C24-methyltransferase in Tobacco modifies the ratio of 24-methyl cholesterol to sitosterol and is associated with growth reduction. *Plant Physiology*. **118**(2), 461–469.

Schreiber, U., Schliwa, U., Bilger, W. (1986) Continuous recording of photochemical and non-photochemical chlorophyll fluorescence quenching with a new type of modulation fluorometer. *Photosynthesis Research*. **10**(1), 51–62.

Schumann, T., Paul, S., Melzer, M., Dörmann, P., Jahns, P. (2017) Plant growth under natural light conditions provides highly flexible short-term acclimation properties toward high light stress. *Frontiers in Plant Science*. **8**, 681.

Schwender, J., Müller, C., Zeidler, J., Lichtenthaler, H.K. (1999) Cloning and heterologous expression of a cDNA encoding 1-deoxy-D-xylulose-5-phosphate reductoisomerase of Arabidopsis thaliana. *FEBS Letters*. **455**(1–2), 140–144.

Shalygo, N., Czarnecki, O., Peter, E., Grimm, B. (2009) Expression of chlorophyll synthase is also involved in feedback-control of chlorophyll biosynthesis. *Plant Molecular Biology*. **71**(4), 425.

Shimoda, Y., Ito, H., Tanaka, A. (2016) Arabidopsis STAY-GREEN, Mendel's green cotyledon gene, encodes magnesium-dechelatase. *The Plant Cell*. **28**(9), 2147–2160.

Shintani, D., DellaPenna, D. (1998) Elevating the vitamin E content of plants through metabolic engineering. *Science*. **282**(5396), 2098–2100.

Simkin, A.J., Guirimand, G., Papon, N., Courdavault, V., Thabet, I., Ginis, O., Bouzid, S., Giglioli-Guivarc'h, N., Clastre, M. (2011) Peroxisomal localisation of the final steps of the mevalonic acid pathway in planta. *Planta*. **234**(5), 903.

Smith, P.K., Krohn, R.I., Hermanson, G.T., Mallia, A.K., Gartner, F.H., Provenzano, M.D., Fujimoto, E.K., Goeke, N.M., Olson, B.J., Klenk, D.C. (1985) Measurement of protein using bicinchoninic acid. *Analytical Biochemistry*. **150**(1), 76–85.

Soll, J., Kemmerling, M., Schultz, G. (1980) Tocopherol and plastoquinone synthesis in spinach chloroplasts subfractions. *Archives of Biochemistry and Biophysics*. **204**(2), 544–550.

Stacey, M.G., Cahoon, R.E., Nguyen, H.T., Cui, Y., Sato, S., Nguyen, C.T., Phoka, N., Clark, K.M., Liang, Y., Forrester, J., Batek, J., Do, P.T., Sleper, D.A., Clemente, T.E., Cahoon, E.B., Stacey, G. (2016) Identification of homogentisate dioxygenase as a target for vitamin E biofortification in oilseeds. *Plant Physiology*. **172**(3), 1506–1518.

Tanaka, R., Oster, U., Kruse, E., Rüdiger, W., Grimm, B. (1999) Reduced activity of geranylgeranyl reductase leads to loss of chlorophyll and tocopherol and to partially geranylgeranylated chlorophyll in transgenic Tobacco plants expressing antisense RNA for geranylgeranyl reductase. *Plant Physiology*. **120**(3), 695–704.

Thai, L., Rush, J.S., Maul, J.E., Devarenne, T., Rodgers, D.L., Chappell, J., Waechter, C.J. (1999) Farnesol is utilized for isoprenoid biosynthesis in plant cells via farnesyl pyrophosphate formed by successive monophosphorylation reactions. *Proceedings of the National Academy of Sciences of the United States of America*. **96**(23), 13080–13085.

Tsegaye, Y., Shintani, D.K., DellaPenna, D. (2002) Overexpression of the enzyme p-hydroxyphenolpyruvate dioxygenase in Arabidopsis and its relation to tocopherol biosynthesis. *Plant Physiology and Biochemistry*. **40**(11), 913–920.

Valentin, H.E., Lincoln, K., Moshiri, F., Jensen, P.K., Qi, Q., Venkatesh, T. V, Karunanandaa, B., Baszis, S.R., Norris, S.R., Savidge, B., Gruys, K.J., Last, R.L. (2006) The Arabidopsis vitamin E pathway gene 5-1 mutant reveals a critical role for phytol kinase in seed tocopherol biosynthesis. *The Plant Cell*. **18**(1), 212–224.

Vidi, P.-A., Kanwischer, M., Baginsky, S., Austin, J.R., Csucs, G., Dörmann, P., Kessler, F., Bréhélin, C. (2006) Tocopherol Cyclase (VTE1) localization and vitamin E accumulation in chloroplast plastoglobule lipoprotein particles. *Journal of Biological Chemistry*. **281**(16), 11225–11234.

Voinnet, O., Lederer, C., Baulcombe, D.C. (2000) A viral movement protein prevents spread of the gene silencing signal in Nicotiana benthamiana. *Cell*. **103**(1), 157–167.

Wang, L., Li, Q., Zhang, A., Zhou, W., Jiang, R., Yang, Z., Yang, H., Qin, X., Ding, S., Lu, Q., Wen, X., Lu, C. (2017) The phytol phosphorylation pathway is essential for the biosynthesis of phylloquinone, which is required for photosystem I stability in Arabidopsis. *Molecular Plant*. **10**(1), 183–196.

Wang, Pingyu, Li, C., Wang, Y., Huang, R., Sun, C., Xu, Z., Zhu, J., Gao, X., Deng, X., Wang, Pingrong (2014) Identification of a geranylgeranyl reductase gene for chlorophyll synthesis in rice. *SpringerPlus*. **3**(1), 201.

Wehler, R. (2017) *Phytyl ester synthases from Arabidopsis thaliana and Solanum lycopersicum*. PhD thesis, University of Bonn, Germany.

von Wettstein, D., Gough, S., Kannangara, C.G. (1995) Chlorophyll biosynthesis. *The Plant Cell*. **7**(7), 1039–1057.

Xiong, L., Zhu, J.-K. (2003) Regulation of abscisic acid biosynthesis. *Plant Physiology*. **133**(1), 29–36.

Yang, W., Cahoon, R.E., Hunter, S.C., Zhang, C., Han, J., Borgschulte, T., Cahoon, E.B. (2011) Vitamin E biosynthesis: functional characterization of the monocot homogentisate geranylgeranyl transferase. *The Plant Journal*. **65**(2), 206–217.

Zhang, C., Cahoon, R.E., Hunter, S.C., Chen, M., Han, J., Cahoon, E.B. (2013) Genetic and biochemical basis for alternative routes of tocotrienol biosynthesis for enhanced vitamin E antioxidant production. *The Plant Journal*. **73**(4), 628–639.

Zhang, Y., Nielsen, J., Liu, Z. (2017) Engineering yeast metabolism for production of terpenoids for use as perfume ingredients, pharmaceuticals and biofuels. *FEMS Yeast Research*. **17**(8).

Zybailov, B., Rutschow, H., Friso, G., Rudella, A., Emanuelsson, O., Sun, Q., van Wijk, K.J. (2008) Sorting signals, N-terminal modifications and abundance of the chloroplast proteome. *PLOS ONE*. **3**(4), e1994.

7 Appendix

7.1 Cloning strategies and vector maps

7.1.1 *E. coli* Rosetta pET Duet FOLK/- and pET Duet VTE5/-

For cloning of the pETDuet FOLK/- and pETDuet VTE5/- vectors, FOLK and VTE5 cDNA sequences were amplified by PCR (section 2.5.4.2) using *Arabidopsis* cDNA obtained by RT-PCR from leaf RNA as template. For VTE5 amplification the oligonucleotides bn3266 and bn3202 were used, for amplification of FOLK, bn3263 and bn3264 were used. In both constructs, BamHI and SalI restriction sides were attached to the cDNA sequence at the 5' and 3' ends, respectively. PCR products (inserts) were ligated into the pJet1.2/blunt vector using the CloneJET PCR Cloning Kit (Thermo Scientific). Ligated plasmids were transformed into self-made electrocompetent *E. coli* Electroshox cells (section 2.4.2). Afterward, single colonies were tested for the presence of the insert by colony PCR (section 2.5.4.2). Positive clones were cultivated in liquid culture overnight and plasmids isolated with the NucleoSpin plasmid kit (Macherey & Nagel). Isolated plasmids were digested (section 2.5.3)with suitable restriction enzymes (NEB) according to the supplier's protocol or sent for sequencing. Correct inserts in the pJet1.2 constructs, and the pETDuet-1 empty vector isolated from bn1132, were digested using the restriction enzymes BamHI and SalI. Then the VTE5 or FOLK inserts were ligated into the pETDuet-1 vector using T4 DNA ligase (NEB) according to the supplier's protocol. After ligation, constructs were always first transformed into *E. coli* Electroshox cells to achieve high plasmid yield. Plasmids were tested for the correct insert (by digestion) and transferred into the bacteria strain for expression. Expression of pETDuet ev, FOLK/- and VTE5/- was performed in *E. coli Rosetta* (DE3).

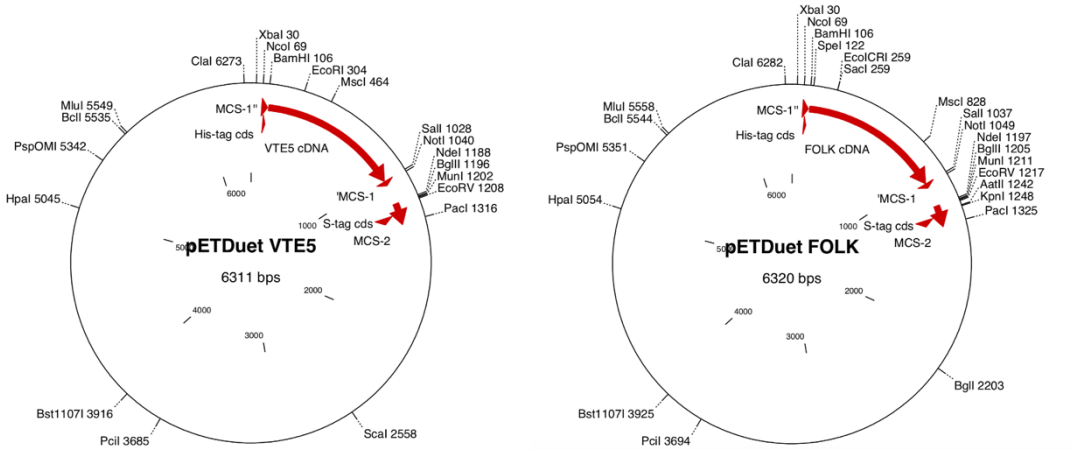

Figure 36 Vector maps of pETDuet VTE5/- and pETDuet FOLK/-

7.1.2 *A. tumefaciens* pLH9000 VTE5-eGFP and FOLK-eGFP

For cloning of the pLH9000 VTE5-eGFP and pLH9000 FOLK-eGFP vectors, FOLK and VTE5 cDNA sequences were amplified by PCR (section 2.5.4.2) using *Arabidopsis* cDNA obtained from leaf RNA by RT-PCR as template. For VTE5 amplification the oligonucleotides bn3203 and bn3205 were used, where the stop codon of VTE5 was removed and the restriction sites SpeI and BamHI added. For amplification of FOLK, bn3173 and bn3174 were used, where the stop codon of FOLK was removed and the restriction sites XbaI and BamHI added. Additionally, the eGFP sequence was amplified with the restriction sites BamHI and SalI from the recombinant plasmid pJet VTE6-eGFP isolated from the stock bn573. PCR products (inserts) were ligated into the pJet1.2/blunt vector using the CloneJET PCR Cloning Kit (Thermo Scientific) and transformed into self-made electrocompetent *E. coli* Electroshox cells (section 2.4.2). Afterwards single colonies were tested for the presence of the insert by colony PCR (section 2.5.4.2). Positive clones were cultivated in liquid culture overnight and plasmids isolated with the NucleoSpin plasmid kit (Macherey & Nagel). Isolated plasmids were control digested to test the sequence orientation (section 2.5.3) with suitable restriction enzymes (NEB) according to the supplier's protocol or sent for sequencing. All pJet1.2 plasmids (pJet VTE5, pJet FOLK and pJet eGFP) were afterwards digested with PstI and BamHI. The digested pJet eGFP was used as vector backbone while the digested fragments of FOLK and VTE5 were used as inserts to generate VTE5-eGFP and FOLK-eGFP fusion

constructs. Ligation was performed using T4 DNA ligase (NEB). After ligation, constructs were transformed into *E. coli* Electroshox cells, positive clones control digested, and plasmids isolated. The binary vector pLH9000 vector carrying a 35S-promotor (bn1176) was isolated and cut with SpeI, HindIII, and SalI. The digested pLH9000 vector (SalI/SpeI) was used for ligation with VTE5-eGFP and FOLK-eGFP which were released from the pJet1.2 constructs with SpeI/SalI or XbaI/SalI, respectively. The recombinant plasmids pLH9000-35S-VTE5-eGFP and pLH9000-35S-FOLK-eGFP were first transformed in *E. coli* Electroshox cells, and afterwards into self-made electrocompetent *A. tumefaciens* cells for transformation of *N. benthamiana* leaves for localization studies.

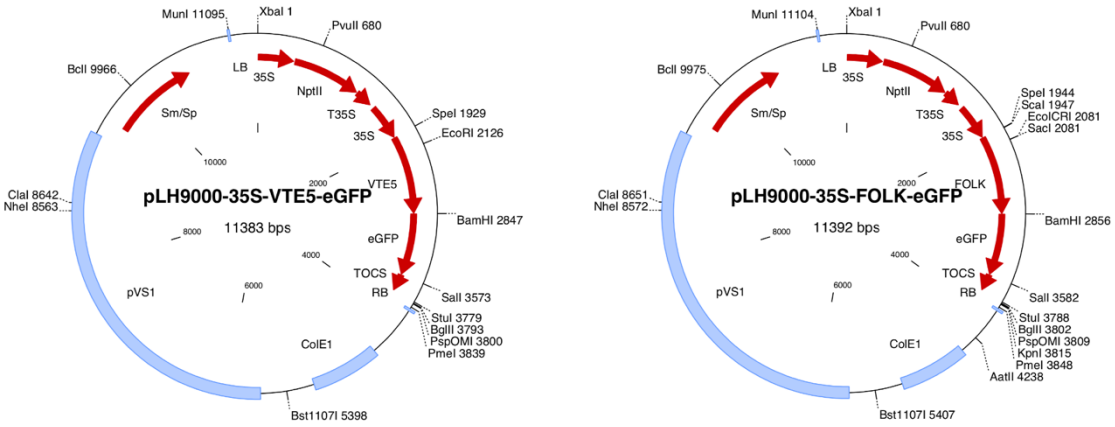

Figure 37 Vector maps of pLH9000 35S-VTE5-eGFP and pLH9000 35S-FOLK-eGFP.

7.2 Synthetic oligonucleotides

Table 8 Synthetic oligonucleotides

Oligonucleotides used for this work were ordered from IDT Genomics (Leuven, BE). Restriction sites in the oligonucleotide sequences are written in lower case letters and underlined.

Primer	Sequence (5' → 3')	Description
bn78	ATTTTGCCGATTTCGGAAC	LBb1.2 SALK, Arabidopsis genotyping
bn232	CCGGATCGTATCGGTTTTCG	Ds3-2a, Arabidopsis genotyping
bn233	ATGGCAACGATTTCGTCAACTC	*vte6-1* genotyping
bn234	GTCCAGCCAATGTTCCTTCAAG	*vte6-1* genotyping
bn771	ACTGTACCTCCGTCAATCGCC	*vte5-2* genotyping
bn772	AAGCTTAAGACAAGCGCGTATG	*vte5-2* genotyping
bn2692	CGACTCACTATAGGGAGAGCGGC	pJet1.2/blunt forward primer
bn2693	AAGAACATCGATTTTCCATGGCAG	pJet1.2/blunt reverse primer
bn2801	GATTATGCGGCCGTGTACAA	pETDuet-1 downstream primer
bn2802	ATGCGTCCGGCGTAGA	pETDuet-1 upstream primer
bn2853	AGATGGGAACAATGAATGCAG	*folk-2* genotyping
bn2854	CATCTGTGGTTGACATTGGTG	*folk-2* genotyping
bn3004	GGCTCACCTGACGCTTGGTTA	*pao1* genotyping
bn3005	CGACGGTGACAATTCAAAGGG	*pao1* genotyping
bn3173	GGGtctagaATGGCAACTACTAGTAC TACTAC	FOLK amplification for cloning (XbaI) (destiny vector: pLH9000)
bn3174	GGGggatccGAAGAGTAAGAATCCG GCCAA	FOLK amplification for cloning without stop codon (BamHI) (destiny vector: pLH9000)
bn3202	CTAgtcgacCTAATATCCGAAACTTA A	VTE5 amplification for cloning (SalI) (destiny vector: pETDuet)
bn3203	CTAactagtATGGCAGCAACCTTACC TCTA	VTE5 amplification for cloning (SpeI) (destiny vector: pLH9000)
bn3205	CTAggatccATATCCGAAACTTAA	VTE5 amplification for cloning without stop codon (BamHI) (destiny vector: pLH9000)
bn3263	CTAggatccAATGGCAACTACTAGT ACTAC	FOLK amplification for cloning (BamHI) (destiny vector: pETDuet)
bn3264	CTAgtcgacTTAGAAGAGTAAGAAT CCGG	FOLK amplification for cloning (SalI) (destiny vector: pETDuet)
bn3266	TTTggatccAATGGCAGCAACCTTAC CTCT	VTE5 amplification for cloning (BamHI) (destiny vector: pETDuet)

7.3 Targeted lists for MS analysis

Table 9 Targeted list for GC-MS analysis of isoprenoid alcohols.

Phytol, farnesol, and geranylgeraniol were quantified using GC-MS after derivatization with MSTFA to produce trimethylsilyl (TMS) ethers. The fragment ion of the TMS group was used to determine the amount of the internal standard octadecenol, as well as of farnesol and geranylgeraniol. A fragment ion derived from the isoprenoid alcohol moiety was used for the quantification of phytol.

Isoprenoid Alcohols	Formula	M	M+TMS	Product Ion m/z
Octadecenol (I.S.)	$C_{18}H_{36}O$	268.2766	340	73
Farnesol	$C_{15}H_{26}O$	222.3663	294	73
Phytol	$C_{20}H_{40}O$	296.3079	368	143
Geranylgeraniol	$C_{20}H_{34}O$	290.4833	362	73

Table 10 Targeted list for GC-MS analysis of free sterols.

Free sterols were quantified using GC-MS after derivatization with MSTFA to produce trimethylsilyl (TMS) ethers. A fragment of the TMS group was used to determine the amount of free sterols.

Free Sterols	Formula	M	M+TMS	Product Ion m/z
Cholestanol (I.S.)	$C_{27}H_{48}O$	388.67	460	460
Cholesterol	$C_{27}H_{46}O$	386.65	458	368
Campesterol	$C_{28}H_{48}O$	400.68	472	382
Stigmasterol	$C_{29}H_{48}O$	412.69	484	394
β-Sitosterol	$C_{29}H_{50}O$	414.71	486	396

Table 11 Targeted list for Q-Trap MS/MS analysis of isoprenoid alcohol phosphates.

Isoprenoid alcohol phosphates were measured as deprotonated ions by LC MS/MS with Q-Trap in the negative ion mode by scanning for a fragment of the phosphate group, m/z 78.9591 (vom Dorp, 2015).

Isoprenoid Alcohol Phosphates	Formula	M	Parental Ion $[M-H]^-$	Product Ion $[HPO_3]^-$
10:0ol-P (I.S.)	$C_{10}H_{23}O_4P$	238.13	237.1256	78.9591
10:0ol-PP (I.S.)	$C_{10}H_{24}O_7P_2$	318.10	317.0919	
Farnesyl-P	$C_{15}H_{27}O_4P$	302.35	301.1569	
Farnesyl-PP	$C_{15}H_{28}O_7P_2$	382.33	381.1232	
Geranylgeranyl-P	$C_{20}H_{35}O_4P$	370.23	369.2195	
Geranylgeranyl-PP	$C_{20}H_{36}O_7P_2$	450.19	449.1858	
Phytyl-P	$C_{20}H_{41}O_4P$	376.27	375.2664	
Phytyl-PP	$C_{20}H_{42}O_7P_2$	456.24	455.2328	

Table 12 Targeted list for Q-TOF-MS/MS analysis of fatty acid isoprenoid alcohol esters.

Fatty acid isoprenoid alcohol esters were measured as ammonium adducts (NH_4^+) using direct infusion Q-TOF MS/MS in the positive ion mode by neutral loss scanning of the respective isoprenoid alcohol (farnesol, phytol, or geranylgeraniol) -H_2O moiety (vom Dorp, 2015).

Fatty Acid Isoprenoid Alcohol Esters	Formula	Parental Ion $[M+NH_4]^+$	Neutral Loss [Isoprenyl alcohol-H_20]
8:0-farnesol	$C_{23}H_{39}O_2$	366.3372	204.1878
10:0-farnesol	$C_{25}H_{43}O_2$	394.3685	
12:0-farnesol	$C_{27}H_{47}O_2$	422.3998	
14:0-farnesol	$C_{29}H_{51}O_2$	450.4311	
16:0-farnesol	$C_{31}H_{55}O_2$	478.4624	
16:3-farnesol	$C_{31}H_{49}O_2$	472.4155	
17:0-farnesol	$C_{32}H_{57}O_2$	492.4781	
18:0-farnesol	$C_{33}H_{59}O_2$	506.4937	
18:1-farnesol	$C_{33}H_{57}O_2$	504.4781	
18:2-farnesol	$C_{33}H_{55}O_2$	502.4624	
18:3-farnesol	$C_{33}H_{53}O_2$	500.4468	
20:0-farnesol	$C_{35}H_{63}O_2$	534.5250	
22:0-farnesol	$C_{37}H_{67}O_2$	562.5563	
8:0-phytol	$C_{28}H_{54}O_2$	440.4468	278.2974
10:0-phytol	$C_{30}H_{58}O_2$	468.4781	
12:0-phytol	$C_{32}H_{62}O_2$	496.5094	
14:0-phytol	$C_{34}H_{66}O_2$	524.5407	
16:0-phytol	$C_{36}H_{70}O_2$	552.5720	
16:3-phytol	$C_{36}H_{64}O_2$	546.5250	
17:0-phytol	$C_{37}H_{72}O_2$	566.5876	
18:0-phytol	$C_{38}H_{74}O_2$	580.6033	
18:1-phytol	$C_{38}H_{72}O_2$	578.5876	
18:2-phytol	$C_{38}H_{70}O_2$	576.5720	
18:3-phytol	$C_{38}H_{68}O_2$	574.5563	
20:0-phytol	$C_{40}H_{78}O_2$	608.6346	
22:0-phytol	$C_{42}H_{82}O_2$	636.6659	
8:0-geranylgeraniol	$C_{28}H_{48}O_2$	434.3998	272.2504
10:0-geranylgeraniol	$C_{30}H_{52}O_2$	462.4311	
12:0-geranylgeraniol	$C_{32}H_{56}O_2$	490.4624	
14:0-geranylgeraniol	$C_{34}H_{60}O_2$	518.4937	
16:0-geranylgeraniol	$C_{36}H_{64}O_2$	546.5250	
16:3-geranylgeraniol	$C_{36}H_{58}O_2$	540.4781	
17:0-geranylgeraniol	$C_{37}H_{66}O_2$	560.5407	
18:0-geranylgeraniol	$C_{38}H_{68}O_2$	574.5563	
18:1-geranylgeraniol	$C_{38}H_{66}O_2$	572.5407	
18:2-geranylgeraniol	$C_{38}H_{64}O_2$	570.5250	
18:3-geranylgeraniol	$C_{38}H_{62}O_2$	568.5094	
20:0-geranylgeraniol	$C_{40}H_{72}O_2$	602.5876	
22:0-geranylgeraniol	$C_{42}H_{76}O_2$	630.6189	

Table 13 Targeted list for LC Q-TOF and Q-Trap MS/MS analysis of prenylquinones (tocopherols and tocotrienols).

Tocopherols and tocotrienols were analyzed by LC MS/MS with either Q-TOF or Q-Trap.

Tocopherol	Formula	M	Parental Ion $[M+H]^+$	Neutral Loss
α-Tocopherol	$C_{29}H_{50}O_2$	430.71	431.4	165.1
β- and γ-Tocopherol	$C_{28}H_{48}O_2$	416.68	417.4	151.1
δ-Tocopherol	$C_{27}H_{46}O_2$	402.65	403.4	137.1
α-Tocotrienol	$C_{29}H_{44}O_2$	424.66	425.3	165.1
β- and γ-Tocotrienol	$C_{28}H_{42}O_2$	410.63	411.3	151.1
δ-Tocotrienol	$C_{29}H_{44}O_2$	424.66	397.3	137.1

7.4 Identification of tocotrienols in Arabidopsis lines by LC MS/MS

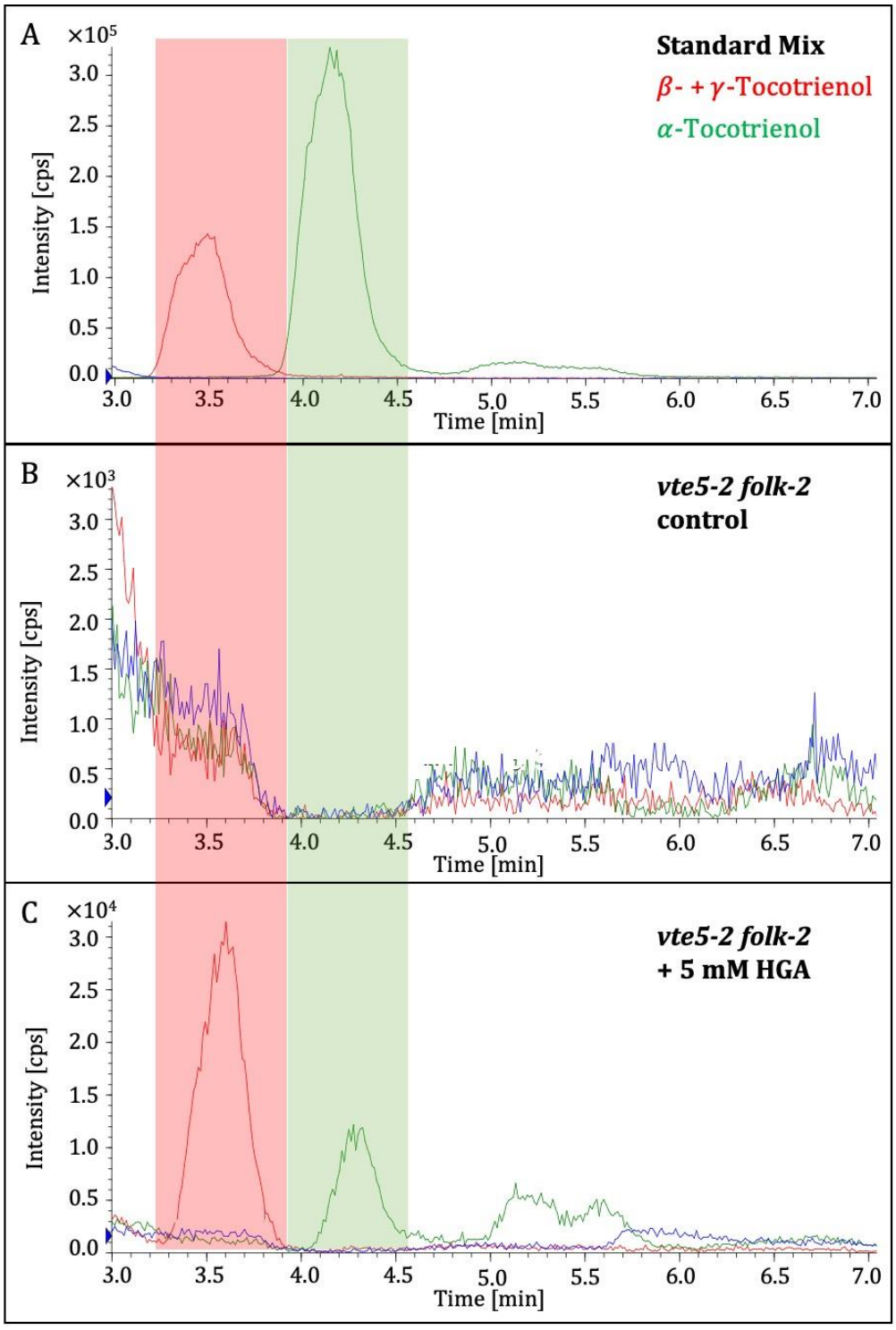

Figure 38 Tocotrienol analysis via LC MS/MS with Q-Trap in *vte5-2 folk-2* after HGA supplementation

The presence of tocotrienols in leaf extracts from Arabidopsis plants after HGA supplementation was confirmed by LC MS/MS analysis with a Q-Trap. As reference a standard mix of α-, β-, γ- and δ-tocotrienol was used (A). Two-week old Arabidopsis *vte5-2 folk-2* seedlings were transferred to control MS medium (B) or to MS medium containing 5 mM HGA (C) for nine days. Highlighted in green is α-tocotrienol (m/z 225.3→165.1) and highlighted in red are β- and γ-tocotrienol (m/z 411.3→151.1). Data represent representative MRM without normalization of one sample each.

7.5 SDS PAGE and Western blot analysis of VTE5 and FOLK

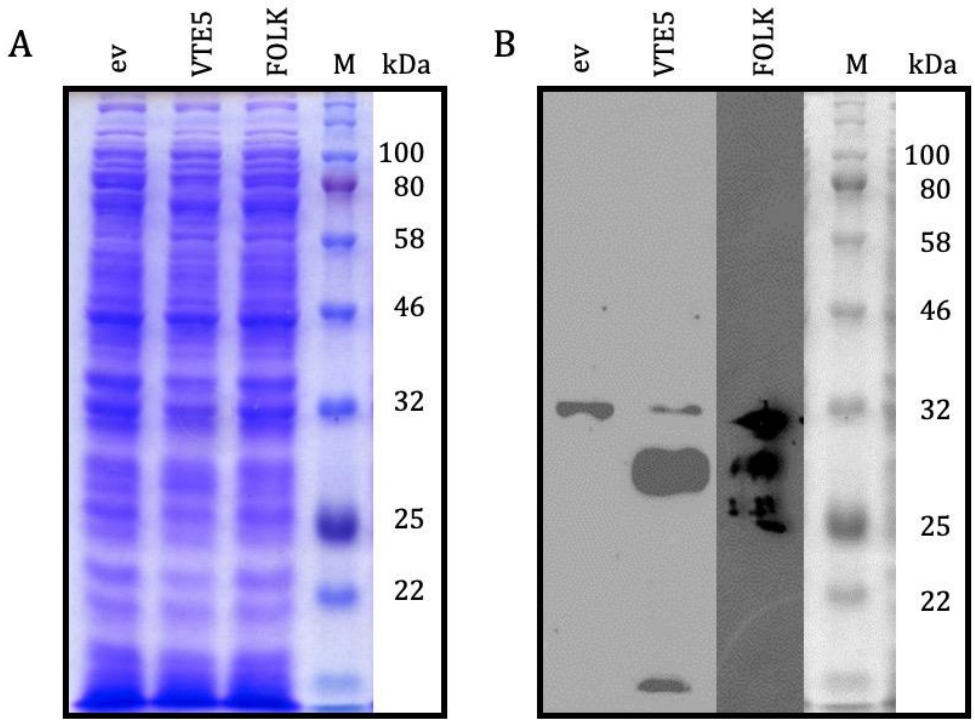

Figure 39 SDS PAGE and Western blot analysis of VTE5 and FOLK protein after heterologous expression in *E. coli*.

His-tagged protein was analyzed after heterologous expression of VTE5 (33.1 kDa) and FOLK (33.2 kDa) in *E. coli* Rosetta (DE3) pETDuet-1 (MCS1) constructs with SDS PAGE (A) and Western blot (B). No differences in protein amount to the ev control were observed by SDS PAGE. Western blot analysis using the His detector kit showed unspecific protein bands in the ev control with a size of around 32 kDa. Samples with VTE5 or FOLK showed several His-tagged protein bands between 25 and 32 kDa